

15 **Abstract**

16 Trait-based approaches are of increasing concern in predicting vegetation changes and
17 linking ecosystem structures to functions at large scales. However, a critical challenge for such
18 approaches is acquiring spatially continuous plant functional trait maps. Here, six key plant
19 functional traits were selected as they can reflect plant resource acquisition strategies and
20 ecosystem functions, including specific leaf area (SLA), leaf dry matter content (LDMC), leaf N
21 concentration (LNC), leaf P concentration (LPC), leaf area (LA) and wood density (WD). A total
22 of 34589 in-situ trait measurements of 3447 seed plant species were collected from 1430 sampling
23 sites in China and were used to generate spatial plant functional trait maps (~1 km), together with
24 environmental variables and vegetation indices based on two machine learning models (random
25 forest and boosted regression trees). To obtain the optimal estimates, a weighted average algorithm
26 was further applied to merge the predictions of the two models to derive the final spatial plant
27 functional trait maps. The models showed a good accuracy in estimating WD, LPC and SLA, with
28 average R^2 values ranging from 0.48 to 0.68. In contrast, both the models had weak performance
29 in estimating LDMC, with average R^2 values less than 0.30. Meanwhile, LA showed considerable
30 differences between two models in some regions. Climatic effects were more important than those
31 of edaphic factors in predicting the spatial distribution of plant functional traits. Estimates of plant
32 functional traits in northeast China and the Qinghai-Tibet Plateau had relatively high uncertainties
33 due to sparse samplings, implying a need of more observations in these regions in future. Our
34 spatial trait maps could provide critical supports for trait-based vegetation models and allow
35 exploration into the relationships between vegetation characteristics and ecosystem functions at
36 large scales. The six plant functional traits maps for China with 1 km spatial resolution are now
37 available at <https://figshare.com/s/c527c12d310cb8156ed2> (An et al., 2023).

38 **1 Introduction**

39 Climate change has been affecting vegetation distributions and biogeochemical cycling globally
40 and altering their feedbacks to climate system (Kirilenko et al., 2000; Finzi et al., 2011; Jónsdóttir
41 et al., 2022). Dynamic global vegetation models (DGVMs) are powerful tools for predicting
42 changes in vegetation and ecosystem-atmosphere exchanges (e.g., water, carbon and nutrient
43 cycling) in a changing climate (Foley et al., 1996; Peng, 2000). However, conventional DGVMs
44 are still insufficient realistic, largely due to their dependence on the plant functional types (PFTs)
45 assumption (Sitch et al., 2008; Yurova and Volodin, 2011; Scheiter et al., 2013). PFTs in
46 conventional DGVMs commonly have fixed attributes (mostly trait values) (Van Bodegom et al.,
47 2012; Wullschleger et al., 2014) that do not reflect plant adaptation to environments, limiting the
48 quantification of carbon-water-nutrient feedback between terrestrial ecosystems and the
49 atmosphere (Zaehle and Friend, 2010; Liu and Yin, 2013). Trait-based approaches can provide
50 robust theoretical basis for developing the next generation of DGVMs (Van Bodegom et al., 2012;
51 Sakschewski et al., 2015; Matheny et al., 2017). Plant functional traits, which are closely
52 associated with ecosystem functions (Diaz et al., 2004; Yan et al., 2023), can effectively reflect
53 response and adaptation of plants to environmental conditions (Myers-Smith et al., 2019; Qiao et
54 al., 2023).

55 Attempts to predict spatially continuous trait maps have been conducted at regional to global
56 scales (Madani et al., 2018; Moreno-Martínez et al., 2018; Boonman et al., 2020; Loozen et al.,
57 2020; Dong et al., 2023). Webb et al. (2010) proposed that the environment creates a filtered trait
58 distribution along an environmental gradient, and such trait-environment relationships offer
59 fundamental supports to predict the spatial distribution of plant functional traits through
60 extrapolating local trait measurements. Boonman et al. (2020) mapped the global patterns of
61 specific leaf area (SLA), leaf N concentration (LNC) and wood density (WD) based on a set of
62 climate and soil variables. As the number of available regional and global trait databases increases
63 (Wang et al., 2018; Kattge et al., 2020), trait-environment relationships are becoming increasingly
64 quantitative and accurate (Bruehlheide et al., 2018; Myers-Smith et al., 2019). Alternatively, remote
65 sensing approaches, such as empirical methods and physical radiative transfer models (e.g., partial
66 least squares regression and PROSPECT model), have been developed to estimate plant
67 physiological, morphological and chemical traits (e.g., leaf chlorophyll content, SLA, LNC and
68 leaf dry matter content (LDMC)) (Darvishzadeh et al., 2008; Romero et al., 2012; Ali et al., 2016).
69 Vegetation indices, such as normalized difference vegetation index (NDVI) and enhanced
70 vegetation index (EVI), have been successful in estimating plant functional traits of crops,
71 grasslands and forests (Clevers and Gitelson, 2013; Li et al., 2018; Loozen et al., 2018). Loozen et
72 al. (2020) demonstrated that EVI was the most important predictor for mapping the spatial pattern
73 of canopy nitrogen in European forests. Admittedly, a recent study has suggested that combining
74 environmental variables and vegetation indices can improve the predictive accuracy of canopy

75 nitrogen compared to those based on vegetation indices alone (Loozen et al., 2020).

76 Although there have been reports on plant functional trait distribution in China in some
77 global or regional researches (Yang et al., 2016; Butler et al., 2017; Madani et al., 2018; Moreno-
78 Mart ínez et al., 2018; Boonman et al., 2020), they are still large uncertainties in characterizing the
79 spatial distribution of plant functional traits in China. First, global studies generally have relatively
80 few, unevenly distributed sampling sites across China (Butler et al., 2017; Madani et al., 2018;
81 Boonman et al., 2020), impeding our understanding of the true spatial characteristics of trait
82 variability. Second, the spatial pattern of traits among these studies are usually inconsistent. For
83 example, Moreno-Mart ínez et al. (2018) and Madani et al. (2018) demonstrated that SLA values
84 were low in the southeast areas but high in the southwest areas of China, whereas Boonman et al.
85 (2020) found the opposite. Third, most studies focused on leaf traits (Yang et al., 2016; Loozen et
86 al., 2018; Moreno-Mart ínez et al., 2018), whereas traits associated with the whole-plant strategies,
87 such as WD, were ignored. Therefore, mapping and verifying the spatial patterns of key functional
88 traits that reflect the whole plant economics spectrum in China is a top priority.

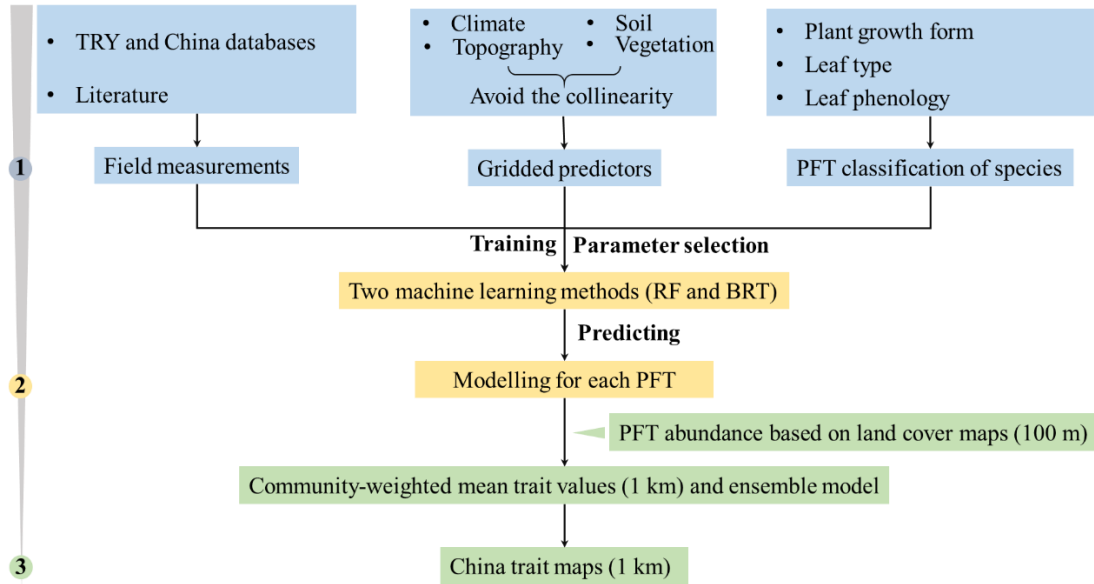
89 In this study, our main objective was to generate spatial maps for several key plant functional
90 traits, through combining field measurements, environmental variables and vegetation indices. We
91 selected six plant functional traits including SLA, LDMC, LNC, LPC, LA and WD. As key leaf
92 economics traits, SLA, LDMC, LNC and LPC were selected because they are closely linked to
93 plant growth rate, resource acquisition and ecosystem functions (Wright et al., 2004; Diaz et al.,
94 2016). LA is indicative of the trade-off between carbon assimilation and water-use efficiency
95 (Wright et al., 2017), and WD reflects the trade-off between plant growth rate and support cost,
96 with a higher WD linked to a lower growth rate, a higher survival rate and a higher biomass
97 support cost (King et al., 2006). For each plant functional trait, we predicted spatial patterns at a 1
98 km resolution using an ensemble modelling algorithm based on two machine learning methods
99 (i.e., random forest and boosted regression trees).

100 **2 Materials and Methods**

101 **2.1 Overview**

102 The spatial maps of plant functional traits in China were generated based on machine learning
103 methods trained by a large dataset of in-situ field measurements, environmental variables and
104 vegetation indices in three steps (Fig. 1). First, in-situ field measurements of six plant functional
105 traits were collected from TRY and China databases as well as published literature, and the PFTs
106 of plant species were classified based on plant growth form, leaf type and leaf phenology. Multiple
107 gridded predictors of climate, soil, topography and vegetation indices were used after avoiding the
108 collinearity among them. Second, random forest and boosted regression trees were used to train
109 the relationships between plant functional traits and predictors for each PFT individually. Third,
110 the spatial abundance of each PFT within 1 km grid cell was calculated using land cover map (100

111 m). Community-weighted trait values within 1 km grid cell were calculated based on these
 112 abundances of each PFT and their predicted trait values in Step 2. To reduce the variability of
 113 different single-models, we derived the final spatial maps of plant functional traits using ensemble
 114 model algorithm to merge the predictions of random forest and boosted regression trees according
 115 to their cross-validated R^2 values.



116
 117 **Figure 1.** Methodological workflow for spatial mapping of plant functional traits. Trait
 118 mapping is performed in three steps. Step 1: in-situ field measurement of plant functional traits,
 119 PFT classification of plant species and gridded predictors were collected. Step 2: two machine
 120 learning methods were used to predict trait values by training the field measurements and
 121 predictors for each PFT. Step 3: spatialization of trait maps by calculating the abundance of each
 122 PFT using 100 m land cover map and predicted trait values within 1 km grid cells. PFT, plant
 123 functional type; RF, random forest; BRT, boosted regression trees.

124 2.2 Plant functional trait collection and data processing

125 The information on the six plant functional traits and their ecological meanings are described in
 126 Table 1. Plant trait data was obtained and collected via two main sources. The first source was
 127 public trait databases, including the TRY database (Kattge et al., 2020) and the China Plant Trait
 128 Database (Wang et al., 2018). The second source was from literature (listed in Appendix A). To
 129 ensure data quality and comparability, we only included trait observations that met the following
 130 five criteria: 1) Measurements must be obtained from natural terrestrial fields in order to minimize
 131 the influences of management disturbance, and observations from cropland, aquatic habitat,
 132 control experiments and gardens were excluded; 2) According to the mass ratio hypothesis, the
 133 effect of plant species on ecosystem functioning is determined to an overwhelming extent by the
 134 traits and functional diversity of the dominant species and is relatively insensitive to the richness
 135 of subordinate species (Grime, 1998). Thus, we only included studies that measured plant trait

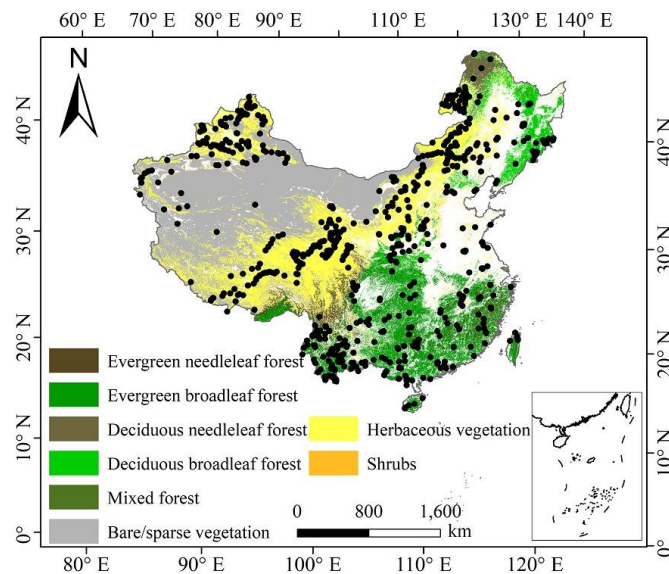
136 observations from all species or dominant species within a community; 3) In order to consider the
 137 intraspecific trait variation, when the same species occurred in the same sampling site from
 138 different studies, we included all original observed data from different studies rather than
 139 averaging the values at the species level (Jung et al., 2010; Siefert et al., 2015); 4) Plant trait
 140 observations must be made on mature and healthy plant individuals, so some specific growth
 141 stages (e.g., seedling) and size classes (e.g., sapling) were excluded to reduce the confounding
 142 effect of ontogeny and seasonality (Thomas, 2010); 5) We only included studies with clear
 143 geographical coordinates to match predictor variables. The sampling location and sampling time
 144 information were also included in the dataset. The sampling time mostly focused on the growing
 145 season of a year (i.e., May-October), which ensures the relative consistency of sampling time to
 146 minimize the effects of seasonality. Plant functional traits must be sampled and measured
 147 according to standardized measurement procedures (Perez-Harguindeguy et al., 2013) to reduce
 148 the variation and uncertainty among different data sources. In this study, we included SLA
 149 measurements on sun-leaves, and WD measurements on main stem of woody species.

150 **Table 1** Description of plant functional traits selected in this study and their relevant
 151 ecosystem functions.

Trait	Abbreviation	Description	Relevant ecosystem functions
Specific leaf area	SLA	As a core leaf economics trait (Wright et al., 2004), it is related to trade-off between leaf lifespan and C acquisition as well as light competition (Reich et al., 1991)	Productivity, litter decomposition, competitive ability (Bakker et al., 2011; Smart et al., 2017)
Leaf dry matter content	LDMC	Strongly related to resource availability and potential growth rate (Hodgson et al., 2011)	Productivity, litter decomposition, herbivore resistance, and drought tolerance (Bakker et al., 2011; Smart et al., 2017; Blumenthal et al., 2020)
Leaf N concentration	LNC	As a core leaf economics trait, it is strongly related to photosynthetic capacity (Wright et al., 2004)	Productivity, nutrient cycling, litter decomposition (LeBauer and Treseder, 2008; Bakker et al., 2011)
Leaf P concentration	LPC	As a core leaf economics trait, it is strongly related to photosynthetic capacity (Wright et al., 2004)	Productivity, nutrient cycling, litter decomposition (LeBauer and Treseder, 2008; Bakker et al., 2011)
Leaf area	LA	Trade-off between C assimilation and water use efficiency, it is related to energy balance (Wright et al., 2017)	Productivity (Li et al., 2020)
Wood density	WD	A measure of carbon investment, representing the trade-off between growth and mechanical support (Martínez-Vilalta et al., 2010)	Drought tolerance, productivity (Hoeber et al., 2014; Liang et al., 2021)

152 The plant trait data was checked for possible errors and corrected in three steps as follows.
 153 First, species name and taxonomic nomenclature were corrected and standardized according to the
 154 Plant List (<http://www.theplantlist.org/>) using the “plantlist” package. Second, illogical values,
 155 repeated values and outliers were removed, which were defined by observations exceeding 1.5

156 standard deviations of the mean trait value for a given species (Kattge et al., 2011). Third, we
 157 appended information on plant growth form, leaf type and leaf phenology from the TRY
 158 categorical traits database (<https://www.try-db.org/TryWeb/Data.php#3>) and *Flora Reipublicae*
 159 *Popularis Sinicae* (<http://www.iplant.cn/frps>), which were used to match species names to PFTs.
 160 We associated each species with a corresponding PFT based on plant growth form (tree, shrub and
 161 grass), leaf type (broadleaf and needleleaf) and leaf phenology (evergreen and deciduous). For
 162 example, the information on *Salix matsudana* is: tree, deciduous and broadleaf, thus, we were able
 163 to associate the PFT of deciduous broadleaf forest (DBF) to this species. The species that did not
 164 correspond to any PFT were discarded. After these treatments, we collected a total of 34589 trait
 165 measurements from 1430 sampling sites for our database, representing 3447 species from 195
 166 families and 1066 genera (Fig. 2). Information on the statistics for the six plant functional traits
 167 collected in this study is shown in Table B1 in Appendix B.
 168



169
 170 **Figure 2.** Location distribution and land cover map in China.

171 2.3 Preparing predictor variables

172 2.3.1 Climate data

173 Twenty-one climate variables were used in this study, including 19 bioclimate variables, solar
 174 radiation (RAD) and aridity index (AI) (Table B2 in Appendix B). The 19 bioclimate variables and
 175 RAD were obtained from the WorldClim version 2.1 for the period from 1970 to 2000
 176 (<https://www.worldclim.org/data/worldclim21.html>). The AI data was extracted from the CGIAR
 177 Consortium of Spatial Information (CGIAR-CSI) website for the period from 1970 to 2000
 178 (<http://www.csi.cgiar.org>) (Trabucco and Zomer, 2018). The spatial resolution of climate data is 1
 179 km.

180 2.3.2 Soil data

181 Twelve soil variables were included in this study, representing the different aspects of soil
 182 properties, i.e. soil texture, bulk density (BD), pH and soil nutrients (Table B2 in Appendix B). All

183 soil variables were extracted from the Soil Database of China for Land Surface Modeling
184 (<http://globalchange.bnu.edu.cn/research/soil2>) (Shangguan et al., 2013). Given the importance of
185 topsoil properties on community composition (Bohner, 2005), we averaged the first four layers to
186 represent the topsoil properties (~ 30 cm) in our study. The spatial resolution is 1 km.

187 **2.3.3 Topography**

188 The topographic variable was elevation. Elevation data was extracted from the STRM 90m dataset
189 in China, based on the SRTM V4.1 database (<https://www.resdc.cn/data.aspx?DATAID=123>). The
190 spatial resolution is 1 km.

191 Given the collinearity among climate and soil variables, we reduced the dimensionality of
192 these predictors based on Pearson's correlation coefficient (r) (Figs. B1 and B2 in Appendix B).
193 Among a set of highly correlated variables ($r > 0.75$), only one variable was retained in subsequent
194 analysis to ensure a combination of different environmental variables. The final selection of
195 environment predictors included nineteen variables: mean annual temperature (MAT), mean
196 diurnal range (MDR), min temperature of coldest quarter (Tmin), max temperature of warmest
197 quarter (Tmax), temperature seasonality (TS), mean annual precipitation (MAP), precipitation
198 seasonality (PS), precipitation of wettest quarter (PEQ), precipitation of driest quarter (PDQ), AI,
199 RAD, elevation, soil sand content (SAND), pH, BD, soil total N (STN), soil total P (STP), soil
200 available P (SAP), soil alkali-hydrolyzable N (SAN) and cation exchange capacity (CEC).

201 **2.3.4 Vegetation indices**

202 Three categories of vegetation indices were included in this study (Table B2 in Appendix B). First,
203 EVI was extracted from the MOD13A3 V006 product
204 (<https://lpdaac.usgs.gov/products/mod13a3v006/>). This product is available as a monthly average
205 with spatial resolution of 1 km, ranging from January 2000 to December 2018. Second, MODIS
206 reflectance data was also extracted from the MOD13A3 V006 product, including MIR reflectance,
207 NIR reflectance, red reflectance and blue reflectance. Third, the MERIS terrestrial chlorophyll
208 index (MTCI) was extracted from the Natural Environment Research Council Earth Observation
209 Data Centre (NERC-NEODC, 2005) (<https://data.ceda.ac.uk/>). MTCI data is available globally as
210 a monthly average at 4.63 km spatial resolution, and ranges from June 2002 to December 2011. It
211 is noted that valid MTCI values should be greater than 1, so our study deleted any values less than
212 1.

213 To avoid collinearity, we also reduced the dimensionality of vegetation indices based on
214 Pearson's correlation coefficient (r) (Fig. B3 in Appendix B). Most selected variables were related
215 to growing seasons due that plant functional traits were measured during the growing season.
216 Furthermore, based on the results of Pearson's correlation coefficient (r), MTCI, MIR, NIR, red
217 and blue in January showed low correlations with those in growing season, thus they were
218 included in subsequent analysis. The final selection included 36 variables: annual EVI, EVI (May,
219 June, July, August and September), MTCI, MIR, NIR, red and blue (all for January, June, July,
220 August and September).

221 Both environmental variables and vegetation indices variables were resampled to a consistent
222 spatial resolution of 1 km using the nearest neighborhood method.

223 PFT is also an important factor in influencing the variation of plant functional traits
224 (Verheijen et al., 2016; Loozen et al., 2020), thus the trait predictions were performed for each
225 PFT individually. We used the 2015 land cover map at a 100 m spatial resolution to calculate the
226 relative abundance of each PFT within 1 km grid cells, which was extracted from the Copernicus
227 Global Land Service (CGLS-LC100, Version 3) (<https://land.copernicus.eu/global/products/lc>)
228 (Buchhorn et al., 2020). We focused on natural terrestrial vegetation, so all artificial or crop areas
229 were thus eliminated in our dataset. Seven categories were included: evergreen needleleaf forest
230 (ENF), evergreen broadleaf forest (EBF), deciduous needleleaf forest (DNF), deciduous broadleaf
231 forest (DBF), shrubland (SHL), grassland (GRL) and bare/sparse vegetation.

232 **2.4 Model fitting and validation**

233 To predict spatial patterns of plant functional traits, we used two machine learning models, i.e.,
234 random forest and boosted regression trees.

235 Random forest is an ensemble machine learning method based on classification and
236 regression trees using collections of regression trees to classify observations according to a set of
237 predictive variables (Breiman, 2001). This method repeatedly constructs a set of trees from
238 random samples of training data, and the final prediction is produced by integrating the results of
239 all individual trees, which makes it a robust method. The model is controlled by two main
240 parameters: the number of sampled variables (mtry) and the number of trees (ntree). The mtry was
241 set to range from 1 to 57 (at an interval of 1), and the ntree was set as 500, 1000, 2000, 5000 and
242 10000 in subsequent runs. This analysis was performed using the ‘randomForest’ function in the
243 ‘randomForest’ package (Liaw and Wiener, 2002).

244 Boosted regression trees are machine learning methods based on generalized boosted
245 regression models and using a boosting algorithm to combine many sample tree models to
246 optimize predictive performance (Elith et al., 2006). There is no need for prior data transformation
247 or the elimination of outliers, and this method can fit complex non-linear relationships while
248 automatically handling interaction effects between predictors (Elith et al., 2008). The four
249 parameters to optimize in these models are the number of trees, interaction depth, learning rate
250 and bag fractions. We varied the parameter settings to find the optimal parameter combination that
251 achieves minimum predictive error. The number of trees was set to 3000, the interaction depth
252 varied from 1 to 7 (at an interval of 1), the learning rate was set to 0.001, 0.01, 0.05 and 0.1, and
253 the bag fraction was set to 0.5, 0.6, 0.7 and 0.75. PFT was used as a dummy variable in the
254 boosted regression trees models. This analysis was conducted using the ‘gbm’ function in the
255 ‘gbm’ package (Ridgeway, 2006).

256 We built separate predictive model for each plant functional trait. To select the optimal
257 parameter combination and to evaluate the final model performance for each trait, we calibrated

258 the models 10 times using randomly selected 80% of the data for training the models and
 259 validating against the remaining 20% based on cross-validation (Table B3 in Appendix B). The
 260 predictive performance was evaluated by regressing the predicted and observed trait values from
 261 all repetitions of the cross-validation. The fitting performances of the random forest and boosted
 262 regression trees were evaluated using determinate coefficient (R^2), normalized root-mean-square
 263 error (NRMSE) and mean absolute error (MAE). These scores are calculated following Eq. (1), Eq.
 264 (2) and Eq. (3):

$$265 \quad R^2 = 1 - \frac{\sum_{i=1}^n (p_i - o_i)^2}{\sum_{i=1}^n (p_i - \hat{o}_i)^2} \quad (1)$$

$$266 \quad \text{NRMSE} = \frac{\sqrt{\frac{1}{n} \sum_{i=1}^n (p_i - o_i)^2}}{p_{\max} - p_{\min}} \quad (2)$$

$$267 \quad \text{MAE} = \frac{1}{n} \sum_{i=1}^n |o_i - p_i| \quad (3)$$

268 where p_i and o_i are the predictive values and observed values, respectively; \hat{o}_i is the mean of the
 269 observed values.

270 To quantify the relative importance of each predictor across the two models consistently, we
 271 used the method proposed by Thuiller et al. (2009). This method applies correlation between the
 272 standard predictions fitted with the original data and predictions where the variable under
 273 investigation has been randomly permuted. If the correlation is high, which indicates little
 274 difference between the two predictions, the variable permuted is considered not important for the
 275 model. This step was repeated multiple times for each predictor, and the mean correlation
 276 coefficient over runs was recorded. Then the relative importance of each predictor was quantified
 277 as one minus the Spearman rank correlation coefficient (see Boonman et al., 2020). In addition,
 278 we used generalized additive models to fit the relationships between plant functional traits and the
 279 most important variables using the ‘gam’ function in the ‘mgcv’ package.

280 **2.5 Generation of plant functional trait maps and model performance**

281 The generation of spatial maps of plant functional was performed in three steps. First, we
 282 predicted trait values for each natural PFT (e.g., EBF, ENF, DBF, DNF, SHL and GRL) within 1
 283 km grid cell separately. Second, the abundance of individual natural PFT within 1 km grid cell
 284 was estimated using a land cover map with a spatial resolution of 100 m. Third, refer to the Eq. (4)
 285 that has been widely applied in a community (Garnier et al., 2004), the final trait value in a given
 286 1 km grid cell was calculated as the sum of the predicted trait values multiplying by corresponding
 287 abundance of each natural PFT.

$$288 \quad \text{CWM} = \sum_{i=1}^n W_i X_i \quad (4)$$

289 where n is the total number of PFT in a given grid; W_i is the relative abundance of the i th natural
 290 PFT; and X_i is the predicted trait value of the i th natural PFT.

291 To reduce the variability of different single-models and to construct a more stable and
 292 accurate model, the ensemble model was further applied to merge the predictions of random forest

293 and boosted regression trees according to their cross-validated R^2 values. The predictive value of
 294 ensemble model was calculated in a given grid cell as described by Eq. (5) (Marmion et al., 2009).
 295 The model accuracy was calculated by regressing the predictive values of ensemble model against
 296 the observed trait values.

$$297 \quad Pred_EM_t = \frac{\sum_{m=1}^2 (pred_{m,t} \times r_{m,t}^2)}{\sum_{m=1}^2 r_{m,t}^2} \quad (5)$$

298 where $Pred_EM_t$ is the predictive values of t trait in the ensemble model; $pred_{m,t}$ is the
 299 predictive values of t trait in m model; $r_{m,t}^2$ is the cross-validated R^2 of t trait in m model.

300 To evaluate the model performance (i.e. the variability in the prediction across models), the
 301 coefficient of variation (CV) was calculated as the difference between the predictions of random
 302 forest and boosted regression trees methods and the ensemble prediction. CV is calculated as
 303 following Eq. (6):

$$304 \quad CV_t = \frac{\sqrt{\sum_{m=1}^2 (pred_{m,t} - obs_t)^2 \times r_{m,t}^2}}{\sum_{m=1}^2 r_{m,t}^2} \quad (6)$$

305 where $pred_{m,t}$ is the predictive values of t trait in m model; obs_t is the values of t trait in the
 306 ensemble model; $r_{m,t}^2$ is the cross-validated R^2 of t trait in m model.

307 **2.6 Uncertainty assessments**

308 Multivariate environmental similarity surface analysis (MESS) was used to identify the range of
 309 the extrapolated predictor values across the locations in the plant trait dataset (Elith et al., 2010).
 310 This method is often used to evaluate the extent of extrapolation and the applicability domain. If
 311 the values are negative, this indicates that at a given grid cell, at least one predictor variable is
 312 outside the extent of referenced predictor layer. This analysis was conducted using the ‘mess’
 313 function in the ‘dismo’ package.

314 All analyses were performed in R 4.0.2 (R Core Team, 2020).

315 **3 Results**

316 **3.1 Performances of prediction models**

317 Cross-validation showed that the performance of the predictive models differed greatly among the
 318 plant functional traits (Table 2, Tables C1 and C2 in Appendix C). WD had the best performance
 319 in all three models, with R^2 values of 0.64, 0.68 and 0.67 for random forest, boosted regression
 320 trees and ensemble model, respectively. SLA and LPC had R^2 values greater than 0.45, while
 321 LDMC performed the worst, with R^2 values below 0.30.

322 **Table 2** Results of plant functional traits for cross-validated R^2 , NRMSE and MAE for
 323 random forest, boosted regression trees and ensemble model.

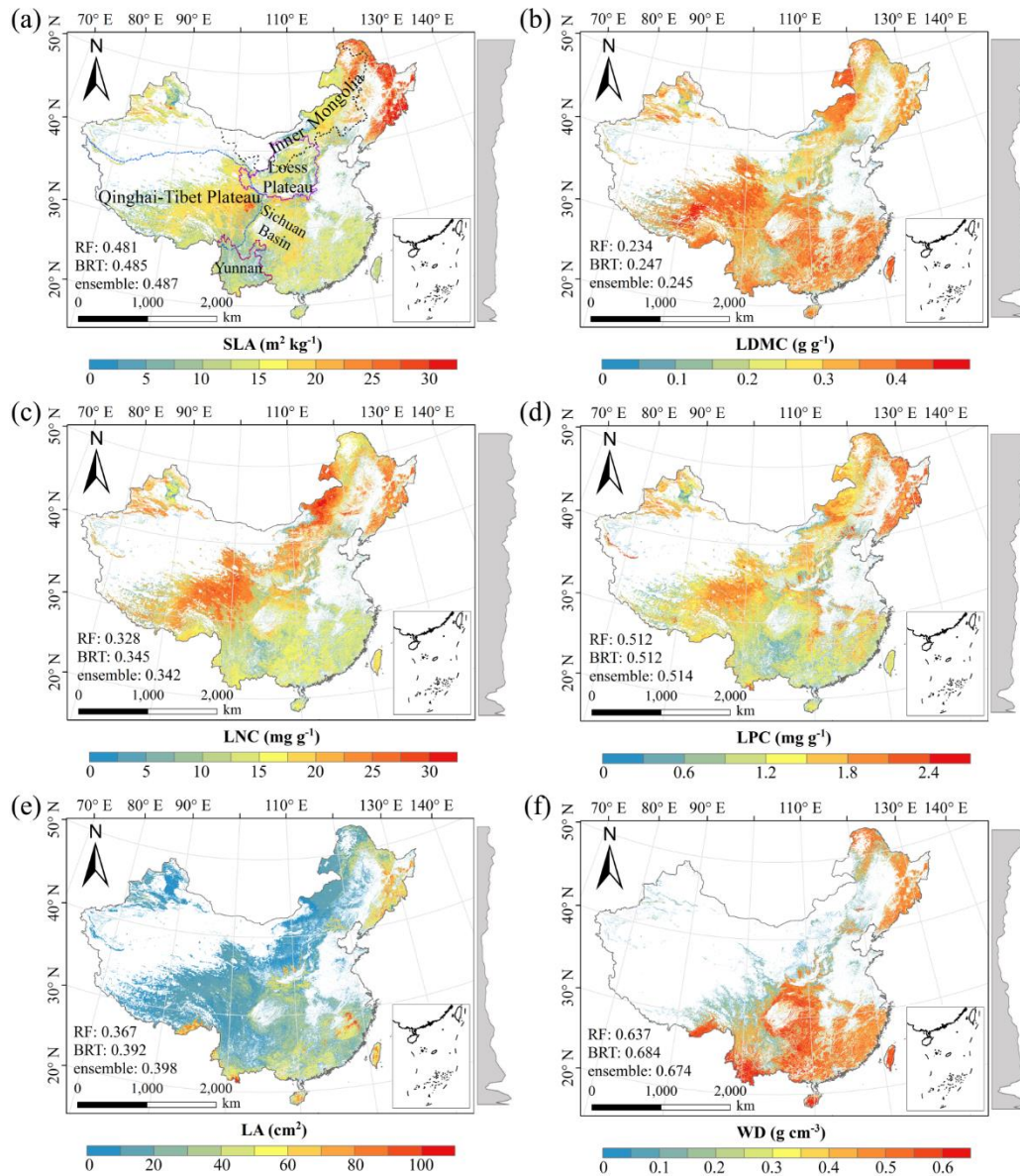
Traits	Random forest			Boosted regression trees			Ensemble model		
	R^2	NRMSE	MAE	R^2	NRMSE	MAE	R^2	NRMSE	MAE
SLA	0.48	0.22	5.10	0.48	0.20	5.08	0.49	0.21	5.07
LDMC	0.23	0.21	0.07	0.28	0.18	0.07	0.24	0.20	0.07
LNC	0.33	0.19	4.92	0.34	0.18	4.85	0.34	0.19	4.85
LPC	0.51	0.24	0.53	0.51	0.22	0.53	0.51	0.27	0.53
LA	0.37	0.45	26.76	0.39	0.51	27.47	0.40	0.58	26.59
WD	0.64	0.20	0.10	0.68	0.13	0.10	0.67	0.17	0.10

324 SLA, specific leaf area ($\text{m}^2 \text{kg}^{-1}$); LDMC, leaf dry matter content (g g^{-1}); LNC, leaf N concentration
 325 (mg g^{-1}); LPC, leaf P concentration (mg g^{-1}); LA, leaf area (cm^2); WD, wood density (g cm^{-3}); R^2 ,
 326 determinate coefficient; NRMSE, normalized root-mean-square error; MAE, mean absolute error.

327 **3.2 Spatial patterns of predicted plant functional traits**

328 There were relatively consistent spatial patterns for SLA, LNC and LPC, with high values in the
 329 northeastern and northwestern regions and the southeastern Qinghai-Tibet Plateau, and low values
 330 in southwestern China (Figs. 3a, 3c and 3d, Figs. D1, D2, D3, D5 and D6 in Appendix D). SLA
 331 and LPC increased with latitude, while LNC did not vary significantly along the latitudinal
 332 gradient. For SLA, LNC and LPC, the variability was low among random forest, boosted
 333 regression trees and ensemble model, with an overall CV less than 0.3 (Figs. 4a, 4c and 4d).
 334 LDMC values were relatively high in most regions of China, and the low values were mainly
 335 located in eastern Yunnan and the Loess Plateau (Fig. 3b, Figs. D1, D2 and D4 in Appendix D).
 336 LA showed high values in the northeastern and southern regions (except for the Sichuan Basin),
 337 and the southeastern Qinghai-Tibet Plateau (Fig. 3e, Figs. D1, D2 and D7 in Appendix D). The
 338 strong latitudinal gradient was observed in LA, where the values decreased with latitude.

339 The CV values of LPC decreased with latitude, but other traits did not show latitudinal
 340 patterns (Fig. 4). The CV values of LA were relatively high, especially in the northwestern region
 341 and the Inner Mongolia-Loess Plateau region (Fig. 4e). WD had high values in the northeastern
 342 and southern regions (Fig. 2f, Figs. D1, D2 and D8 in Appendix D), while CV values for WD in
 343 China were low throughout China (Fig. 4f).



344

345

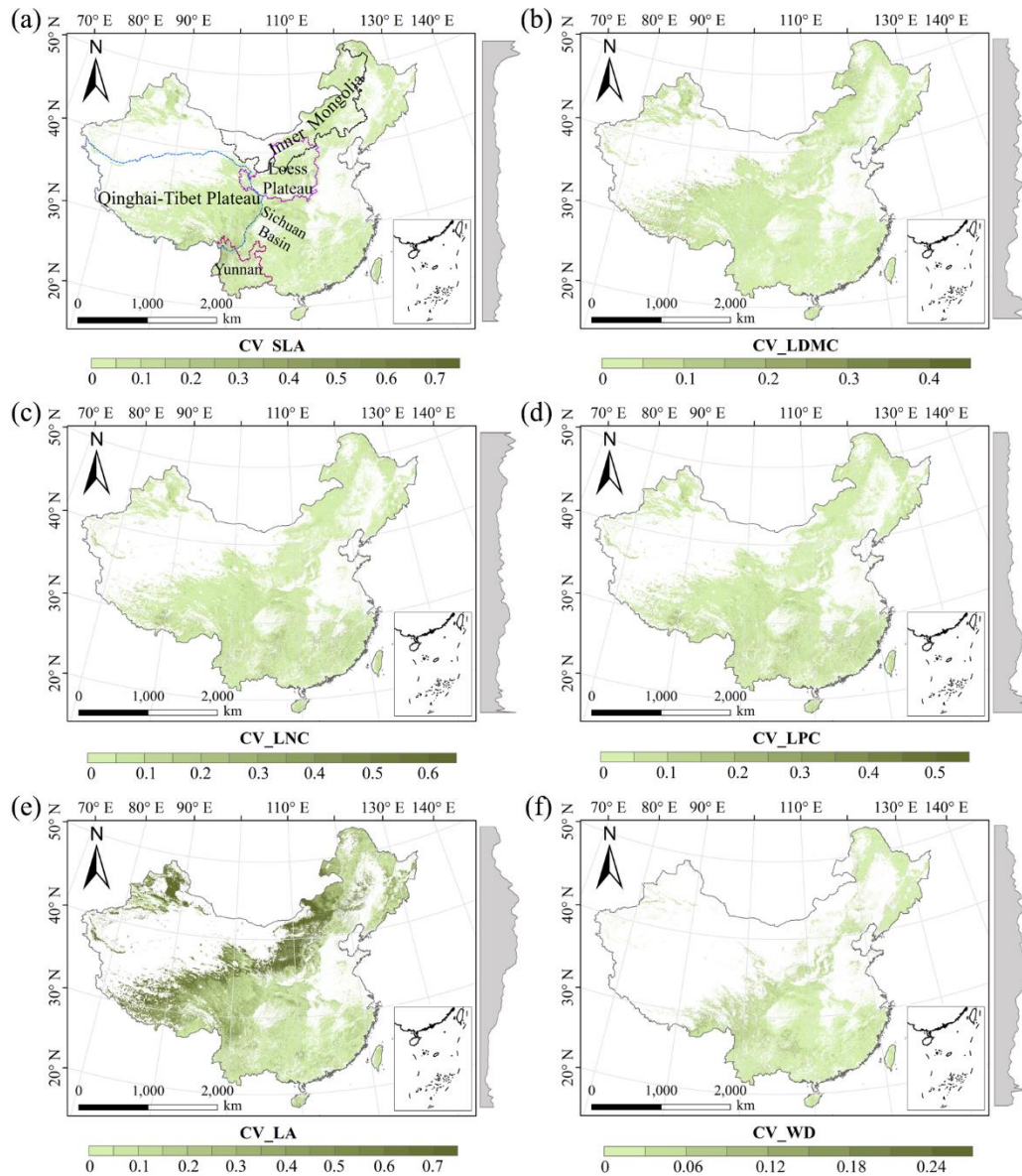
346

347

348

349

Figure 3. Spatial patterns of predicted plant functional traits in China based on the ensemble model. The grey curves to the right of the maps display trait distribution along with latitude. The white areas represent artificial land cover types. RF, random forest; BRT, boosted regression trees; ensemble, ensemble model; SLA, specific leaf area; LDMC, leaf dry matter content; LNC, leaf N concentration; LPC, leaf P concentration; LA, leaf area; WD, wood density.



350

351 **Figure 4.** The variability in plant functional trait predictions among random forest, boosted
 352 regression trees and ensemble model. The grey curves to the right of the maps display coefficient
 353 of variation along with latitude. The white areas represent artificial land cover types. SLA, specific
 354 leaf area; LDMC, leaf dry matter content; LNC, leaf N concentration; LPC, leaf P concentration;
 355 LA, leaf area; WD, wood density.

356 3.3 Relative importance of predictive variables

357 The dominant factors explaining spatial variation differed greatly among plant functional traits
 358 (Table 3). Overall, climate variables were more important for predicting plant functional traits
 359 than were soil variables. Temperature variables (i.e., MAT, MDR and TS) showed close
 360 relationships with SLA, LDMC, LPC and WD, while precipitation variables (i.e., PS, PEQ, MAP
 361 and PDQ) were more important for predicting the spatial patterns of LNC, LPC and LA. RAD was

362 the fourth most dominant factor in predicting the spatial patterns of SLA and WD. Elevation also
 363 played an important role in the LDMC and LPC predictions. Within soil variables, soil nutrients
 364 (i.e., pH and SAP) showed close associations with SLA and LNC. In addition to the environmental
 365 variables, MTCI emerged as an important predictor for explaining SLA, LDMC and LA. Finally,
 366 EVI was the most important predictor for LA, and MIR in January and May were the primary
 367 predictors of WD. The relationships between plant functional traits and the most important
 368 variables were shown in Figs. E1 and E2 in Appendix E.

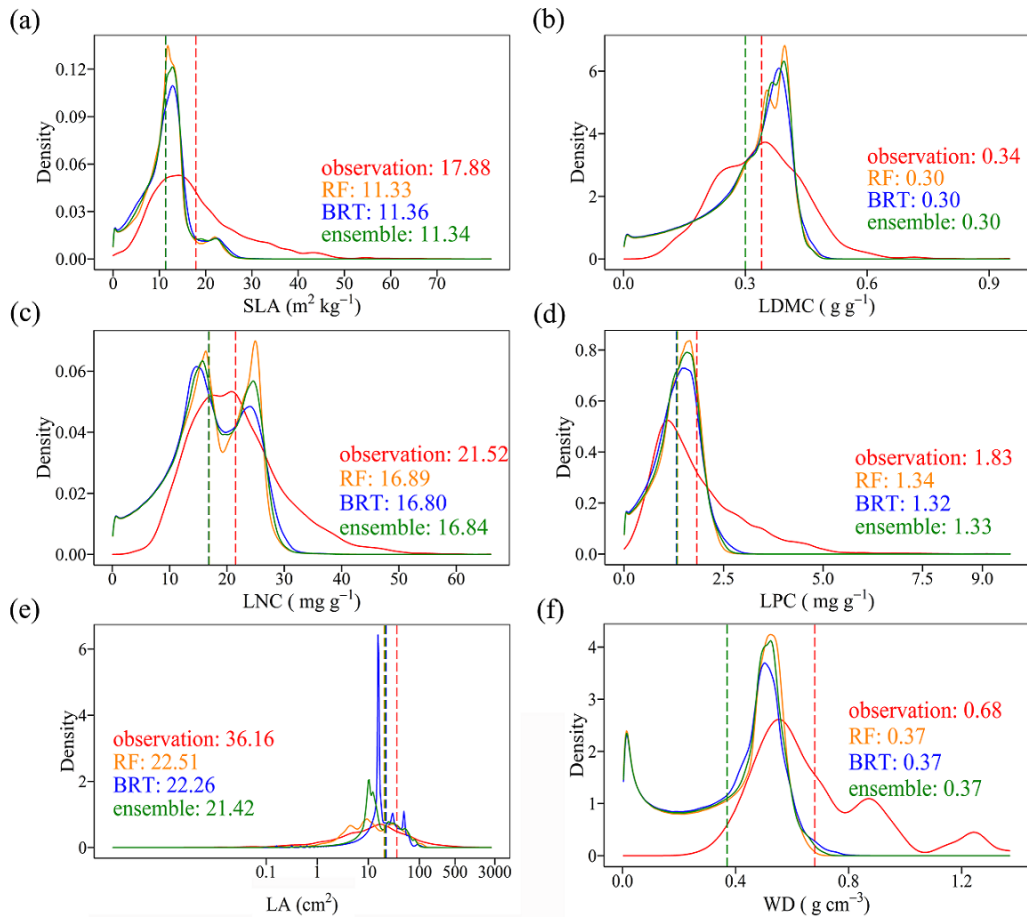
369 **Table 3** List of the eight most important variables for plant functional trait predictions.

Rank	SLA	LDMC	LNC	LPC	LA	WD
1	SAP	MAT	PS	MDR	EVI5	MIR1
2	TS	Elevation	SAP	PDQ	PEQ	TS
3	blue9	MTCI5	pH	Elevation	MTCI9	MIR5
4	RAD	blue8	MDR	MIR8	NIR9	RAD
5	MTCI4	MTCI4	MAP	Tmax	AI	MIR6
6	MTCI6	MTCI6	PEQ	MTCI6	MTCI6	pH
7	Elevation	NIR1	MIR1	MIR7	MAP	red5
8	MTCI7	CEC	Tmax	MIR9	red5	PS

370 SLA, specific leaf area ($\text{m}^2 \text{kg}^{-1}$); LDMC, leaf dry matter content (g g^{-1}); LNC, leaf N concentration
 371 (mg g^{-1}); LPC, leaf P concentration (mg g^{-1}); LA, leaf area (cm^2); WD, wood density (g cm^{-3}); SAP, soil
 372 available P; TS, temperature seasonality; blue, blue reflectance; RAD, solar radiation; MTCI, MERIS
 373 terrestrial chlorophyll index; MAT, mean annual temperature; NIR, near-infrared reflectance; CEC,
 374 cation exchange capacity; PS, precipitation seasonality; MDR, mean diurnal range; MAP, mean annual
 375 precipitation; PEQ, precipitation of wettest quarter of a year; MIR, middle infrared reflectance; Tmax,
 376 max temperature of warmest month of a year; PDQ, precipitation of driest quarter of a year; EVI,
 377 enhanced vegetation index; AI, aridity index; red, red reflectance.

378 3.4 Model performance

379 The distributions of the predictive trait values based on random forest, boosted regression trees,
 380 and ensemble model were consistent with the original trait observations, especially the peak
 381 values (Fig. 5). The mean values of trait observations were relatively higher than those of the
 382 predictive values.

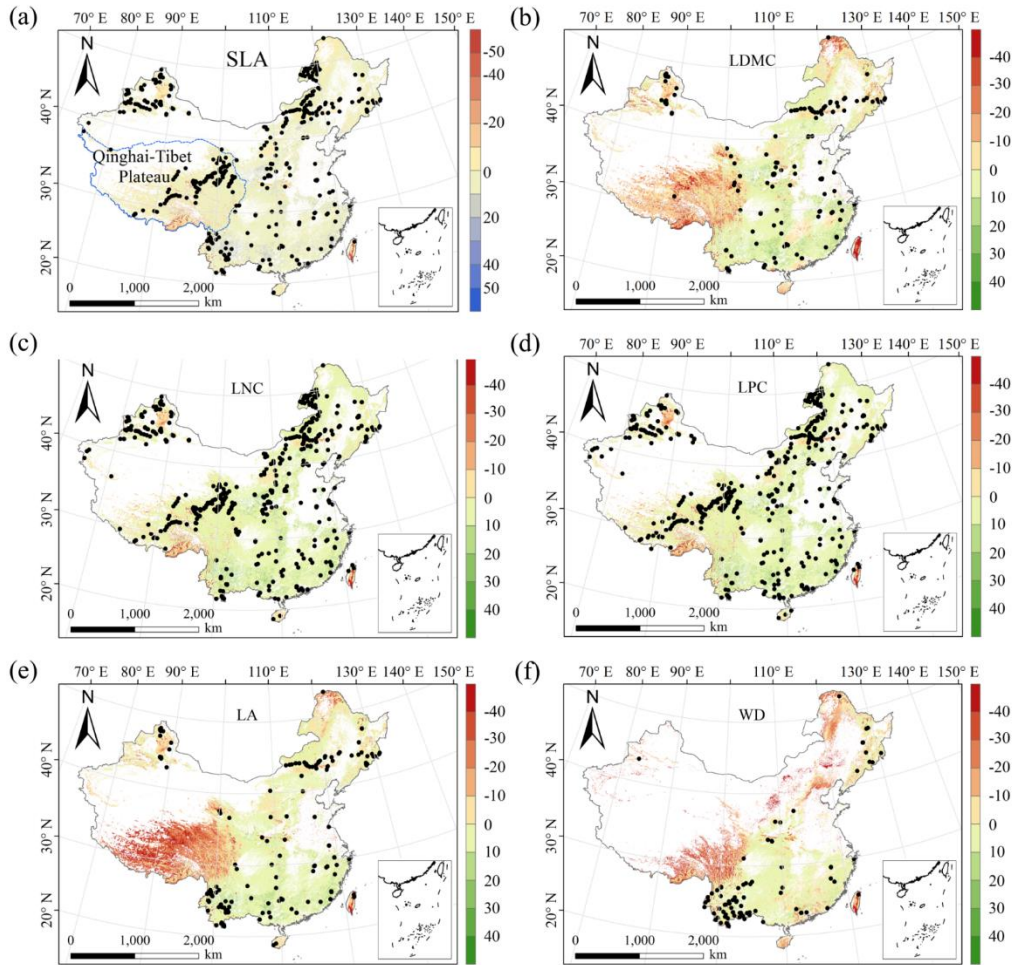


383

384 **Figure 5.** Comparison of trait distribution between observations and predictive values in each
 385 of the different models. Each panel depicts the distribution of observations in solid red, of the
 386 random forest (RF) model in yellow, of the boosted regression trees (BRT) model in blue, and of
 387 the ensemble model in green. The dashed vertical lines indicate mean values. SLA, specific leaf
 388 area; LDMC, leaf dry matter content; LNC, leaf N concentration; LPC, leaf P concentration; LA,
 389 leaf area; WD, wood density.

390 3.5 Uncertainty assessments

391 The MESS values of all plant functional traits were positive in most regions, indicating a wide
 392 applicability domain of our models (Fig. 6). Nevertheless, trait predictions should be interpreted
 393 carefully for northeastern China and the Qinghai-Tibet Plateau due to the sparse samplings in
 394 these regions.



395

396

Figure 6. Multivariate environmental similarity surface (MESS) assessments for the six plant
 397 functional traits. The black dots represented the locations of trait observations. More intense
 398 shades indicate greater similarity (blue) or difference (red) in environmental conditions of the
 399 location compared to the predictive factors covered by the training dataset. The white areas
 400 represent artificial land cover types. SLA, specific leaf area; LDMC, leaf dry matter content; LNC,
 401 leaf N concentration; LPC, leaf P concentration; LA, leaf area; WD, wood density.

402

4 Discussion

403

4.1 Comparison with previous work

404

Our study predicted the spatial patterns of six key plant functional traits across China using
 405 machine learning methods and identified the applicability domain of the models. WD had the
 406 highest precision with an average of R^2 of 0.66, which was higher than the global WD prediction
 407 (Boonman et al., 2020). This improvement in precision may be attributed to the large number and
 408 dense occurrence of sample sites as well as the inclusion of vegetation indices in our study. In
 409 addition, SLA and LPC also showed good accuracy with R^2 values of 0.50, which was higher than
 410 that of Boonman et al. (2020) and consistent with that of Moreno-Martínez et al. (2018). However,

411 LNC and LA showed relatively poor performance, which may be related to the reason that these
412 two traits were more influenced by phylogeny than environmental variables (Yang et al., 2017; An
413 et al., 2021).

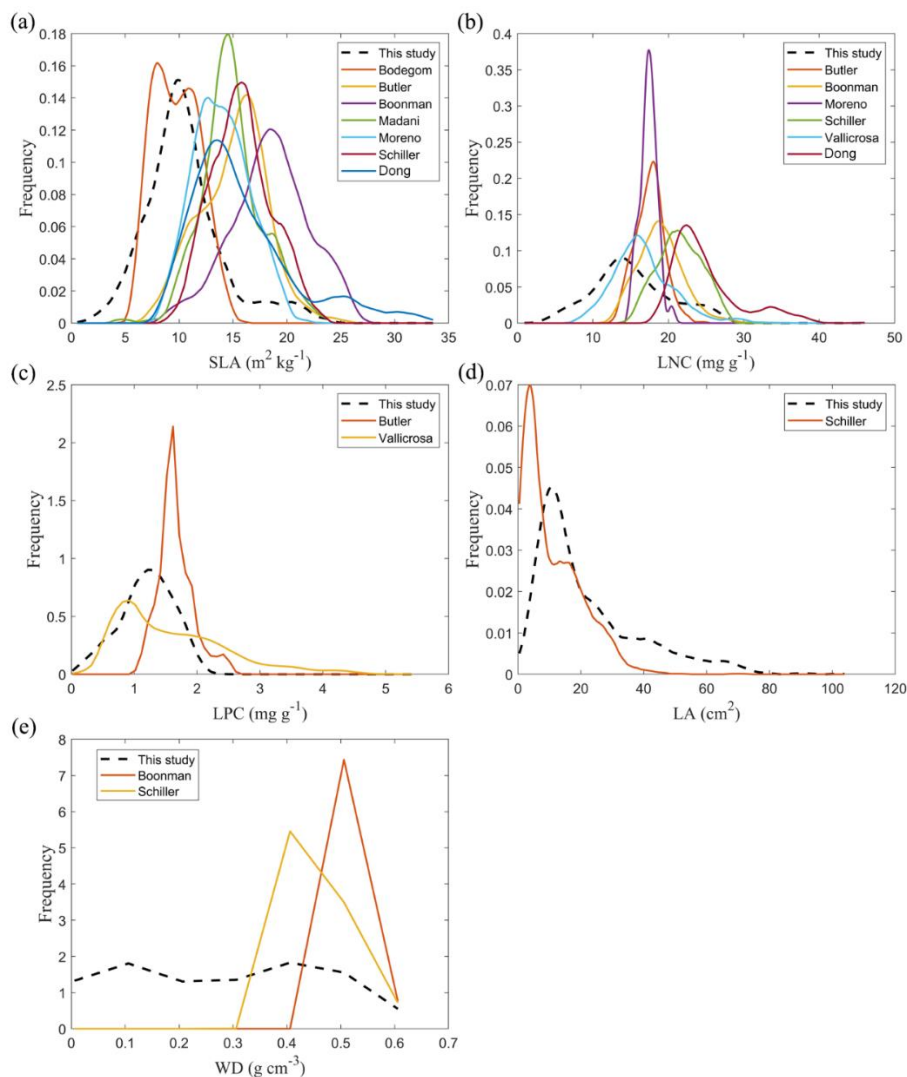
414 The frequency distribution of plant functional traits in China differed between our study and
415 previous studies (Fig. 7, Fig. F1, Table F1 in Appendix F). Given that the spatial resolution of trait
416 maps in most previous studies is 0.5° (except for Moreno-Martínez et al. (2018) and Vallicrosa et
417 al. (2022)), we resampled the data products of previous studies and our study to 0.5° spatial
418 resolution. The distribution in our study contained more predictions at lower values of SLA, LNC
419 and LPC and was broader than those for SLA and LNC in previous global studies. However, the
420 distribution of LNC in our study was consistent with that in Vallicrosa et al. (2022) at the 1 km
421 spatial resolution (Fig. F1 in Appendix F). LA in our study contained more predictions at higher
422 values and was also broader than those in previous global studies. WD did not show the lower and
423 higher predictive values in this study, however, the WD values in the studies of Boonman et al.
424 (2020) and Schiller et al. (2021) had more predictions at higher values and no lower values (< 0.3
425 g cm^{-3}). Our predicted values of SLA showed the highest spatial correlation with those of Dong et
426 al. (2023), and LNC showed the strongest spatial correlation with those of Butler et al. (2017)
427 (Table 5). LA and WD showed the best spatial correlation with those of Schiller et al. (2021), but
428 LPC showed relatively weak spatial correlation with those of published studies.

429 In addition, we compared our results to the other studies focused on China. Yang et al. (2016)
430 predicted the spatial distribution of leaf mass per area (i.e., $1/\text{SLA}$) and LNC based on trait-
431 environment relationships in China and had an R^2 of 0.13-0.16. The lower predictive precision
432 may be because Yang et al. (2016) only used MAT, MAP and RAD as predictors in estimating the
433 spatial patterns of leaf mass per area and LNC, which likely led to poor performance and low
434 heterogeneity. These results also demonstrated the advantage of our methods in mapping the
435 spatial patterns of plant functional traits at a regional scale.

436 **Table 5** Spatial correlations for SLA, LNC, LPC, LA and WD between this study and other
 437 previous trait maps, labelled by the first author of the corresponding publication (see Table F1 in
 438 Appendix F for citations)

Spatial correlation	Dong	Vallicrosa	Schiller	Boonman	Moreno	Madani	Butler	Bodegom
SLA	0.398		-0.082	0.327	0.242	0.136	-0.042	0.319
LNC	0.156	0.359	0.229	0.252			0.394	
LPC		0.136					0.057	
LA			0.514					
WD			0.647	0.107				

439 The spatial correlation of leaf dry matter content (LDMC) between our study and previous studies was
 440 not included, as the LDMC maps were not available. SLA, specific leaf area ($\text{m}^2 \text{kg}^{-1}$); LNC, leaf N
 441 concentration (mg g^{-1}); LPC, leaf P concentration (mg g^{-1}); LA, leaf area (cm^2); WD, wood density (g cm^{-3}).
 442



443 **Figure 7.** Frequency distributions of plant functional traits in our study (“This study”, dashed
 444 black lines) and other trait maps, identified by the first author of the corresponding publication
 445 (see Table F1 for citations). SLA, specific leaf area ($\text{m}^2 \text{kg}^{-1}$); LNC, leaf N concentration (mg g^{-1});
 446

447 LPC, leaf P concentration (mg g^{-1}); LA, leaf area (cm^2); WD, wood density (g cm^{-3}).

448 **4.2 Spatial patterns of plant functional traits in China**

449 Our study revealed the spatial patterns of different plant functional traits across China, and the
450 variability among the two machine learning methods was relatively low. We compared the spatial
451 differences of trait maps between our study and previous studies at the global scale (Figs. F2-F6 in
452 Appendix F). For example, our study showed high SLA values in the southeastern Qinghai-Tibet
453 Plateau, which concurred with the global study of Boonman et al. (2020). The spatial difference of
454 SLA between our study and Bodegom et al. (2014) was relatively low, and the predictive values in
455 most regions were slightly lower in our study than those in Bodegom et al. (2014). The spatial
456 pattern of difference in SLA between our study and Moreno et al. (2018), Bulter et al. (2017) and
457 Bodegom et al. (2020) was consistent, and the values were higher in northeastern China and
458 southwestern Qinghai-Tibet Plateau in our study than those studies. Our study showed higher
459 LNC values in the northern Inner Mongolia-the Loess Plateau-the eastern Qinghai-Tibet Plateau
460 and northwestern China than those studies at the global studies (Butler et al., 2017; Moreno-
461 Mart ínez et al., 2018; Boonman et al., 2020; Vallicrosa et al., 2022; Dong et al., 2023), reflecting
462 the consistent spatial pattern among these studies. However, Yang et al. (2016) predicted high
463 LNC values in northeastern and northwestern China, northern Inner Mongolia and the entire
464 Qinghai-Tibet Plateau, and SLA and LNC had low heterogeneity overall. The discrepancy with
465 Yang et al. (2016) may be attributed to spatial extrapolation based on trait-climate relationships
466 with a low predictive precision. There was no consistent spatial pattern in LPC between our study
467 and previous studies. Consistent with the global pattern (Wright et al., 2017), LA was larger in
468 southern regions than in northern regions and showed a decreasing trend with latitude. In addition,
469 LA and WD values in our study were lower in most regions than those ones at the global scale.
470 These discrepancies between our study and previous studies at the global scale may be related to
471 three reasons. First, there is bias in the available in-situ field measurement data from China in
472 these global studies, with large gaps in western China for SLA and no data in China for WD
473 (Boonman et al., 2020). Second, some trait-environment relationships may be scale-dependent
474 (Bruelheide et al., 2018), and these studies we compared are from the global scale because the trait
475 maps in China are not available. Third, the methods used for trait mapping were different among
476 studies, including eco-evolutionary optimality models (Dong et al., 2023), Convolutional Neural
477 Networks based on RGB photographs (Schiller et al., 2021), machine learning algorithms
478 (Vallicrosa et al., 2022; Boonman et al., 2020) and multiple regression analysis (Bodegom et al.,
479 2014).

480 Moreover, our study also identified the applicability domain of our models for predicting the
481 spatial patterns of plant functional traits across China. Five leaf traits and WD appeared to have
482 poor applicability in northeastern China and the Qinghai-Tibet Plateau, primarily due to sparse
483 samplings. Future studies predicting plant functional traits across a large scale through remote

484 sensing observations or other supplementary data will be needed to re-evaluate our results.

485 **4.3 The role of predictive variables**

486 Our study indicates that environmental variables are important for predicting the spatial patterns
487 of plant functional traits, especially climate variables. Temperature variables were primary
488 predictors for SLA, LDMC, LPC and WD. The relationships between leaf traits and temperature
489 have been widely discussed in global and regional studies (Reich and Oleksyn, 2004; Bruelheide
490 et al., 2018). The positive linkage between WD and temperature may be driven by changes in
491 water viscosity. Plants can adapt to the low water viscosity at high temperatures by reducing the
492 diameter and density of their vessels and by thickening cell walls (Roderick and Berry, 2002;
493 Thomas et al., 2004). Precipitation variables were important predictors for leaf nutrient traits and
494 LA. For example, precipitation of wettest quarter of a year was the factor that most influenced LA
495 variation, which has been confirmed by a previous study (An et al., 2021). A smaller LA could be
496 an adaptive strategy to decrease water loss via reducing the surface area for transpiration under
497 dry environmental conditions (Du et al., 2019). Although the effects of soil on trait predictions
498 were relatively weak, we found that SAP and pH played key roles in SLA and LNC predictions.
499 These results were similar with the previous studies that reported that soil pH was an important
500 driver of trait variation at the global scale and in tundra regions (Maire et al., 2015; Kemppinen et
501 al., 2021). Additionally, from the perspective of cost-efficient theory, the strong effects of SAP
502 reflected that high SLA may be an adaptation for facilitating soil exploration more efficiently in
503 fertile soils (Freschet et al., 2010).

504 Vegetation indices have recently been proposed as important predictors of spatial patterns of
505 plant functional traits (Loozen et al., 2018). Our results corroborated these findings and further
506 suggested that EVI, MTCI and MIR reflectance are important predictors in models. Here, the
507 underlying mechanisms between vegetation indices and plant functional traits are not further
508 discussed due to their complexity and uncertainty. However, our results indicated that vegetation
509 indices and NIR reflectance are not key predictors of LNC estimation, which contrasts the
510 findings from global and regional studies (Wang et al., 2016; Loozen et al., 2018; Moreno-
511 Mart ínez et al., 2018). This may be related to the multitude of factors that influence the
512 relationship between LNC and vegetation indices and NIR reflectance, such as forest type and
513 canopy structure (Dahlin et al., 2013).

514 **4.4 Uncertainties**

515 Although our study mapped the spatial patterns of key functional traits of seed plants in China
516 through large-scale field investigations and compared the predictions with previous studies
517 performed at global and regional scales, there persists some uncertainties in the interpretation of
518 these results. First, the predictive ability of models was relatively worse for certain traits,
519 especially LDMC. Beyond the environmental effects, the variation in plant functional traits is also

520 regulated by phylogenetic structure among plant species (e.g., family, order and phylogenetic
521 clade) (Li et al., 2017). Consequently, incorporating the phylogenetic information will be a
522 promising avenue for further improving the accuracy of spatial predictions of plant functional
523 traits (Butler et al., 2017). A second potential issue is sampling bias; there were major spatial gaps
524 in field investigation in both the northeastern China and the Qinghai-Tibet Plateau. Due to the few
525 measurements for shrubs and the lack of herbs, WD data is mainly confined to eastern forests, and
526 the overall quantity of WD data was much lower than that of leaf traits, even in the TRY database.
527 The environmental information of sampling sites was not always obtained from original literature,
528 thus using the public environmental products is a common resolution in large-scale plant trait
529 studies (Boonman et al., 2020; Vallicrosa et al., 2022). Such mismatch between in-situ trait
530 measurements and predictors should be resolved in further work. Finally, additional key
531 challenges in data availability must be resolved to scale up from the species to the community
532 levels, in particular with data surrounding species co-occurrence and their relative cover or
533 abundance in ecological communities (He et al., 2023). For example, Global biodiversity data
534 (e.g., sPlot and Global Biodiversity Information Agency databases) that contains information on
535 species occurrence or the proportion of species in a community has the potential for enabling the
536 calculation of community-weighted trait values and the re-evaluation of our results in future work
537 (Telenius, 2011; Bruelheide et al., 2019). The lack of consistent time period and spatial resolution
538 of predictors due to limitation of data availability is another key challenge in the spatial mapping
539 of plant functional traits. In addition, although WorldClim version 2.1 product has high spatial
540 resolution and includes various aspects of climatic parameters, there exists certain limitation and
541 uncertainty in predicting trait maps. Therefore, integrating satellite remote sensing monitoring
542 methods with in-situ trait data collection can also provide an effective way to estimate and assess
543 the species diversity at large scales (Cavender-Bares et al., 2022).

544 **4.5 Potential applications**

545 Maps of these key functional traits of seed plants highlighted large-scale variability in space,
546 which will significantly advance ecological analyses and future interdisciplinary research. First,
547 using the spatially continuous trait maps, one can optimize and develop trait-flexible vegetation
548 models to reduce uncertainties of conventional vegetation models based on PFTs, which allows for
549 the exploration of the community assembly rules based on how plants with different trait
550 combinations perform under a given set of environmental conditions (Berzaghi et al., 2020). When
551 trait-flexible vegetation models are available, incorporating trait maps into models will bridge the
552 gap for vegetation classifications and predictions of vegetation distribution under global change
553 (Van Bodegom et al., 2012; Yang et al., 2019). Second, most studies focused on the effects of plant
554 functional traits on ecosystem carbon processes at individual, species and community scales, while
555 how such effects scale up to regional or larger scales remains challenging. In addition, the
556 assessments of China's terrestrial ecosystem carbon sink have had large uncertainties so far (Piao

557 et al., 2022). The spatial continuous trait maps will provide an effective way to link ecosystem
558 characteristics to ecosystem carbon sink estimates in China (Madani et al., 2018; Šímová et al.,
559 2019). These analyses will help shed light on the mechanisms underlying plant functional traits
560 and terrestrial ecosystem carbon storage at a large scale.

561 **5 Data availability**

562 The original plant functional trait data collected in this study that were used for machine learning
563 models (named by Data file used for machine learning models.csv) and final maps of plant
564 functional traits in terrestrial ecosystems in a GeoTIFF format across China (named by plant
565 functional trait category) are now available for the private link
566 <https://figshare.com/s/c527c12d310cb8156ed2> (An et al., 2023). Once the article is accepted, we
567 will publicly publish these maps at the figshare website.

568 **6 Conclusions**

569 We generated a set of spatial continuous trait maps at a 1-km spatial resolution using machine
570 learning methods in combination with field measurements, environmental variables and vegetation
571 indices. Models for leaf traits (except for LDMC) and WD showed good accuracy and robustness,
572 whereas models of LDMC had relatively poor precision and robustness. Temperature variables
573 were the most important predictors for leaf traits (except for LA) and WD, and precipitation
574 variables were the most important predictors for leaf nutrient traits and LA. We caution that plant
575 functional trait predictions should be interpreted carefully for northeastern China and the Qinghai-
576 Tibet Plateau. The spatial continuous trait maps generated in our study are complementary to
577 current terrestrial in-situ observations and offer new avenues for predicting large-scale changes in
578 vegetation and ecosystem function under climate scenarios in China.

579

580 **Appendix A Data collection from literature**

- 581 An H. and Shangguan Z. P. Photosynthetic characteristics of dominant plant species at different succession stages
582 of vegetation on Loess Plateau. Chinese Journal of Applied Ecology, 2007, 18, 1175-1180.
- 583 Bai K. D., Jiang D. B., Wan C. X. Photosynthesis-nitrogen relationship in evergreen and deciduous tree species at
584 different altitudes on Mao'er Mountain, Guangxi. Acta Ecologica Sinica, 2013, 33, 4930-4938.
- 585 Bai W. J., Zheng F. L., Dong L. L., et al. Leaf traits of species in different habits in the water-wind erosion region
586 of the Loess Plateau. Acta Ecologica Sinica, 2010, 30, 2529-2540.
- 587 Chai Y F., Shang H. L., Zhang X. F., et al. Ecological variations of woody species along an altitudinal gradient in
588 the Qinling Mountains of Central China: area-based versus mass-based expression of leaf traits. Journal of
589 Forestry Research, 2021, 32, 599-608.
- 590 Chang Y. N., Zhong Q. L., Cheng D. L., et al. Stoichiometric characteristics of C, N, P and their distribution
591 pattern in plants of *Castanopsis carlesii* natural forest in Youxi. Journal of Plant Resources and Environment,
592 2013, 22, 1-10.

593 Chen F. Y., Luo T. X., Zhang L., et al. Comparison of leaf construction cost in dominant tree species of the
594 evergreen broadleaved forest in Jiulian Mountain, Jiangxi Province. *Acta Ecologica Sinica*, 2006, 26, 2485-
595 2493.

596 Chen H. Y., Huang Y. M., He K. J., et al. Temporal intraspecific trait variability drives responses of functional
597 diversity to interannual aridity variation in grasslands. *Ecology and Evolution*, 2018, 9, 5731-5742.

598 Chen L. X., Xiang W. H., Wu H. L., et al. Tree growth traits and social status affect the wood density of pioneer
599 species in secondary subtropical forest. *Ecology and Evolution*, 2017, 7, 5366-5377.

600 Chen L., Yang X. G., Song N. P., et al. Leaf water uptake strategy of plants in the arid-semiarid region of Ningxia.
601 *Journal of Zhejiang University*, 2013, 39, 565-574.

602 Chen Y. H., Han W. X., Tang L. Y., et al. Leaf nitrogen and phosphorus concentrations of woody plants differ in
603 responses to climate, soil and plant growth form. *Ecography*, 2011, 36, 178-184.

604 Cheng J. H., Chu P. F., Chen D. M., et al. Functional correlations between specific leaf area and specific root length
605 along a regional environmental gradient in Inner Mongolia grasslands. *Functional Ecology*, 2016, 30, 985-997.

606 Cheng W., Yu C. H., Xiong K. N., et al. Leaf functional traits of dominant species in karst plateau-canyon areas.
607 *Guihaia*, 2019, 39, 1039-1049.

608 Dong H. and Shekhar R. B. Negative relationship between interspecies spatial association and trait dissimilarity.
609 *Oikos*, 2019, 128, 659-667.

610 Dong T. F., Feng Y. L., Lei Y. B., et al. Comparison on leaf functional traits of main dominant woody species in
611 wet and dry habitats. *Chinese Journal of Ecology*, 2012, 31, 1043-1049.

612 Du H. D. Ecological responses of foliar anatomical structural & physiological characteristics of dominant plants at
613 different site conditions in north Shaanxi Loss Plateau. 2010, Graduation Thesis.

614 Fan Z. X., Zhang S. B., Hao G. Y., et al. Hydraulic conductivity traits predict growth rates and adult stature of 40
615 Asian tropical tree species better than wood density. *Journal of Ecology*, 2012, 100, 732-741.

616 Feng J. B., Fan S. X., Hou Y. F., et al. Interspecific and intraspecific variation of leaf function traits of herbaceous
617 plants in a forest-steppe zone, Hebei Province, China. *Journal of Northeast Forestry University*, 2021, 49, 23-
618 28.

619 Feng Q. H. The study on the response of foliar $\delta^{13}C$ of different life from plants to altitude in subalpine area of
620 Western Sichuan, China. 2011, Graduation Thesis.

621 Fu P. L., Zhu S. D., Zhang J. L., et al. The contrasting leaf functional traits between a karst forest and a nearby
622 non-karst forest in south-west China. *Functional Plant Biology*, 2019, 46, 907-915.

623 Gao S. P., Li J. X., Xu M. C., et al. Leaf N and P stoichiometry of common species in successional stages of the
624 evergreen broad-leaved forest in Tiantong National Forest Park, Zhejiang Province, China. *Acta Ecologica
625 Sinica*, 2007, 27, 947-952.

626 Geekiyanage N., Goodale, U. M., Cao, K. F., et al. Leaf trait variations associated with habitat affinity of tropical
627 karst tree species. *Ecology and Evolution*, 2017, 8, 286-295.

628 Geng Y., Ma W. H., Wang L., et al. Linking above- and belowground traits to soil and climate variables: an
629 integrated database on China's grassland species. *Ecology*, 2017, 98, 1471.

630 Guo F. C. The photosynthetic characteristics of precious broad-leaved tree species in south subtropics and their
631 relationship with leaf functional traits. 2015, Graduation Thesis.

632 Guo W. J. Exploring the relationship between arbuscular mycorrhizal fungi and plant based on phylogeny and
633 plant traits. 2015, Graduation Thesis.

634 Hau C. H. Tree seed predation on degraded hillsides in Hong Kong. *Forest Ecology & Management*. 1997, 99,
635 215-221.

636 He J. S., Wang Z. H., Wang X. P., et al. A test of the generality of leaf trait relationships on the Tibetan Plateau.

637 New Phytologist, 2006, 170, 835-848.

638 He P. C., Wright I. J., Zhu S. D., et al. Leaf mechanical strength and photosynthetic capacity vary independently
639 across 57 subtropical forest species with contrasting light requirements. *New Phytologist*, 2019, 223, 607-618.

640 He Y. T. Studies on physioecological traits of 30 plant species in the Subalpine Meadow of the Qinling Mountains.
641 2007, Graduation Thesis.

642 Hou M M. Adaptive evolution of some species from sedges (*Carex Cyperaceae*) based on phylogeny and leaf
643 functional traits to habitat in the Poyang Lake Area. 2017, Graduation Thesis.

644 Hou Y., Liu M. X., Sun H. R., et al. Response of plant leaf traits to microhabitat change in a subalpine meadow on
645 the eastern edge of Qinghai-Tibetan Plateau, China. *Chinese Journal of Applied Ecology*, 2017, 28, 71-79.

646 Hu Z. Z., Michaletz S. T., Johnson D. J., et al. Traits drive global wood decomposition rates more than climate.
647 *Global Change Biology*, 2018, 24, 5259-5269.

648 Hua L., He P., Goldstein G., et al. Linking vein properties to leaf biomechanics across 58 woody species from a
649 subtropical forest. *Plant Biology*, 2019, 22, 212-220.

650 Huang J. J. and Wang X. H. Leaf nutrient and structural characteristics of 32 evergreen broad-leaved species.
651 *Journal of East China Normal University (Natural Science)*, 2003, 1, 92-97.

652 Huang Y. L. The research about the turnover patterns and moisture adaptation mechanism of major species on the
653 South-North-facing slope. 2012, Graduation Thesis.

654 Iida Y., Kohyama T. S., Swenson N. G., et al. Linking functional traits and demographic rates in a subtropical tree
655 community: the importance of size dependency. *Journal of Ecology*, 2014, 102, 641-650.

656 Jia Q. Q. Functional traits of fine roots and their relationship with leaf traits of 50 major species in a subtropical
657 forest in Gutianshan. 2011, Graduation Thesis.

658 Jiang Y., Chen X., Ma J., et al., Interspecific and intraspecific variation in functional traits of subtropical evergreen
659 and deciduous broadleaved mixed forests in karst topography, Guilin, Southwest China. *Tropical
660 Conservation Science*, 2016, 9.

661 Jin Y., Wang C. K., Zhou Z. H., et al. Co-ordinated performance of leaf hydraulics and economics in 10 Chinese
662 temperate tree species. *Functional Plant Biology*, 2016, 43, 1082-1090.

663 Jing G. H. Responses of grassland community structure and functions to management practices on the semi-arid
664 area of Loess Plateau. 2017, Graduation Thesis.

665 Kang M. Spatial distribution pattern and its causes of woody plant functional traits in Tiantong region, Zhejiang
666 Province. 2012, Graduation Thesis.

667 Krober W., Li Y., Hardtle W., et al. Early subtropical forest growth is driven by community mean trait values and
668 functional diversity rather than the abiotic environment. *Ecology and Evolution*, 2015, 5, 3541-3556.

669 Krober W., Bohnke M., Welk E., et al. Leaf trait-environment relationships in a subtropical broadleaved forest in
670 south-east China. *PloS One*, 2012, 7, e35742.

671 Krober W., Zhang, S. R. Ehmgig, M., et al. Linking xylem hydraulic conductivity and vulnerability to the leaf
672 economics spectrum-a cross-species study. *PloS One*, 2014, e109211.

673 Li F. Comparison of functional traits in semi-humid evergreen broad-leaved in Western Hill of Kunming. 2011,
674 Graduation Thesis.

675 Li K. and Xiang W. H. Comparison of specific leaf area, SPAD value and seed mass among subtropical tree
676 species in hilly area of Central Hunan, China. *Journal of Central South University of Forestry & Technology*,
677 2011, 31, 213-218.

678 Li L., McCormack M. L., Ma C.G., et al. Leaf economics and hydraulic traits are decoupled in five species-rich
679 tropical-subtropical forests. *Ecology Letters*, 2015, 18, 899-906.

680 Li Q. Leaf functional traits and their relationships with environmental factors in Beishan Mountain of Jinhua,

681 Zhejiang Province. 2020, Graduation Thesis.

682 Li S. J., Su P. X., Zhang H. N., et al. Characteristics and relationships of foliar water and leaf functional traits of
683 desert plants. *Plant Physiology Journal*, 2013, 49, 153-160.

684 Li W. H., Xu F. W., Zheng S. X., et al. Patterns and thresholds of grazing-induced changes in community structure
685 and ecosystem functioning: species-level responses and the critical role of species traits. *Journal of Applied*
686 *Ecology*, 2017, 54, 963-975.

687 Li W. Q., Xu Q., Li J., et al. Quantification of ecotone width of returned forest land from farmland based on
688 specific leaf area. *Journal of West China Forestry Science*, 2017, 46, 117-121.

689 Li X. F., Pei K. Q., Kery M., et al. Decomposing functional trait associations in a Chinese subtropical forest. *PloS*
690 *One*, 2017, 12, e0175727.

691 Li X. F., Schmid B., Wang F., et al. Net assimilation rate determines the growth rates of 14 species of subtropical
692 forest trees. *PloS One*, 2016, 11, e0150644.

693 Li X. L., Li X. H., Jiang D. M., et al. Leaf morphological characters of 22 compositae herbaceous species in
694 Horqin sandy land. *Chinese Journal of Ecology*, 2005, 24, 1397-1401.

695 Li Y. H., Luo T. X., Lu Q., et al. Comparisons of leaf traits among 17 major plant species in Shazhuyu Sand
696 Control Experimental Station of Qinghai Province. *Acta Ecologica Sinica*, 2005, 25, 994-999.

697 Li Y. L., Meng Q. T., Zhao X. Y., et al. Relationships of fresh leaf traits and leaf litter decomposition in Kerqin
698 Sandy Land. *Acta Ecologica Sinica*, 2008, 28, 2486-2494.

699 Li Y., Yao J., Yang S., et al. Trait differences research on leaf function of Liaodong oak forest main species in
700 Dongling mountain. *Guangdong Agricultural Sciences*, 2012, 23, 159-162, 171.

701 Liang X. Y., Ye Q., Liu H., et al. Wood density predicts mortality threshold for diverse trees. *New Phytologist*,
702 2021, 229, 3053-3057.

703 Li, R., Zhu, S., Chen, H. Y. H., et al. Are functional traits a good predictor of global change impacts on tree species
704 abundance dynamics in a subtropical forest? *Ecology Letters*, 2015, 18, 1181-1189.

705 Li Y. Y., Shi H., Shao M. A. Cavitation resistance of dominant trees and shrubs in Loess hilly region and their
706 relationship with xylem structure. *Journal of Beijing Forestry University*, 2010, 32, 8-13.

707 Lin G. G., Guo, D. L., Li, L., et al. Contrasting effects of ectomycorrhizal and arbuscular mycorrhizal tropical tree
708 species on soil nitrogen cycling: the potential mechanisms and corresponding adaptive strategies. *Oikos*, 2018,
709 127, 518-530.

710 Liu C. H. and Li Y. Y. Relationship between leaf traits and PV curve parameters in the typical deciduous woody
711 plants occurring in Southern Huanglong Mountain. *Journal of Northwest Forestry University*, 2013, 28, 1-5.

712 Liu G. F., Freschet G. T., Pan X., et al. Coordinated variation in leaf and root traits across multiple spatial scales in
713 Chinese semi-arid and arid ecosystems. *New Phytologist*, 2010, 188, 543-553.

714 Liu G. F., Wang L., Jiang L., et al. Specific leaf area predicts dryland litter decomposition via two mechanisms.
715 *Journal of Ecology*, 2017, 106, 218-229.

716 Liu J. H., Zeng D. H. and Don K. L. Leaf traits and their interrelationships of main plant species in southeast
717 Horqin sandy land. *Chinese Journal of Ecology*, 2006, 25, 921-925.

718 Liu J. X., Chen J., Jiang M. X., et al. Leaf traits and persistence of relict and endangered tree species in a rare plant
719 community. *Functional Plant Biology*, 2012, 39, 512-518.

720 Liu L. H. The traits and adaptive strategies of main herbaceous plants and lianas on micro-topographical units in
721 Huangcangyu reserves of Anhui Province. 2012, Graduation Thesis.

722 Liu M. C., Kong D. L., Lu X. R., et al. Higher photosynthesis, nutrient- and energy-use efficiencies contribute to
723 invasiveness of exotic plants in a nutrient poor habitat in northeast China. *Physiologia Plantarum*, 2017, 160,
724 373-382.

725 Liu R. H., Bai J. L., Bao H., et al. Variation and correlation in functional traits of main woody plants in the
726 *Cyclobalanopsis glauca* community in the karst hills of Guilin, southwest China. Chinese Journal of Plant
727 Ecology, 2020, 44, 828-841.

728 Liu W. D., Su J. R., Li S. F., et al. Stoichiometry study of C, N and P in plant and soil at different successional
729 stages of monsoon evergreen broad-leaved forest in Pu'er, Yunnan Province. Acta Ecologica Sinica, 2010, 30,
730 6581-6590.

731 Liu X. C., Jia H. B., Wang Q. Y. Genetic variation and correlation in wood properties of *Betula platyphlla* in
732 natural Stands. Journal of Northeast Forestry University, 2018, 36, 8-10.

733 Liu Y. Y. Spatial distribution and habitat associations of trees in a typical mixed broad-leaved Korean pine (*Pinus*
734 *koraiensis*) forest. 2014, Graduation Thesis.

735 Luo Y. H., Cadotte M. W., Burgess K. S., et al. Greater than the sum of the parts: how the species composition in
736 different forest strata influence ecosystem function. Ecology Letters, 2019, 22, 1449-1461.

737 Lv J. Z., Miao Y. M., Zhang H. F., et al. Comparisons of leaf traits among different functional types of plant from
738 Huoshan Mountain in the Shanxi Province. Plant Science Journal, 2010, 28, 460-465.

739 Ma J., Wu L. F., Wei X., et al. Habitat adaptation of two dominant tree species in a subtropical monsoon forest:
740 leaf functional traits and hydraulic properties. Guihaia, 2015, 35, 261-268.

741 Mo J. M., Zhang D. Q., Huang Z. L., et al. Distribution pattern of nutrient elements in plants of Dinghushan Lower
742 Subtropical Evergreen Broad-Leaved Forest. Journal of Tropical and Subtropical Botany, 2000, 8, 198-206.

743 Niu C. Y., Meinzer F. C. and Hao G. Y. Divergence in strategies for coping with winter embolism among co-
744 occurring temperate tree species: the role of positive xylem pressure, wood type and tree stature. Functional
745 Ecology, 2017, 31, 1550-1560.

746 Niu D. C., Li Q., Jiang S. G., et al. Seasonal variations of leaf C:N:P stoichiometry of six shrubs in desert of
747 China's Alxa Plateau. Chinese Journal of Plant Ecology, 2013, 37, 317-325.

748 Niu K. C., He J. S. and Lechowicz M. J. Grazing-induced shifts in community functional composition and soil
749 nutrient availability in Tibetan alpine meadows. Journal of Applied Ecology, 2016, 53, 1554-1564.

750 Niu K. C., Zhang S. and Lechowicz M. Harsh environmental regimes increase the functional significance of
751 intraspecific variation in plant communities. Functional Ecology, 2020, 34, 1666-1677.

752 Niu S. L. Photosynthesis research on the predominant legume species in Hunshandak Sandland. 2004, Graduation
753 Thesis.

754 Qi L. X. Response of leaf traits of *Pinus mongoliensis* and *Pinus massoniana* to elevation gradient in Daiyun
755 Mountain. 2015, Graduation Thesis.

756 Ren Q. J., Li Q. J., Bu H. Y., et al. Comparison of physiological and leaf morphological traits for photosynthesis of
757 the 51 plant species in the Maqu alpine swamp meadow. Chinese Journal of Plant Ecology, 2015, 39, 593-603.

758 Ren Y. T. The study of leaf functional traits of typical plants across the Alashan Desert. 2017, Graduation Thesis.

759 Ren Y., Wei C. G. and Guo X. Y. Comparison on leaf function traits of six kinds of plant in Ordos. Journal of Inner
760 Mongolia Forestry Science & Technology, 2019, 45, 43-46, 55.

761 Rios R. S., Salgado-Luarte C. and Gianoli E. Species divergence and phylogenetic variation of ecophysiological
762 traits in lianas and trees. PloS One, 2007, 9, e99871.

763 Shang K. K. Differentiation and maintenance of relict deciduous broad-leaved forest patterns along micro-
764 topographic gradient in subtropical area, East China. 2011, Graduation Thesis.

765 Song Y T. Study on functional plant ecology in Songnen Grassland Northeast China. 2012, Graduation Thesis.

766 Song Y T., Zhou D. W., Li Q., et al. Leaf nitrogen and phosphorus stoichiometry in 80 herbaceous plant species of
767 Songnen grassland in Northeast China. Chinese Journal of Plant Ecology, 2012, 36, 222-230.

768 Tan X. Y. Research on leaf functional diversity of forest communities in rainy area of south-west China. 2014,

769 Graduation Thesis.

770 Tang Q. Q. Variation in functional traits of plants in the Subtropical Evergreen and Deciduous Broad-leaved Mixed
771 Forest. 2016, Graduation Thesis.

772 Tang Y. Inter-specific variations and relationship in leaf traits of major temperate species in northern China. 2011,
773 Graduation Thesis.

774 Tao J. P., Zuo J., He Z., et al. Traits including leaf dry matter content and leaf pH dominate over forest soil pH as
775 drivers of litter decomposition among 60 species. *Functional Ecology*, 2019, 33, 1798-1810.

776 Tian M., Yu G. R., He N. P., et al. Leaf morphological and anatomical traits from tropical to temperate coniferous
777 forests: Mechanisms and influencing factors. *Scientific Reports*, 2016, 6, 19703.

778 Wang B. Analysis of leaf functional traits of 13 species trees in northwestern Fujian Province. 2019, Graduation
779 Thesis.

780 Wang B. B. A study on ecological stoichiometry of six kinds of dominant shrubs in Huangcangyu Nature Reserve.
781 2015, Graduation Thesis.

782 Wang G. H. Leaf trait co-variation, response and effect in a chronosequence. *Journal of Vegetation Science*, 2007,
783 18, 563-570.

784 Wang G. H., Liu J. L. and Meng T. T. Leaf trait variation captures climate differences but differs with species
785 irrespective of functional group. *Journal of Plant Ecology*, 2015, 8, 61-69.

786 Wang J. Y., Wang S. Q., Li R. L., et al. C:N:P stoichiometric characteristics of four forest types' dominant tree
787 species in China. *Chinese Journal of Plant Ecology*, 2011, 35, 587-595.

788 Wang K. B. Vegetation ecological features and net primary productivity simulation in Yanggou watershed in the
789 Loess hill-gully areas of China. 2011, Graduation Thesis.

790 Wang S. S. The traits and adaptive strategies of main herbaceous plants and lianas on micro-topographical units in
791 Longjishan reserves of Anhui Province. 2016, Graduation Thesis.

792 Wei L. P. Variations in functional traits of main tree species along tree-crown in broadleaved Korean Pine Forest in
793 Jiaohe, Jilin Province. 2014, Graduation Thesis.

794 Wei L. P., Hou J. H. and Jiang S. S. Changes of leaf functional traits of two main species along tree height in
795 broad-leaved Korean pine forest. *Guangdong Agricultural Sciences*, 2014, 12, 55-58, 71.

796 Wei L. Y. and Shanguan Z. P. Relation between specific leaf areas and leaf nutrient contents of plants growing on
797 slopelands with different farming-abandoned periods in the Loess Plateau. *Acta Ecologica Sinica*, 2008, 28,
798 2526-2535.

799 Wei L. Y., Zhou J. W., Xiao H. G., et al. Variations in leaf functional traits among plant species grouped by growth
800 and leaf types in Zhenjiang, China. *Journal of Forestry Research*, 2011, 28, 241-248.

801 Wu D. H., Pietsch K. A., Staab M., et al. Wood species identity alters dominant factors driving fine wood
802 decomposition along a subtropical plantation forests tree diversity gradient in subtropical plantation forests.
803 *Biotropica*, 2021, 53, 643-657.

804 Wu T. G., Chen B. F., Xiao Y. H., et al. Leaf stoichiometry of trees in three forest types in Pearl River Delta, South
805 China. *Chinese Journal of Plant Ecology*, 2009, 34, 58-63.

806 Xie Y. J. The characteristics of 20 dominant plant functional traits in evergreen broad-leaf forest in Daming
807 Mountain Nature Reserve, Guangxi. 2013, Graduation Thesis.

808 Xu M. F., Ke X. H., Zhang Y., et al. Wood densities of six hardwood tree species in Eastern Guangdong and
809 influencing factors. *Journal of South China Agricultural University*, 2016, 37, 100-106.

810 Xu M. S., Zhao Y. T., Yang X. D., et al. Geostatistical analysis of spatial variations in leaf traits of woody plants in
811 Tiantong, Zhejiang Province. *Chinese Journal of Plant Ecology*, 2016, 40, 48-59.

812 Xu Y. Z. Biomass estimate and storage mechanisms in northern subtropical forest ecosystems, central China. 2016,

813 Graduation Thesis.

814 Xun Y. H., Di X. Y. and Jin G. Z. Vertical variation and economic strategy of leaf trait of major tree species in a
815 typical mixed broadleaved-Korean pine forest. *Chinese Journal of Plant Ecology*, 2020, 44, 730-741.

816 Yan E. R., Wang X. H., Guo M., et al. C:N:P stoichiometry across evergreen broad-leaved forests, evergreen
817 coniferous forests and deciduous broad-leaved forests in the Tiantong region, Zhejiang Province, eastern
818 China. *Chinese Journal of Plant Ecology*, 2010, 34, 48-57.

819 Yang S. The adaptive strategies of main herbaceous plants traits to different micro-topographical units in
820 Dashushan Mountain, Hefei. 2017, Graduation Thesis.

821 Yang Y., Xu X., Xu M., et al. Adaptation strategies of three dominant plants in the trough-valley karst region of
822 northern Guizhou Province, Southwestern China, evidence from associated plant functional traits and
823 ecostochiometry. *Earth and Environment*, 2020, 48, 413-423.

824 Yang Z., Fan S. X., Zhou B. C., et al. Leaf function and soil nutrient differences of dominant tree species on
825 different slope aspects at the south foothills of Taihang Mountains. *Journal of Henan Agricultural University*,
826 2020, 54, 408-414.

827 Yin Q. L., Wang L., Lei, M. L., et al. The relationships between leaf economics and hydraulic traits of woody
828 plants depend on water availability. *Science of the Total Environment*, 2018, 621, 245-252.

829 Yu Y. H., Zhong X. P. and Chen W. Analysis of relationship among leaf functional traits and economics spectrum
830 of dominant species in northwestern Guizhou Province. *Journal of Forest and Environment*, 2018, 38, 196-
831 201.

832 Yuan S. Preliminary research on plant functional traits and the capability of carbon sequestration of major tree
833 species in Changbai Mountain Area. 2011, Graduation Thesis.

834 Zhang H., Chen H. Y. H., Lian J. Y., et al. Using functional trait diversity patterns to disentangle the scale-
835 dependent ecological processes in a subtropical forest. *Functional Ecology*, 2018, 32, 1379-1389.

836 Zhang J. G., Fu S. L., Wen Z. D., et al. Relationship of key leaf traits of 16 woody plant species in Low
837 Subtropical China. *Journal of Tropical and Subtropical Botany*, 2009, 17, 395-400.

838 Zhang J. L., Poorter L., Cao K. F. Productive leaf functional traits of Chinese savanna species. *Plant Ecology*, 2012,
839 213, 1449-1460.

840 Zhang J. Y. Comparative study on the different plant functional groups leaf traits at the Maoershan Region. 2008,
841 Graduation Thesis.

842 Zhang Q. W., Zhu S. D., Jansen S., et al. Topography strongly affects drought stress and xylem embolism
843 resistance in woody plants from a karst forest in Southwest China. *Functional Ecology*, 2020, 35, 566-577.

844 Zhang S. B. and Cao K. F. Stem hydraulics mediates leaf water status, carbon gain, nutrient use efficiencies and
845 plant growth rates across dipterocarp species. *Functional Ecology*, 2009, 23, 658-667.

846 Zhang S. B., Cao K. F., Fan Z. X., et al. Potential hydraulic efficiency in angiosperm trees increases with growth-
847 site temperature but has no trade-off with mechanical strength. *Global Ecology and Biogeography*, 2013, 22,
848 971-981.

849 Zhang Y., Ren Y. X., Yao J., et al. Leaf nitrogen and phosphorous stoichiometry of trees in *Pinus tabulaeformis*
850 Carr stands, North China. *Journal of Anhui Agricultural University*, 2012, 39, 247-251.

851 Zhao Y. T., Ali, A. and Yan, E. R. The plant economics spectrum is structured by leaf habits and growth forms
852 across subtropical species. *Tree Physiology*, 2016, 37, 173-185.

853 Zheng X. J., Li S. and Li Y. Leaf water uptake strategy of desert plants in the Junggar Basin, China. *Chinese*
854 *Journal of Plant Ecology*, 2011, 35, 893-905.

855 Zheng Y. M. Carbon, nitrogen and phosphorus stoichiometry of plant and soil in the sandy hills of Poyang Lake.
856 2014, Graduation Thesis.

- 857 Zheng Z. X. Comparison of plant leaf, height and seed functional traits in dry-hot valleys. 2010, Graduation Thesis.
- 858 Zhou J. Y., He J. J., Guo Z. Y., et al. A study on specific leaf area and leaf dry matter content of five dominant
859 species in Xiangshan Mountain, Huaibei City, Anhui Province. *Journal of Huaibei Normal University*
860 (Natural Sciences), 2013, 34, 51-54.
- 861 Zhou X., Zuo X. A., Zhao X. Y., et al. Plant functional traits and interrelationship of 34 plant species in south
862 central Horqin Sandy Land, China. *Journal of Desert Research*, 2015, 35, 1489-1495.
- 863 Zhu B. R., Xu B. and Zhang D. Y. Extent and sources of variation in plant functional traits in grassland. *Journal of*
864 *Beijing Normal University (Natural Science)*, 2011, 47, 485-489.
- 865 Zhu S. D., Song J. J., Li R. H., et al. Plant hydraulics and photosynthesis of 34 woody species from different
866 successional stages of subtropical forests. *Plant Cell and Environment*, 2013, 36, 879-891.
- 867 Zhu X B, Liu Y. M. and Sun S. C. Leaf expansion of the dominant woody species of three deciduous oak forests in
868 Nanjing, East China. *Chinese Journal of Plant Ecology*, 2005, 29, 125-136.

869 **Appendix B**

870 **Table B1** Summary of statistics in plant functional traits, environmental variables and geographical
 871 distribution in China.

Trait	Unit	Range	Mean	CV (%)	No. of species	Entries	Sites
SLA	m ² kg ⁻¹	0.06–81.68	17.88	54.96	2463	9195	1032
LDMC	g g ⁻¹	0.06–0.95	0.34	100.00	1582	3957	193
LNC	mg g ⁻¹	3.41–66.02	21.52	37.44	2335	7407	567
LPC	mg g ⁻¹	0.09–9.70	1.83	62.19	2074	6266	515
LA	cm ²	0.0033–2553.33	36.16	259.64	1838	5976	691
WD	g cm ⁻³	0.25–1.37	0.68	33.16	768	1788	639
Altitude	m	-144–5454					1430
MAT	°C	-12.07–24.32					1430
MAP	mm	15–2982					1430
Soil total N	g kg ⁻¹	0.11–10.25					1430
Bulk density	g cm ⁻³	0.83–1.45					1430

872 SLA, specific leaf area; LDMC, leaf dry matter content; LNC, leaf N concentration; LPC, leaf P concentration; LA,
 873 leaf area; WD, wood density; MAT, mean annual temperature; MAP, mean annual precipitation.

874 **Table B2** List of all the predictors including environment and remote sensing variables used in this
 875 study.

Type of variables	Variable name	Abbreviations	Units	Time periods	Spatial resolution	Source
Climate	Mean annual temperature	MAT	°C	1970-2000	1 km	WorldClim version 2.1
	Mean diurnal range	MDR	°C	1970-2000	1 km	WorldClim version 2.1
	Temperature seasonality	TS	°C	1970-2000	1 km	WorldClim version 2.1
	Max temperature of warmest month	Tmin	°C	1970-2000	1 km	WorldClim version 2.1
	Min temperature of coldest month	Tmax	°C	1970-2000	1 km	WorldClim version 2.1
	Temperature annual range	TAR	°C	1970-2000	1 km	WorldClim version 2.1
	Isothermality	IS	%	1970-2000	1 km	WorldClim version 2.1
	Mean temperature of wettest quarter	MTEQ	°C	1970-2000	1 km	WorldClim version 2.1
	Mean temperature of driest quarter	MTDQ	°C	1970-2000	1 km	WorldClim version 2.1
	Mean temperature of warmest quarter	MTWQ	°C	1970-2000	1 km	WorldClim version 2.1
	Mean temperature of coldest quarter	MTCQ	°C	1970-2000	1 km	WorldClim version 2.1
	Mean annual precipitation	MAP	mm	1970-2000	1 km	WorldClim version 2.1
	Precipitation of wettest month	PEM	mm	1970-2000	1 km	WorldClim version 2.1
	Precipitation of driest month	PDM	mm	1970-2000	1 km	WorldClim version 2.1
	Precipitation seasonality	PS	%	1970-2000	1 km	WorldClim version 2.1
	Precipitation of wettest quarter	PEQ	mm	1970-2000	1 km	WorldClim version 2.1
	Precipitation of driest quarter	PDQ	mm	1970-2000	1 km	WorldClim version 2.1
	Precipitation of warmest quarter	PWQ	mm	1970-2000	1 km	WorldClim version 2.1
	Precipitation of coldest quarter	PCQ	mm	1970-2000	1 km	WorldClim version 2.1
	Aridity index	AI	/	1970-2000	1 km	Global CGIAR-CSI
	Solar radiation	RAD	$\text{kJ m}^{-2} \text{day}^{-1}$	1970-2000	1 km	WorldClim version 2.1
Topography	Elevation	/	m		1 km	SRTM 90m V4.1
Soil	Soil sand content	SAND	%	/	1 km	Shangguan et al. (2013)
	Soil silt content	SILT	%	/	1 km	Shangguan et al. (2013)
	Soil clay content	CLAY	%	/	1 km	Shangguan et al. (2013)
	Bulk density	BD	g cm^{-3}	/	1 km	Shangguan et al. (2013)
	Soil pH	pH	/	/	1 km	Shangguan et al. (2013)
	Soil organic matter	SOC	g kg^{-1}	/	1 km	Shangguan et al. (2013)
	Soil total N	STN	g kg^{-1}	/	1 km	Shangguan et al. (2013)
	Soil total P	STP	g kg^{-1}	/	1 km	Shangguan et al. (2013)
	Soil alkali-hydrolysable N	SAN	mg kg^{-1}	/	1 km	Shangguan et al. (2013)
	Soil available P	SAP	mg kg^{-1}	/	1 km	Shangguan et al. (2013)
	Soil available K	SAK	mg kg^{-1}	/	1 km	Shangguan et al. (2013)
	Cation exchange capacity	CEC	me kg^{-1}	/	1 km	Shangguan et al. (2013)

Continued

Type of variables	Variable name	Abbreviations	Units	Time periods	Spatial resolution	Source
EVI	MODIS EVI long-term monthly averages		/	2001-2018	1 km	MOD13A3 V006
NIR	MODIS NIR long-term monthly averages		/	2001-2018	1 km	MOD13A3 V006
MIR	MODIS MIR long-term monthly averages		/	2001-2018	1 km	MOD13A3 V006
Red	MODIS red long-term monthly averages		/	2001-2018	1 km	MOD13A3 V006
Blue	MODIS blue long-term monthly averages		/	2001-2018	1 km	MOD13A3 V006
MTCI	MTCI long-term monthly averages		/	2003-2011	4.63 km	MTCI level 3 product
Land cover	Land cover map		/	2015	100 m	Copernicus Global Land Service Collection 3

876 The remote sensing variables are calculated as long-term monthly averages from 2001 to 2018. Thus 12 variables
 877 of each remote sensing category are obtained.

878

879

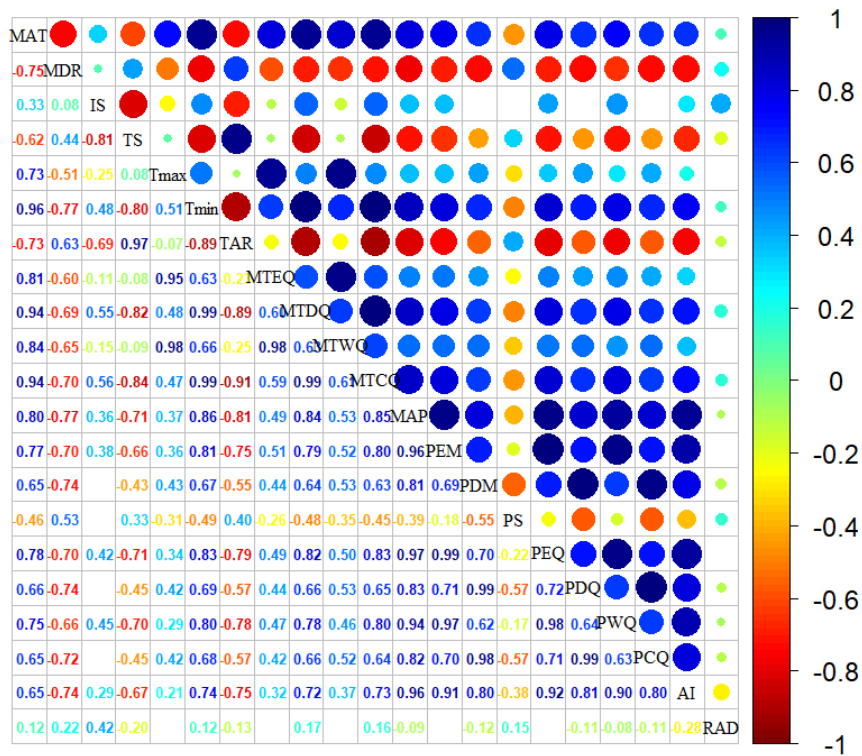
880

881

882 **Table B3** The number of samples of eight plant functional trait used for model training (80%) and
 883 validation (20%).

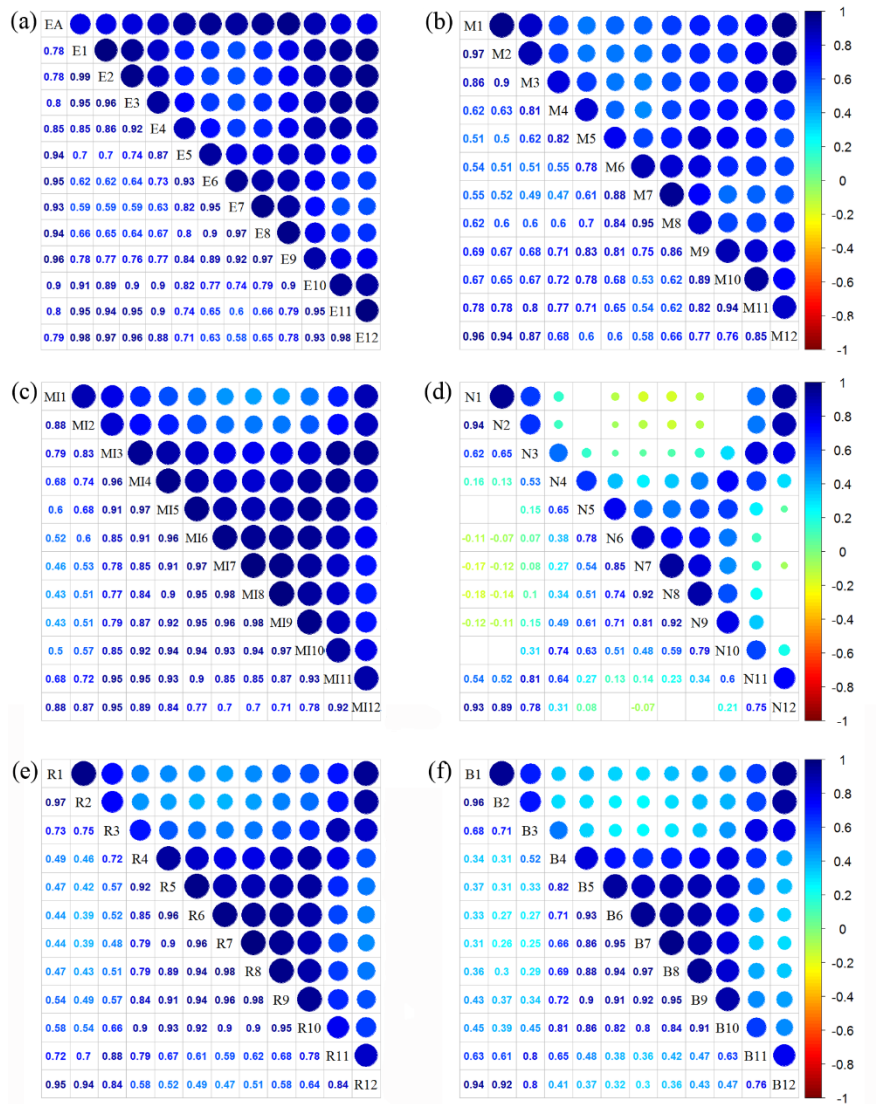
Traits	No. of samples	No. of samples used for model training	No. of samples used for model validation
SLA	9195	7356	1839
LDMC	3957	3166	791
LNC	7407	5926	1481
LPC	6266	5013	1253
LA	5976	4781	1195
WD	1787	1430	357

884 SLA, specific leaf area ($\text{m}^2 \text{kg}^{-1}$); LDMC, leaf dry matter content (g g^{-1}); LNC, leaf N concentration
 885 (mg g^{-1}); LPC, leaf P concentration (mg g^{-1}); LA, leaf area (cm^2); WD, wood density (g cm^{-3}).



886

887 **Figure B1.** Correlations among climate variables. The blank indicates that the correlations are not
 888 significant ($P > 0.05$). The size of the circles is proportional to the correlation coefficient. The
 889 abbreviation of climate variables is seen in Table B2.



894

895 **Figure B3.** Correlations among monthly remote sensing variables. The blank indicates that the
 896 correlations are not significant ($P > 0.05$). The size of the circles is proportional to the correlation
 897 coefficient. (a) enhanced vegetation index (EVI); (b) MERIS terrestrial chlorophyll index (MTCI);
 898 (c) MIR reflectance; (d) NIR reflectance; (e) red reflectance; (f) blue reflectance.

899 **Appendix C**

900 **Table C1** Optimal parameter combination and model performance of random forest for plant functional
 901 traits

Traits	n.tree	mtry	R ²	NRMSE	MAE
SLA	1000	24	0.476	0.22	5.134
LDMC	1000	11	0.234	0.20	0.072
LNC	1000	57	0.392	0.00	0.098
LPC	1000	20	0.587	0.05	0.129
LA	1000	18	0.278	0.48	26.622
WD	1000	9	0.531	0.02	0.072

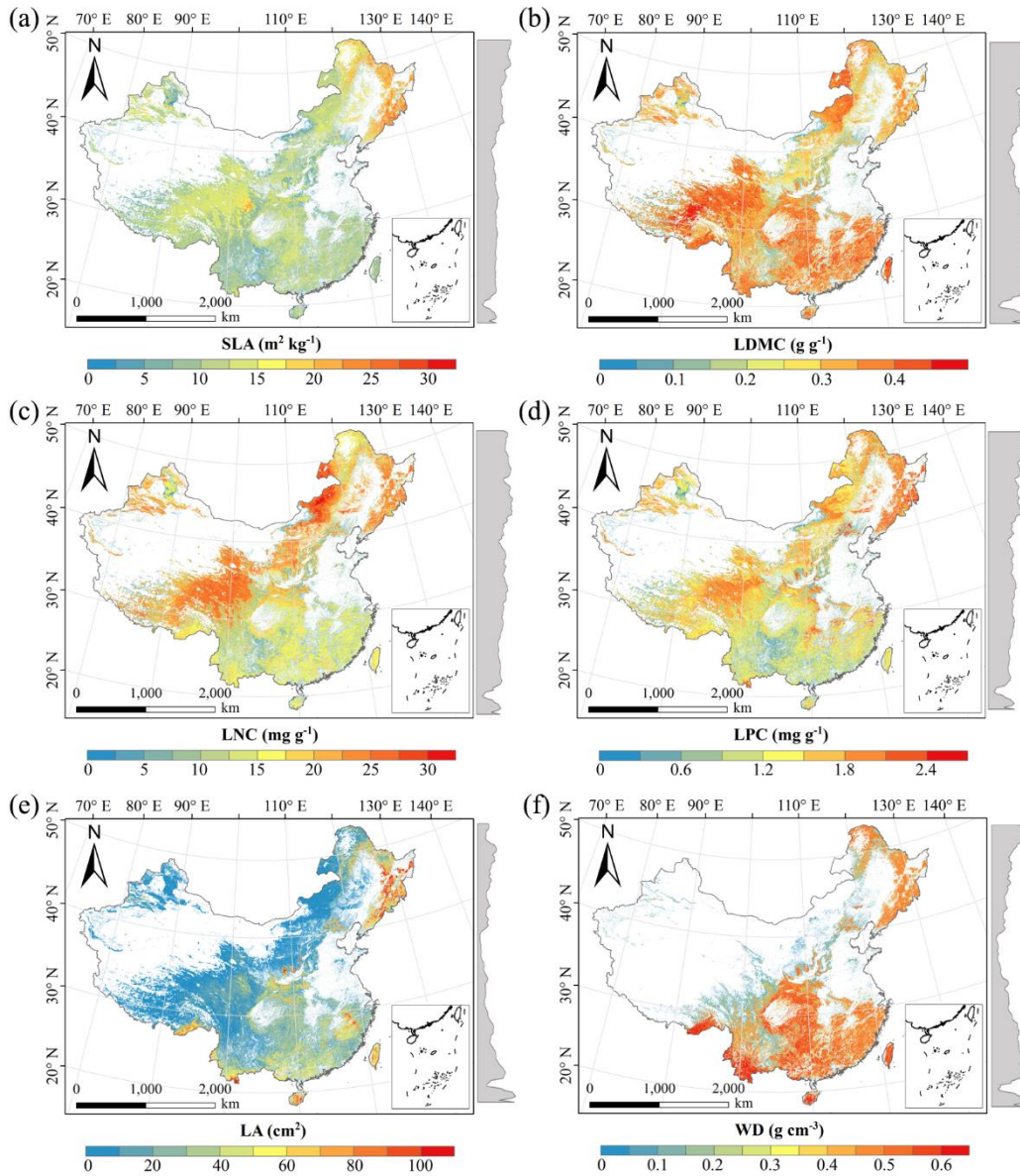
902 SLA, specific leaf area; LDMC, leaf dry matter content; LNC, leaf N concentration; LPC, leaf P
 903 concentration; LA, leaf area; WD, wood density.

904

905 **Table C2** Optimal parameter combination and model performance of boosted regression trees for plant
 906 functional traits

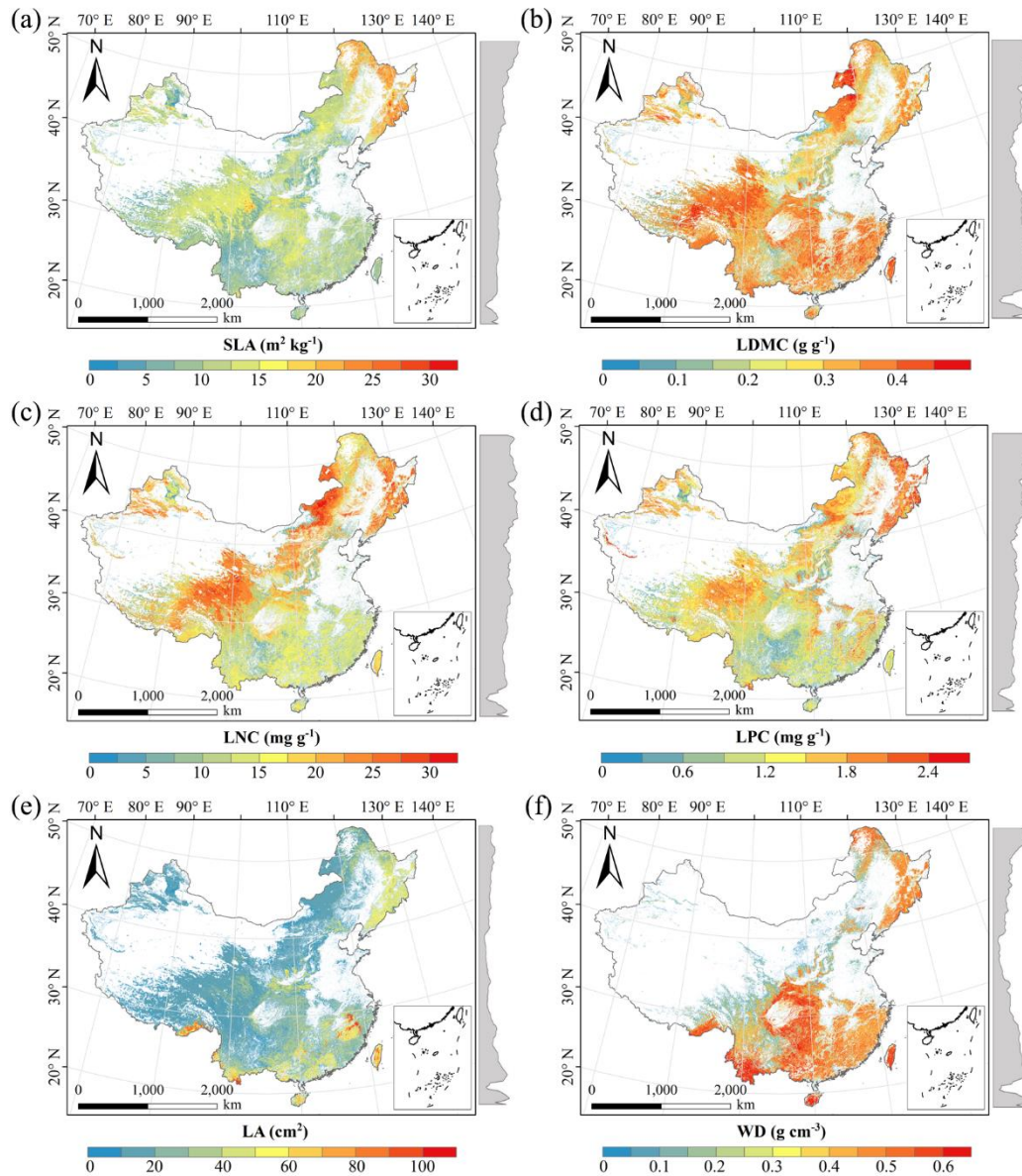
Traits	n.tree	interaction. depth	shrinkage	learning rate	bag fractions	R ²	NRMSE	MAE
SLA	3000	6	0.01	10	0.75	0.486	0.20	5.082
LDMC	3000	2	0.01	10	0.75	0.247	0.19	0.071
LNC	3000	6	0.01	10	0.70	0.414	0.00	0.096
LPC	3000	7	0.01	10	0.75	0.591	0.05	0.129
LA	3000	3	0.001	10	0.75	0.282	0.55	27.556
WD	3000	4	0.01	10	0.70	0.627	0.01	0.066

907 SLA, specific leaf area; LDMC, leaf dry matter content; LNC, leaf N concentration; LPC, leaf P
 908 concentration; LA, leaf area; WD, wood density.



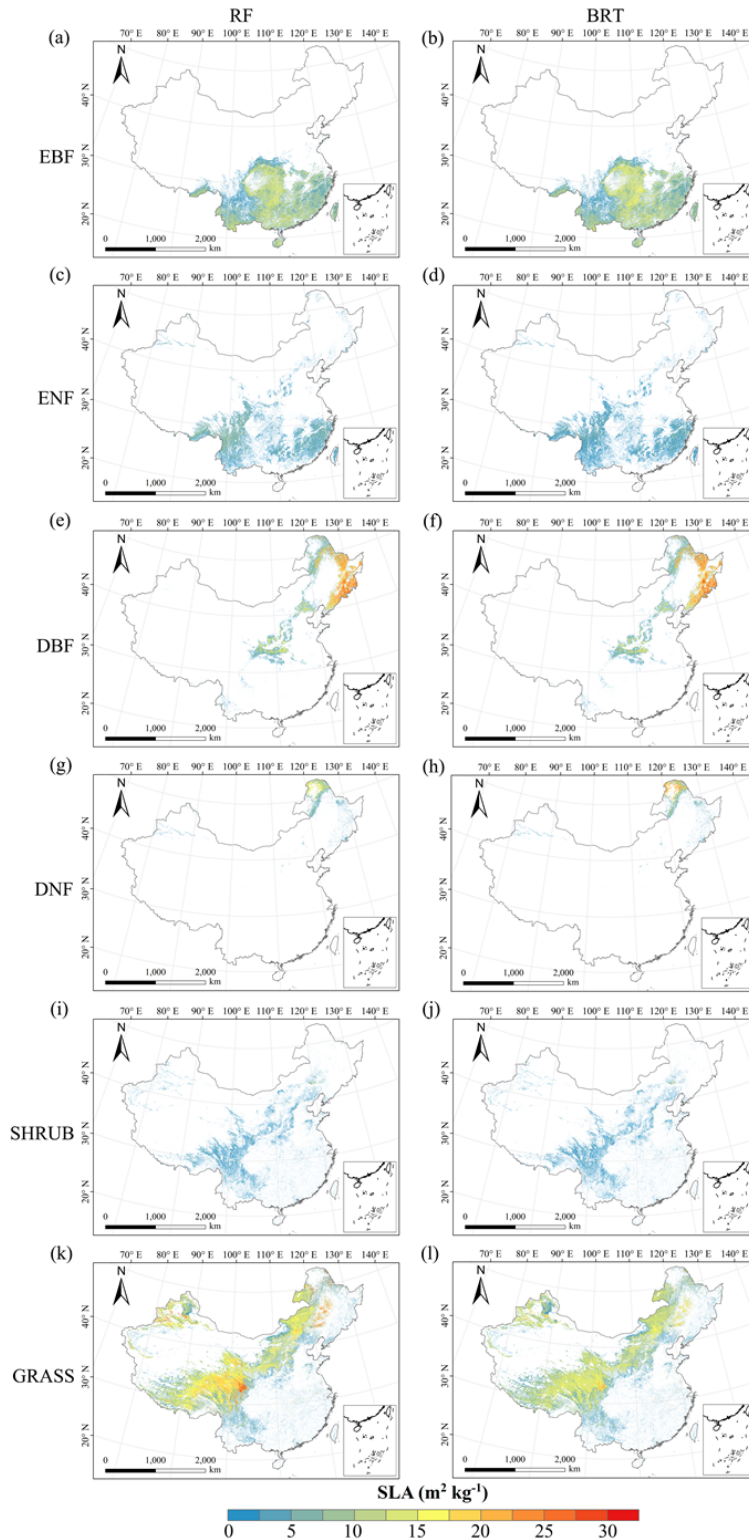
910

911 **Figure D1.** Spatial distribution of plant functional traits based on random forest. The grey curves
 912 on the right of maps were trait distribution along with latitude. The white areas represent artificial
 913 land cover types. SLA, specific leaf area; LDMC, leaf dry matter content; LNC, leaf N
 914 concentration; LPC, leaf P concentration; LA, leaf area; WD, wood density.



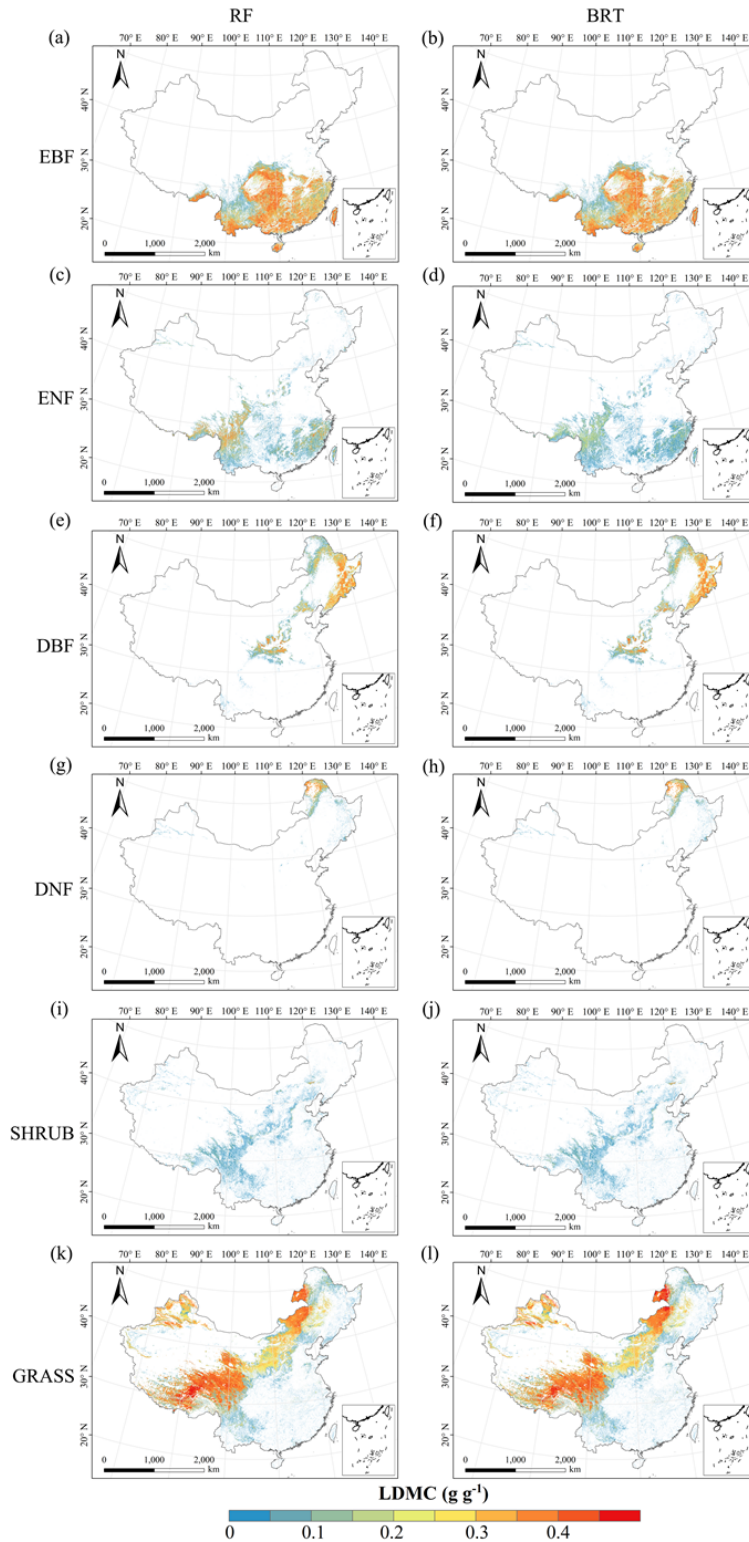
915

916 **Figure D2.** Spatial distribution of plant functional traits based on boosted regression trees. The
 917 grey curves on the right of maps were trait distribution along with latitude. The white areas
 918 represent artificial land cover types. SLA, specific leaf area; LDMC, leaf dry matter content; LNC,
 919 leaf N concentration; LPC, leaf P concentration; LA, leaf area; WD, wood density.



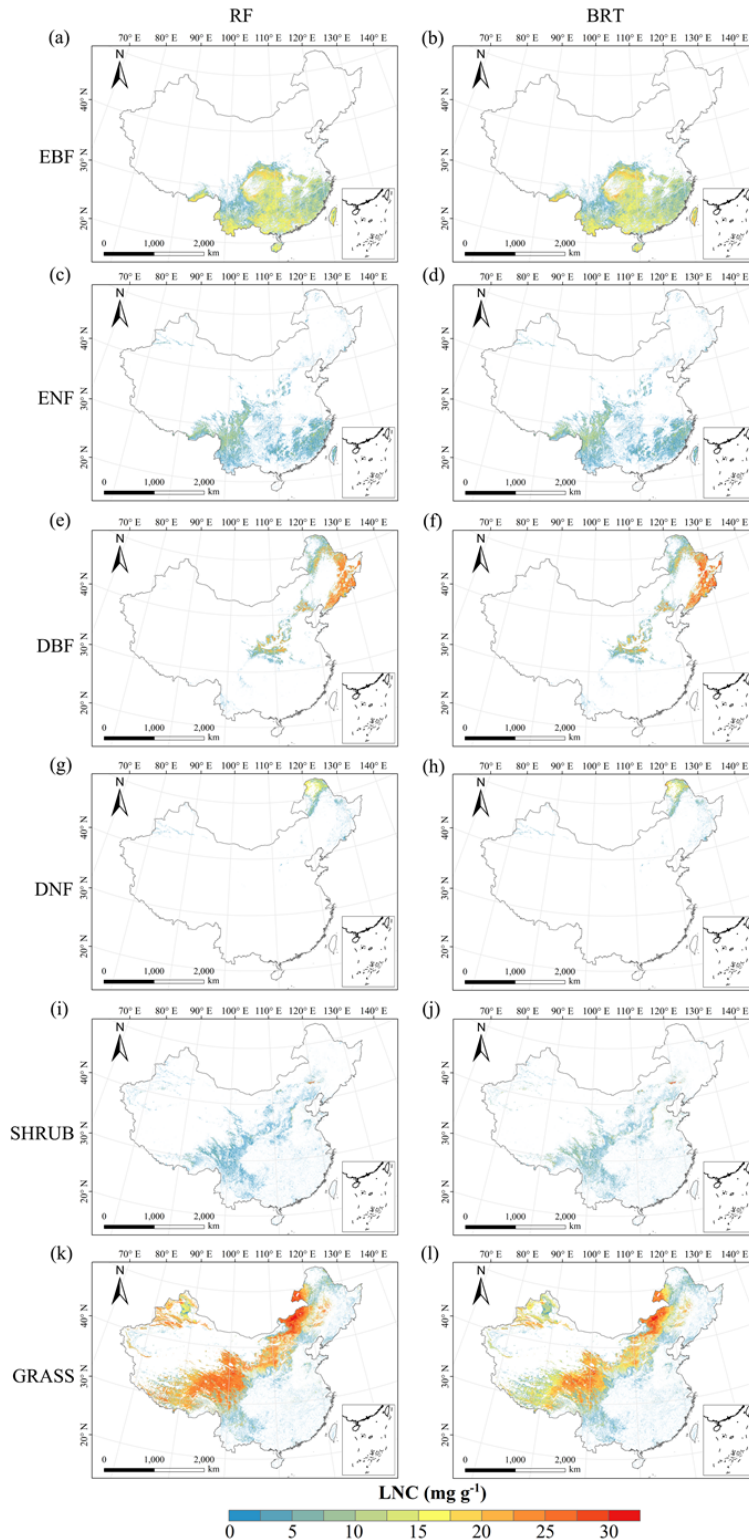
920

921 **Figure D3.** Spatial distribution of specific leaf area for each plant functional type. The left penal
 922 was obtained from RF method (random forest), the right penal was obtained from BRT method
 923 (boosted regression trees). The white areas represent other natural vegetation types and artificial
 924 land cover types. EBF, evergreen broadleaf forest; ENF, evergreen needleleaf forest; DBF,
 925 deciduous broadleaf forest; DNF, deciduous needleleaf forest; SHRUB, shrubland; GRASS,
 926 grassland.



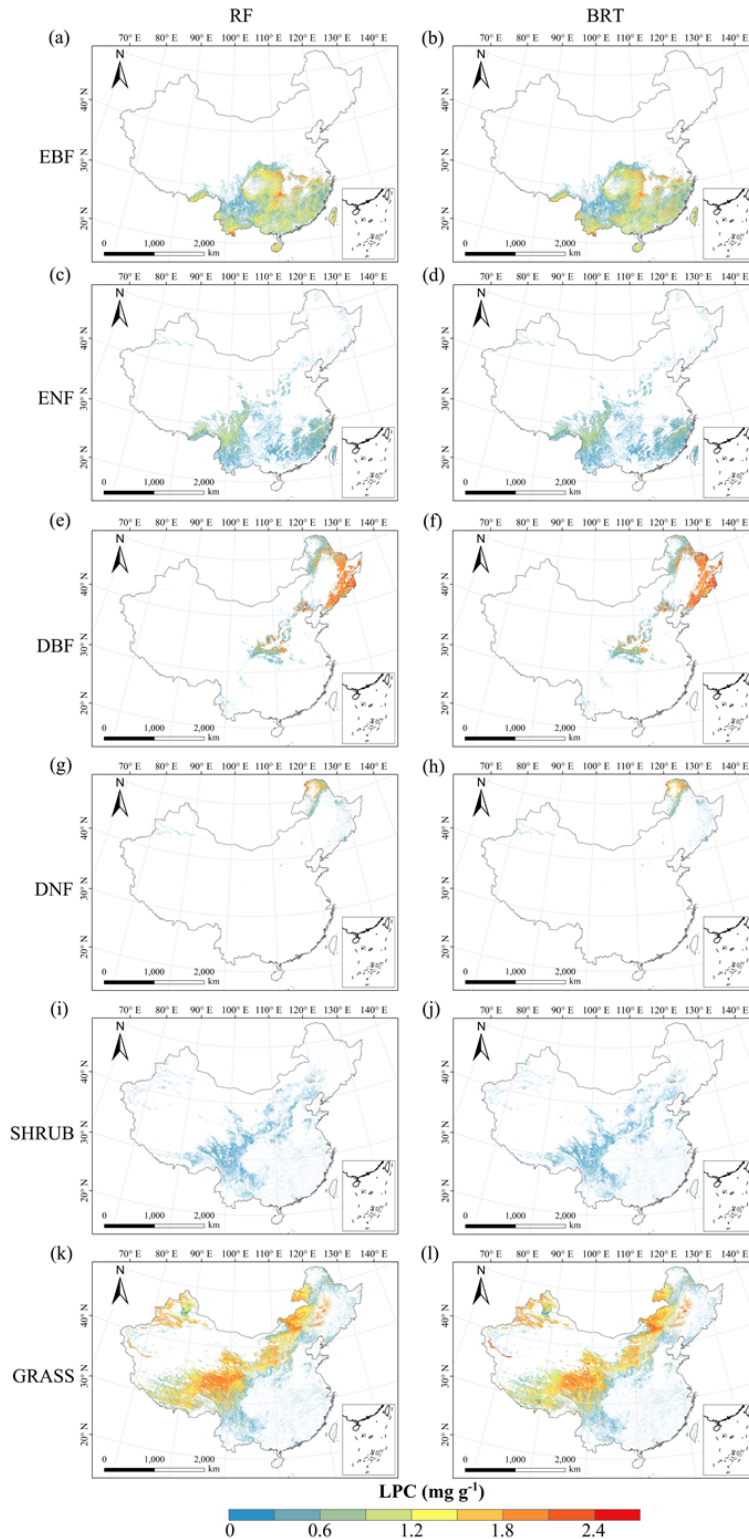
927

928 **Figure D4.** Spatial distribution of leaf dry matter content for each plant functional type. The left
 929 penal was obtained from RF method (random forest), the right penal was obtained from BRT
 930 method (boosted regression trees). The white areas represent other natural vegetation types and
 931 artificial land cover types. EBF, evergreen broadleaf forest; ENF, evergreen needleleaf forest; DBF,
 932 deciduous broadleaf forest; DNF, deciduous needleleaf forest; SHRUB, shrubland; GRASS,
 933 grassland.



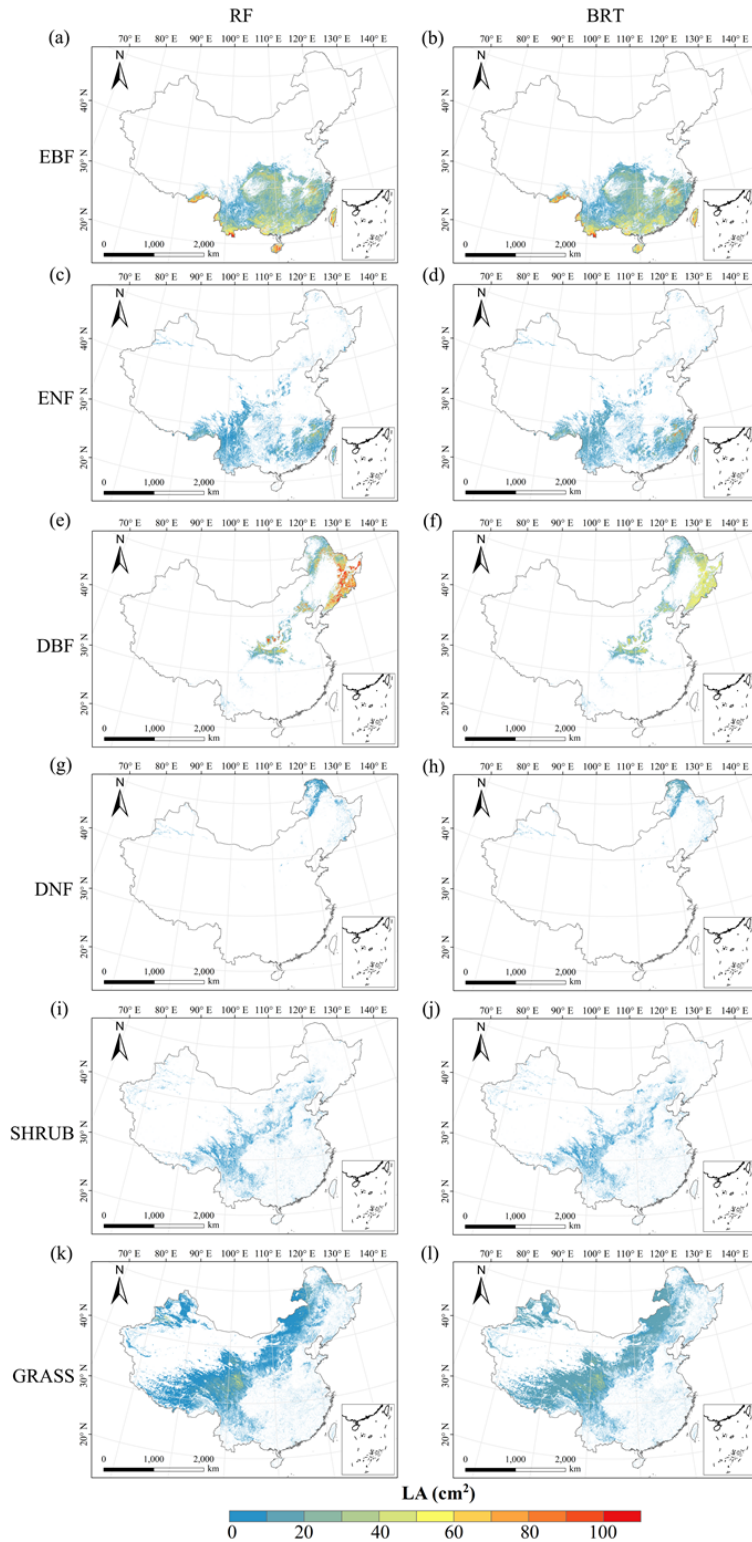
934

935 **Figure D5.** Spatial distribution of leaf N concentration for each plant functional type. The left
 936 penal was obtained from RF method (random forest), the right penal was obtained from BRT
 937 method (boosted regression trees). The white areas represent other natural vegetation types and
 938 artificial land cover types. EBF, evergreen broadleaf forest; ENF, evergreen needleleaf forest; DBF,
 939 deciduous broadleaf forest; DNF, deciduous needleleaf forest; SHRUB, shrubland; GRASS,
 940 grassland.



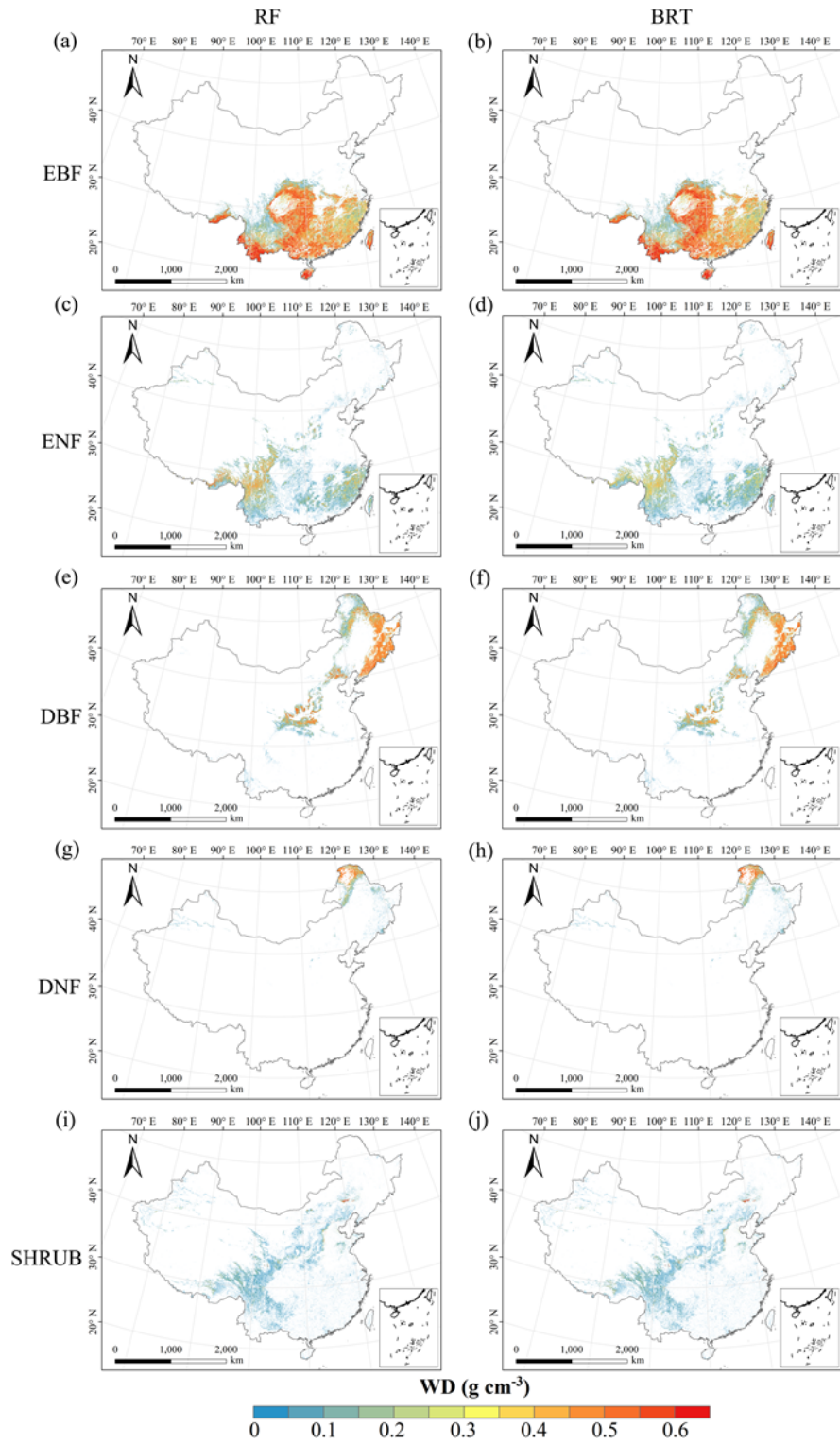
941

942 **Figure D6.** Spatial distribution of leaf P concentration for each plant functional type. The left
 943 penal was obtained from RF method (random forest), the right penal was obtained from BRT
 944 method (boosted regression trees). The white areas represent other natural vegetation types and
 945 artificial land cover types. EBF, evergreen broadleaf forest; ENF, evergreen needleleaf forest; DBF,
 946 deciduous broadleaf forest; DNF, deciduous needleleaf forest; SHRUB, shrubland; GRASS,
 947 grassland.



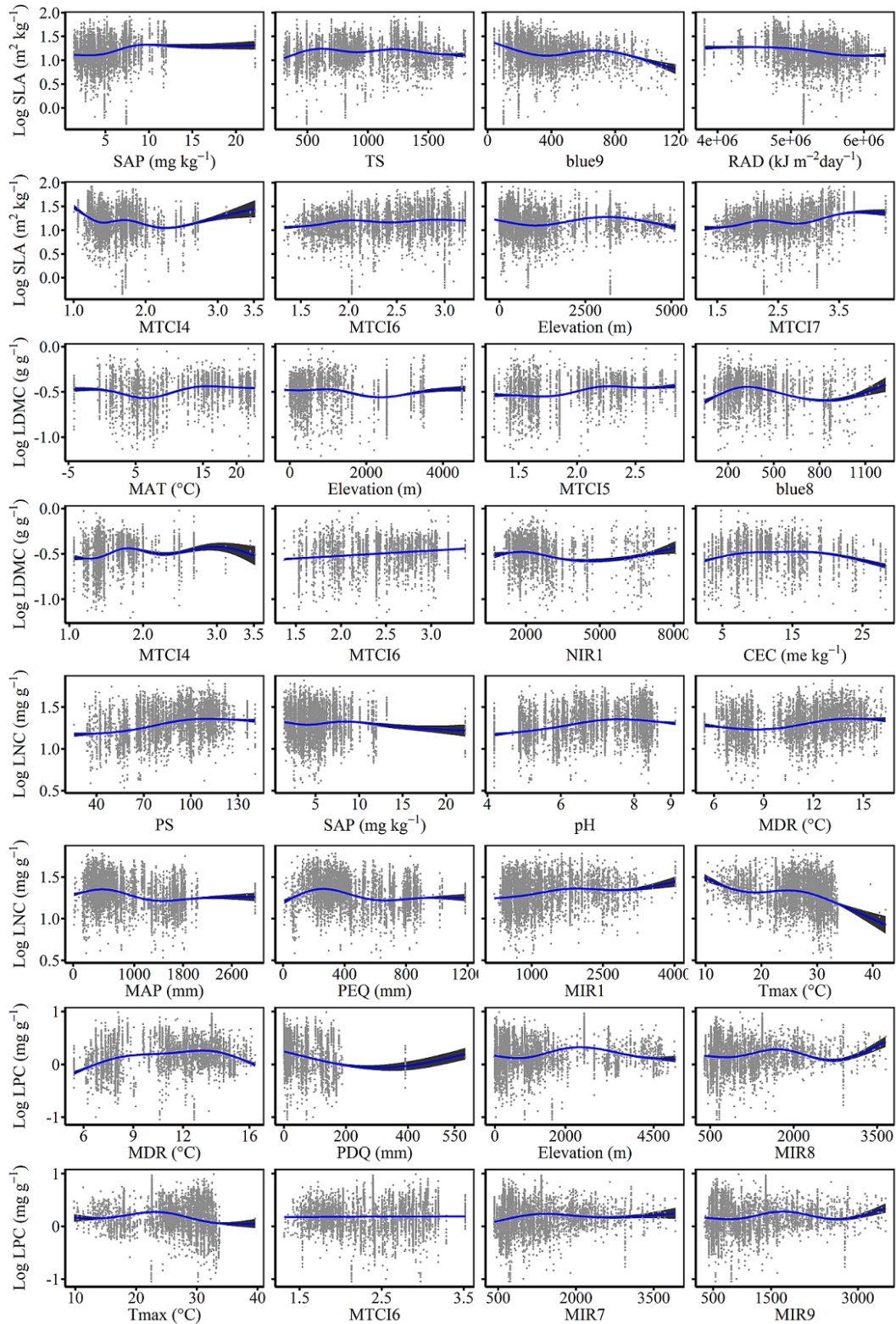
948

949 **Figure D7.** Spatial distribution of leaf area for each plant functional type. The left panel was
 950 obtained from RF method (random forest), the right panel was obtained from BRT method
 951 (boosted regression trees). The white areas represent other natural vegetation types and artificial
 952 land cover types. EBF, evergreen broadleaf forest; ENF, evergreen needleleaf forest; DBF,
 953 deciduous broadleaf forest; DNF, deciduous needleleaf forest; SHRUB, shrubland; GRASS,
 954 grassland.

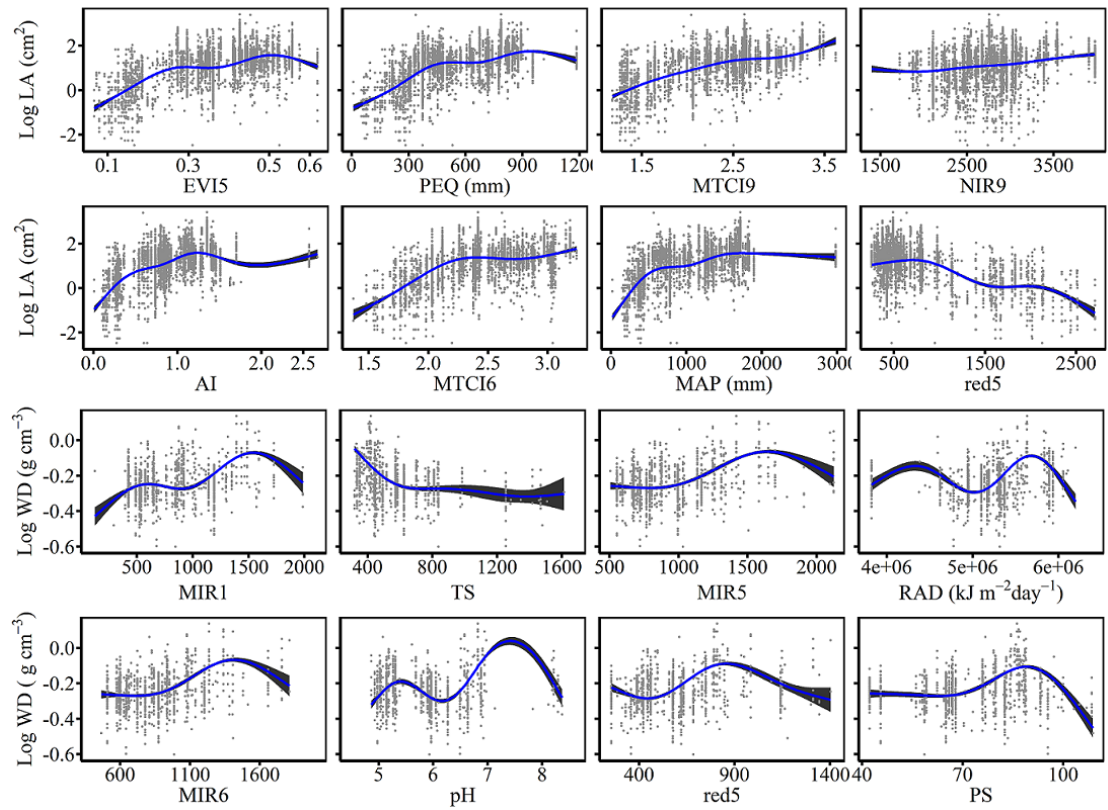


955

956 **Figure D8.** Spatial distribution of wood density for each plant functional type. The left panel was
 957 obtained from RF method (random forest), the right panel was obtained from BRT method
 958 (boosted regression trees). The white areas represent other natural vegetation types and artificial
 959 land cover types. EBF, evergreen broadleaf forest; ENF, evergreen needleleaf forest; DBF,
 960 deciduous broadleaf forest; DNF, deciduous needleleaf forest; SHRUB, shrubland.



962
 963 **Figure E1.** The relationships between SLA (specific leaf area), LDMC (leaf dry matter content),
 964 LNC (leaf N concentration), LPC (leaf P concentration) and their eight most important predictors.



965
 966
 967

Figure E2. The relationships between LA (leaf area), WD (wood density) and their eight most important predictors.

968 **Appendix F Comparisons between our study with trait maps from previous**
 969 **studies**

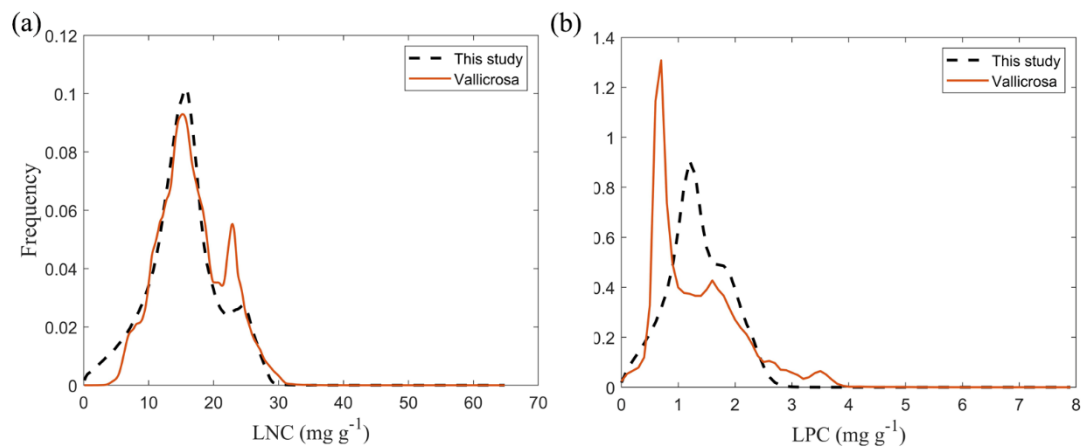
970 Given that the trait maps predicted for China were not available from the literature and
 971 authors, we compared our study with those studies performed at the global scale (see Table F1).
 972 Thus, we extracted the data in China from global trait maps. Before the quantitative comparisons
 973 with previous studies, we performed two steps to make the data products as comparable as
 974 possible and improve the consistency between different studies. First, due to different spatial
 975 resolution of global trait maps (mainly 0.5 °) and our study, we resampled the data products of
 976 previous studies and our maps to 0.5 ° spatial resolution. In addition, Vallicrosa et al. (2022)
 977 generated the global maps of LNC and LPC with a 1 km spatial resolution, we also compared the
 978 frequency distribution of Vallicrosa et al. (2022) with that of our study at a 1 km spatial resolution.
 979 Second, our study focused on natural vegetation, so the global trait maps were used to filter out
 980 non-natural vegetation (e.g., croplands). For example, Madani et al. (2018) predicted the spatial
 981 distributions of SLA that included croplands. We quantitatively compared our maps with previous
 982 studies from two perspectives. The comparisons among trait maps were made using frequency
 983 plots and spatial correlations (Figure 7 and Table 5). And the maps of spatial differences between
 984 our study and previous studies were displayed as Figs F1-F5 in Appendix F.

985 **Table F1** Summary table of related trait maps of previous studies used in this study.

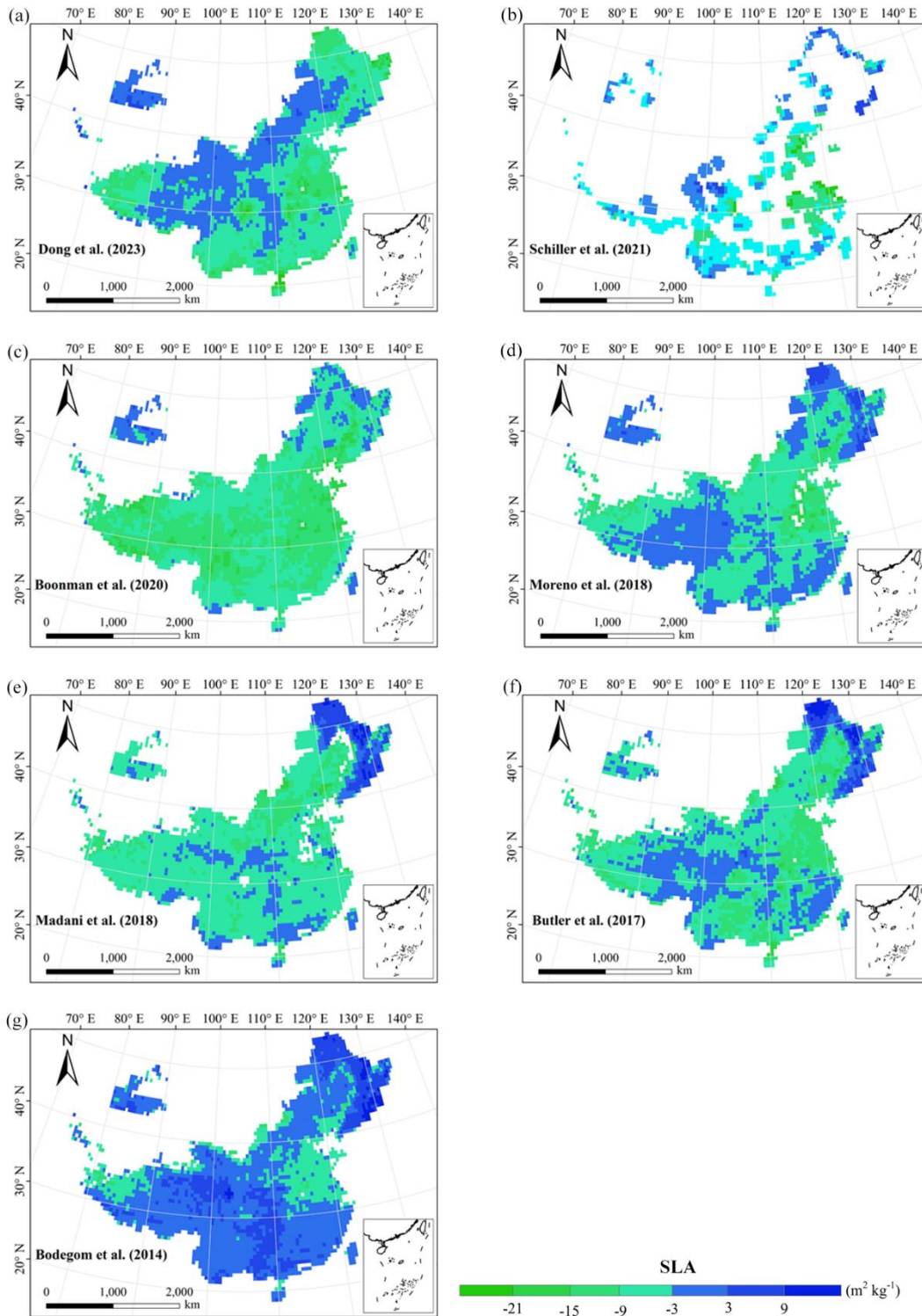
References	Related traits	Methods	Predictors	Consideration of PFT	Resolution
Dong et al. (2023)	SLA LNC	Optimality models	Climate	Yes	0.5 °
Vallicrosa et al. (2022)	LNC LPC	Neural networks	Climate Soil N and P deposition	Yes	0.0083 °
Schiller et al. (2021)	SLA LNC LA WD	Convolutional Neural Networks	Climate In-situ RGB images	No	0.5 °
Boonman et al. (2020)	SLA LNC WD	Generalized linear model, Generalized additive model, Random forest, Boosted regression trees, Ensemble model	Climate Soil	No	0.5 °
Moreno et al. (2018)	SLA LNC LPC LDMC	Regularized regression, forest, networks, Kernel networks	Climate Elevation Reflectance	Yes	0.0045 °

Madani et al. (2018)	SLA	Generalized additive model	Climate	No	0.5 °
Butler et al. (2017)	SLA LNC LPC	Bayesian model	Climate Soil	Yes	0.5 °
Bodegom et al. (2014)	SLA WD	Multiple regression analysis	Climate Soil	No	0.5 °

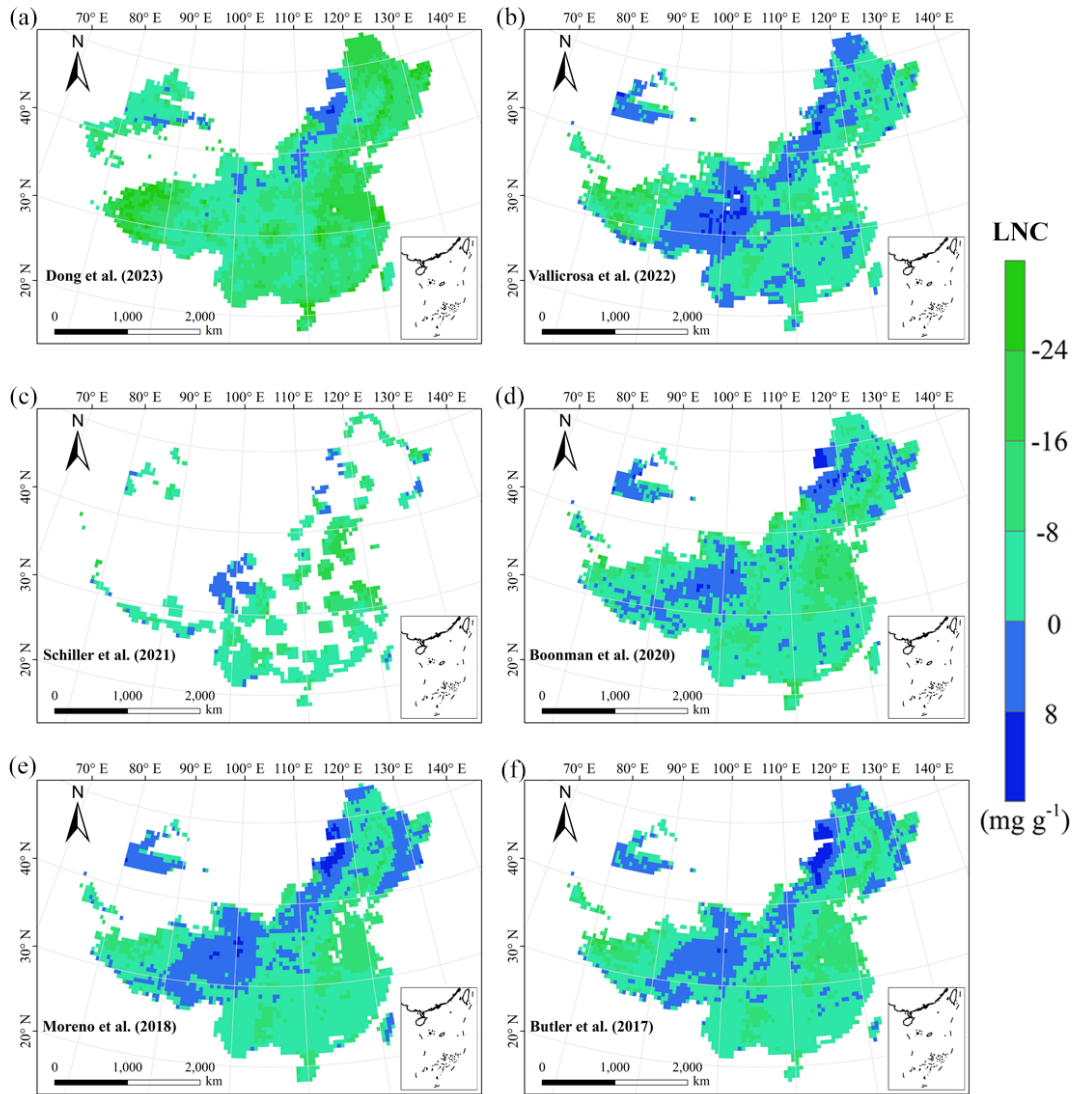
986 The resolutions 0.5 °, 0.0083 ° and 0.0045 ° correspond to square grid cell sizes of about 50 km, 1 km
987 and 500 m at the equator. PFT, plant functional type; SLA, specific leaf area; LDMC, leaf dry matter
988 content; LNC, leaf N concentration; LPC, leaf P concentration; LA, leaf area; WD, wood density.
989



990
991 **Figure F1.** Frequency distributions of plant functional traits in our study (“This study”, dashed
992 black lines) and Vallicrosa et al. (2022) at 1 km spatial resolution. (a) LNC, leaf N concentration
993 (mg g⁻¹); (b) LPC, leaf P concentration (mg g⁻¹).



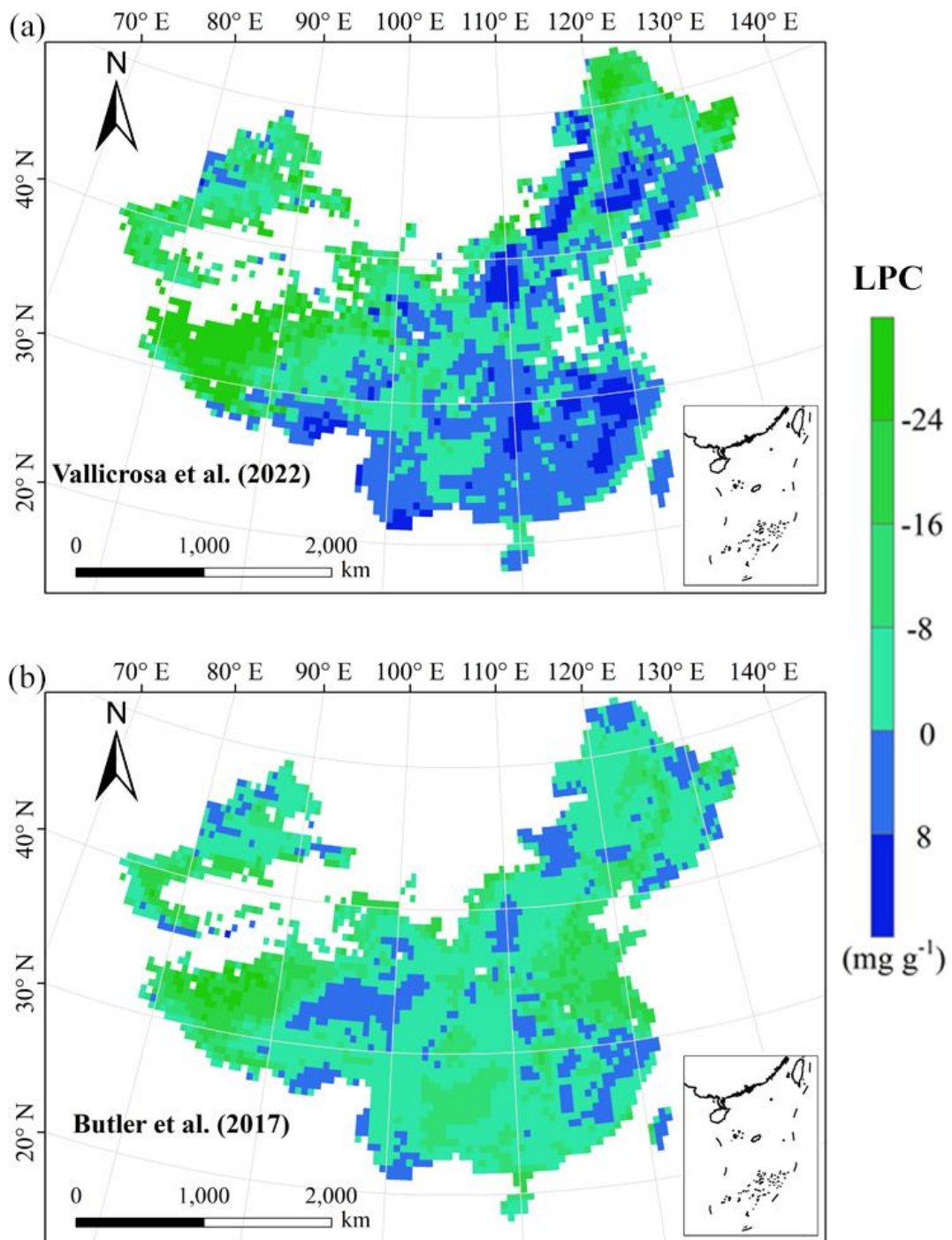
994
 995 **Figure F2.** Spatial differences in SLA (specific leaf area, $\text{m}^2 \text{kg}^{-1}$) between our study and trait maps
 996 from previous studies (see Table F1 for citations).



997

998 **Figure F3.** Spatial differences in LNC (leaf N concentration, mg g^{-1}) between our study and trait maps

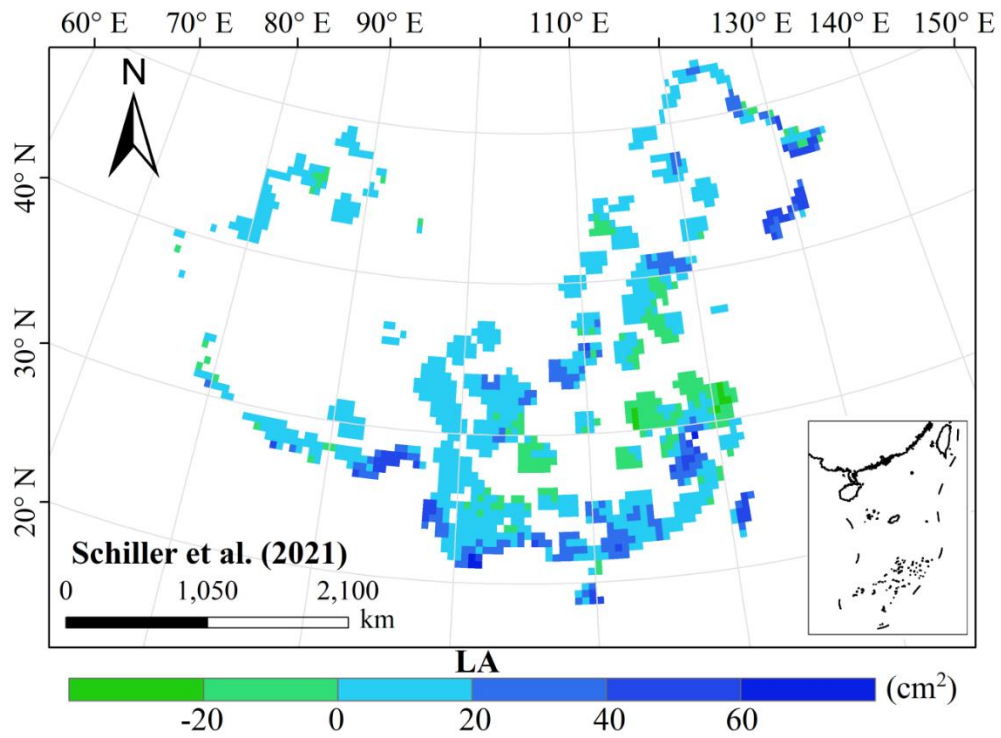
999 from previous studies (see Table F1 for citations).



1000

1001 **Figure F4.** Spatial differences in LPC (leaf P concentration, mg g⁻¹) between our study and trait maps

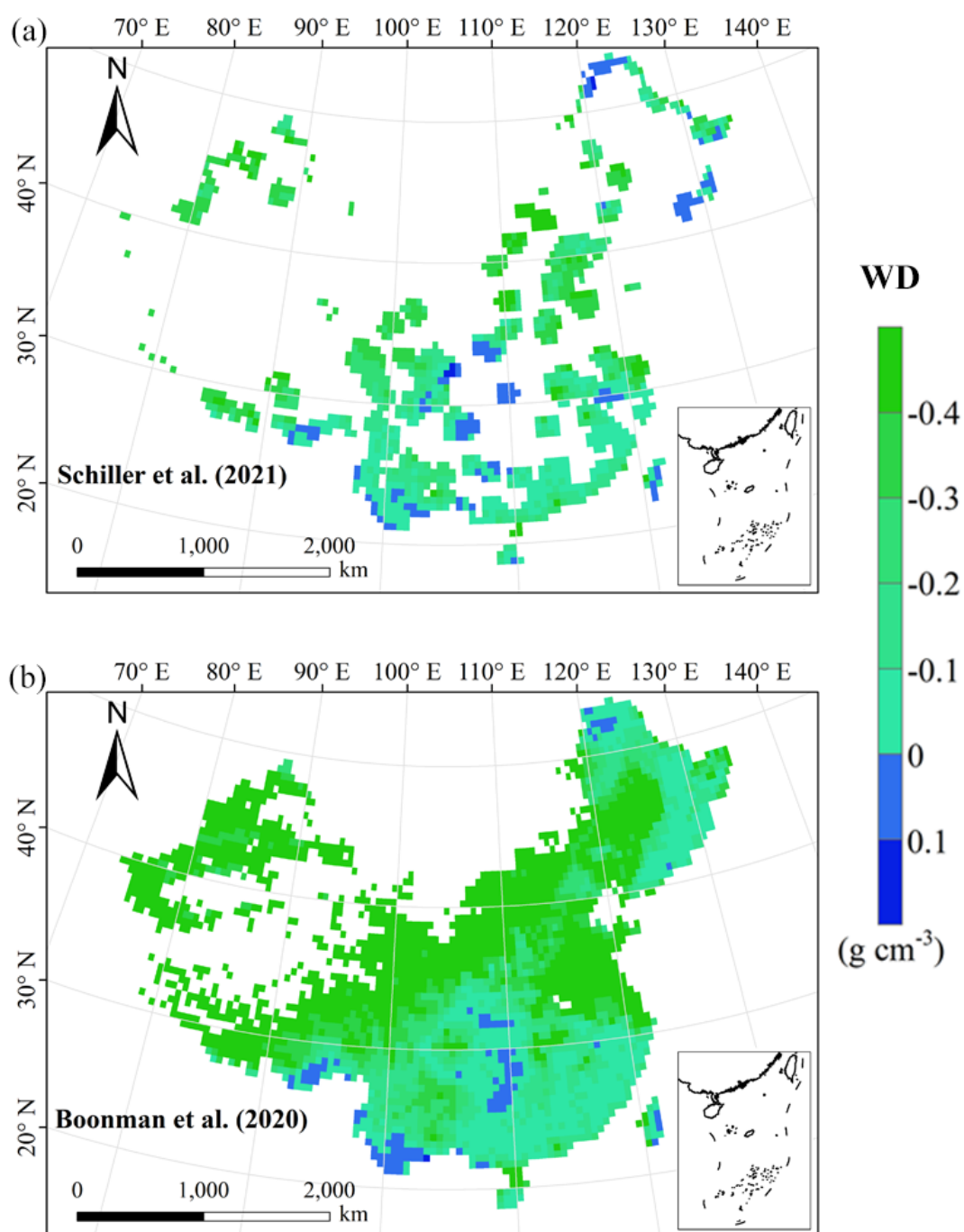
1002 from previous studies (see Table F1 for citations).



1003

1004 **Figure F5.** Spatial differences in LA (leaf area, cm²) between our study and trait maps from previous

1005 studies (see Table F1 for citations).



1006

1007 **Figure F6.** Spatial differences in WD (wood density, g cm^{-3}) between our study and trait maps from

1008 previous studies (see Table F1 for citations).

1009 **Author contributions.** NA and NL designed the research. NA did the analysis, processed the data
1010 and wrote the draft of the paper. All co-authors commented on the manuscript and agreed upon the
1011 final version of the paper.

1012
1013 **Competing interests.** The contact author has declared that none of the authors has any competing
1014 interests.

1015
1016 **Disclaimer.** Publisher's note: Copernicus Publications remains neutral with regard to
1017 jurisdictional claims in published maps and institutional affiliations.

1018
1019 **Acknowledgement.** We acknowledge financial supports from the National Natural Science
1020 Foundation of China (41991234) and the Joint CAS-MPG Research Project (HZXM20225001MI).

1021
1022 **Financial support.** This work has been supported by the National Natural Science Foundation of
1023 China (grant no. 41991234) and the Joint CAS-MPG Research Project (grant no.
1024 HZXM20225001MI).

1025

1026 **References**

1027 Ali, A. M., Darvishzadeh, R., Skidmore, A. K., van Duren, I., Heiden, U., and Heurich, M.:
1028 Estimating leaf functional traits by inversion of PROSPECT: assessing leaf dry matter
1029 content and specific leaf area in mixed mountainous forest. *Int. J. Appl. Earth Obs. Geoinf.*,
1030 45, 66–76, <https://doi.org/10.1016/j.jag.2015.11.004>, 2016.

1031 An, N. N., Lu, N., Fu, B. J., Wang, M. Y., and He, N. P.: Distinct responses of leaf traits to
1032 environment and phylogeny between herbaceous and woody angiosperm species in China.
1033 *Front. Plant Sci.* 12, 799401, <https://doi.org/10.3389/fpls.2021.799401>, 2021.

1034 Bakker, M. A., Carreño-Rocabado, G., and Poorter, L.: Leaf economics traits predict litter
1035 decomposition of tropical plants and differ among land use types. *Funct. Ecol.*, 25, 473–483,
1036 <https://doi.org/10.1111/j.1365-2435.2010.01802.x>, 2011.

1037 Berzaghi, F., Wright, I. J., Kramer, K., Oddou-Muratorio, S., Bohn, F. J., Reyer, C. P. O., Sabate,
1038 S., Sanders, T. G. M., and Hartig, F.: Towards a new generation of trait-flexible vegetation
1039 models. *Trends Ecol. Evol.*, 35, 191–205, <https://doi.org/10.1016/j.tree.2019.11.006>, 2020.

1040 Blumenthal, D. M., Mueller, K. E., Kray, J. A., Ocheltree, T. W., Augustine, D. J., Wilcox, K. R.,
1041 and Cornelissen, H.: Traits link drought resistance with herbivore defence and plant
1042 economics in semi-arid grasslands: The central roles of phenology and leaf dry matter
1043 content. *J. Ecol.*, 108, 2336–2351, <https://doi.org/10.1111/1365-2745.13454>, 2020.

1044 Bohner, A. Soil chemical properties as indicators of plant species richness in grassland
1045 communities. Integrating efficient grassland farming and biodiversity, Proceedings of the
1046 13th International Occasional Symposium of the European Grassland Federation, Tartu,

1047 Estonia, 29–31 August, 48–51, 2005.

1048 Boonman, C. C. F., Benitez-Lopez, A., Schipper, A. M., Thuiller, W., Anand, M., Cerabolini, B. E.
1049 L., Cornelissen, J. H. C., Gonzalez-Melo, A., Hattingh, W. N., Higuchi, P., Laughlin, D. C.,
1050 Onipchenko, V. G., Penuelas, J., Poorter, L., Soudzilovskaia, N. A., Huijbregts, M. A. J., and
1051 Santini, L.: Assessing the reliability of predicted plant trait distributions at the global scale.
1052 *Glob. Ecol. Biogeogr.*, 29, 1034–1051, <https://doi.org/10.1111/geb.13086>, 2020.

1053 Breiman, L.: Random forests. *Mach. Learn.*, 45, 5–32, <https://doi.org/10.1023/a:1010933404324>,
1054 2001.

1055 Bruelheide, H., Dengler, J., Purschke, O., Lenoir, J., Jimenez-Alfaro, B., Hennekens, S. M., Botta-
1056 Dukat, Z., Chytrý, M., Field, R., Jansen, F., Kattge, J., Pillar, V. D., Schrodte, F., Mahecha, M.
1057 D., Peet, R. K., Sandel, B., van Bodegom, P., Altman, J., Alvarez-Davila, E., Arfin Khan, M.
1058 A. S., et al.: Global trait-environment relationships of plant communities. *Nat. Ecol. Evol.*, 2,
1059 1906–1917, <https://doi.org/10.1038/s41559-018-0699-8>, 2018.

1060 Bruelheide, H., Dengler, J., Jiménez-Alfaro, B., Purschke, O., Hennekens, S. M., Chytrý, M.,
1061 Pillar, V. D., Jansen, F., Kattge, J., Sandel, B., Aubin, I., Biurrun, I., Field, R., Haider, S.,
1062 Jandt, U., Lenoir, J., Peet, R. K., Peyre, G., Sabatini, F. M., Schmidt, M., et al.: sPlot – A new
1063 tool for global vegetation analyses. *J. Veg. Sci.*, 30, 161–186,
1064 <https://doi.org/10.1111/jvs.12710>, 2019.

1065 Buchhorn, M., Bertels, L., Smets, B., De Roo, B., Lesiv, M., Tsendbazar, N. E., Masiliunas, D.,
1066 and Linlin, L.: Copernicus Global Land Service: Land Cover 100m: Version 3 Globe 2015-
1067 2019: Algorithm Theoretical Basis Document. <https://doi.org/10.5281/zenodo.3938968>, 2020.

1068 Butler, E. E., Datta, A., Flores-Moreno, H., Chen, M., Wythers, K. R., Fazayeli, F., Banerjee, A.,
1069 Atkin, O. K., Kattge, J., Amiaud, B., Blonder, B., Boenisch, G., Bond-Lamberty, B., Brown,
1070 K. A., Byun, C., Campetella, G., Cerabolini, B. E. L., Cornelissen, J. H. C., Craine, J. M.,
1071 Craven, D., de Vries, F. T., Diaz, S., Domingues, T. F., Forey, E., Gonzalez-Melo, A., Gross,
1072 N., Han, W., Hattingh, W. N., Hickler, T., Jansen, S., Kramer, K., Kraft, N. J. B., Kurokawa,
1073 H., Laughlin, D. C., Meir, P., Minden, V., Niinemets, U., Onoda, Y., Penuelas, J., Read, Q.,
1074 Sack, L., Schamp, B., Soudzilovskaia, N. A., Spasojevic, M. J., Sosinski, E., Thornton, P. E.,
1075 Valladares, F., van Bodegom, P. M., Williams, M., Wirth, C., and Reich, P. B.: Mapping local
1076 and global variability in plant trait distributions. *P. Nat. Acad. Sci. USA*, 114, 10937–10946,
1077 <https://doi.org/10.1073/pnas.1708984114>, 2017.

1078 Cavender-Bares, J., Schneider, F. D., Santos, M. J., Armstrong, A., Carnaval, A., Dahlin, K. M.,
1079 Fatoyinbo, L., Hurr, G. C., Schimel, D., Townsend, P. A., Ustin, S. L., Wang, Z. H., and
1080 Wilson, A. M.: Integrating remote sensing with ecology and evolution to advance
1081 biodiversity conservation. *Nat. Ecol. Evol.*, 6, 506–519, <https://doi.org/10.1038/s41559-022-01702-5>, 2022.

1083 Clevers, J. G. P. W., and Gitelson, A. A.: Remote estimation of crop and grass chlorophyll and
1084 nitrogen content using red-edge bands on Sentinel-2 and -3. *Int. J. Appl. Earth Obs. Geoinf.*,

1085 23, 344–351, <https://doi.org/10.1016/j.jag.2012.10.008>, 2013.

1086 Dahlin, K. M., Asner, G. P., and Field, C. B.: Environmental and community controls on plant
1087 canopy chemistry in a Mediterranean-type ecosystem. *P. Nat. Acad. Sci. USA*, 110, 6895–
1088 6900, <https://doi.org/10.1073/pnas.1215513110>, 2013.

1089 Darvishzadeh, R., Skidmore, A., Schlerf, M., and Atzberger, C.: Inversion of a radiative transfer
1090 model for estimating vegetation LAI and chlorophyll in a heterogeneous grassland. *Remote
1091 Sens. Environ.*, 112, 2592–2604, <https://doi.org/10.1016/j.rse.2007.12.003>, 2008.

1092 Diaz, S., Kattge, J., Cornelissen, J. H., Wright, I. J., Lavorel, S., Dray, S., Reu, B., Kleyer, M.,
1093 Wirth, C., Prentice, I. C., Garnier, E., Bonisch, G., Westoby, M., Poorter, H., Reich, P. B.,
1094 Moles, A. T., Dickie, J., Gillison, A. N., Zanne, A. E., Chave, J., Wright, S. J., Sheremet'ev, S.
1095 N., Jactel, H., Baraloto, C., Cerabolini, B., Pierce, S., Shipley, B., Kirkup, D., Casanoves, F.,
1096 Joswig, J. S., Gunther, A., Falczuk, V., Ruger, N., Mahecha, M. D., and Gorne, L. D.: The
1097 global spectrum of plant form and function. *Nature*, 529, 167–171,
1098 <https://doi.org/10.1038/nature16489>, 2016.

1099 Diaz, S., Hodgson, J. G., Thompson, K., Cabido, M., Cornelissen, J. H. C., Jalili, A., Montserrat-
1100 Marti, G., Grime, J. P., Zarrinkamar, F., Asri, Y., Band, S. R., Basconcelo, S., Castro-Diez, P.,
1101 Funes, G., Hamzehee, B., Khoshnevi, M., Perez-Harguindeguy, N., Perez-Rontome, M. C.,
1102 Shirvany, F. A., Vendramini, F., Yazdani, S., Abbas-Azimi, R., Bogaard, A., Boustani, S.,
1103 Charles, M., Dehghan, M., de Torres-Espuny, L., Falczuk, V., Guerrero-Campo, J., Hynd, A.,
1104 Jones, G., Kowsary, E., Kazemi-Saeed, F., Maestro-Martinez, M., Romo-Diez, A., Shaw, S.,
1105 Siavash, B., Villar-Salvador, P., and Zak, M. R.: The plant traits that drive ecosystems:
1106 evidence from three continents. *J. Veg. Sci.*, 15, 295–304, <https://doi.org/10.1111/j.1654-1103.2004.tb02266.x>, 2004.

1108 Dong, N., Dechant, B., Wang, H., Wright, I. J., and Prentice, IC.: Global leaf-trait mapping based
1109 on optimality theory. *Glob. Ecol. Biogeogr.*, <https://doi.org/10.1111/geb.13680>, 2023.

1110 Du, L., Liu, H., Guan, W., Li, J., and Li, J.: Drought affects the coordination of belowground and
1111 aboveground resource-related traits in *Solidago canadensis* in China. *Ecol. Evol.*, 9, 9948–
1112 9960, <https://doi.org/10.1002/ece3.5536>, 2019.

1113 Elith, J., Leathwick, J. R., and Hastie, T.: A working guide to boosted regression trees. *J. Anim.
1114 Ecol.*, 77, 802–813, <https://doi.org/10.1111/j.1365-2656.2008.01390.x>, 2008.

1115 Elith, J., Kearney, M., and Phillips, S.: The art of modelling range-shifting species. *Methods Ecol.
1116 Evol.*, 1, 330–342, <https://doi.org/10.1111/j.2041-210X.2010.00036.x>, 2010.

1117 Elith, J., Graham, C. H., Anderson, R. P., Dudik, M., Ferrier, S., Guisan, A., Hijmans, R. J.,
1118 Huettmann, F., Leathwick, J. R., Lehmann, A., Li, J., Lohmann, L. G., Loiselle, B. A.,
1119 Manion, G., Moritz, C., Nakamura, M., Nakazawa, Y., Overton, J. M., Peterson, A. T.,
1120 Phillips, S. J., Richardson, K., Scachetti-Pereira, R., Schapire, R. E., Soberon, J., Williams, S.,
1121 Wisz, M. S., and Zimmermann, N. E.: Novel methods improve prediction of species'
1122 distributions from occurrence data. *Ecography*, 29, 129–151,

1123 <https://doi.org/10.1111/j.2006.0906-7590.04596.x>, 2006.

1124 Finzi, A. C., Austin, A. T., Cleland, E. E., Frey, S. D., Houlton, B. Z., and Wallenstein, M. D.:
 1125 Responses and feedbacks of coupled biogeochemical cycles to climate change: examples
 1126 from terrestrial ecosystems. *Front. Ecol. Environ.*, 9, 61–67, <https://doi.org/10.1890/100001>,
 1127 2011.

1128 Foley, J. A., Prentice, I. C., Ramankutty, N., Levis, S., Pollard, D., Sitch, S., and Haxeltine, A.: An
 1129 integrated biosphere model of land surface processes, terrestrial carbon balance, and
 1130 vegetation dynamics. *Global Biogeochem. Cy.*, 10, 603–628,
 1131 <https://doi.org/10.1029/96gb02692>, 1996.

1132 Freschet, G. T., Cornelissen, J. H. C., van Logtestijn, R. S. P., and Aerts, R.: Evidence of the ‘plant
 1133 economics spectrum’ in a subarctic flora. *J. Ecol.*, 98, 362–373,
 1134 <https://doi.org/10.1111/j.1365-2745.2009.01615.x>, 2010.

1135 Grime, J. P.: Benefits of plant diversity to ecosystems: immediate, filter and founder effects. *J.*
 1136 *Ecol.*, 86, 902–910, <https://doi.org/10.1046/j.1365-2745.1998.00306.x>, 1998.

1137 He, N., Yan, P., Liu, C., Xu, L., Li, M., Van Meerbeek, K., Zhou, G., Zhou, G., Liu, S., Zhou, X.,
 1138 Li, S., Niu, S., Han, X., Buckley, T. N., Sack, L., and Yu, G.: Predicting ecosystem
 1139 productivity based on plant community traits. *Trends Plant Sci.*, 28, 43–53,
 1140 <https://doi.org/10.1016/j.tplants.2022.08.015>, 2023.

1141 Hodgson, J. G., Montserrat-Marti, G., Charles, M., Jones, G., Wilson, P., Shipley, B., Sharafi, M.,
 1142 Cerabolini, B. E. L., Cornelissen, J. H. C., Band, S. R., Bogard, A., Castro-Diez, P., Guerrero-
 1143 Campo, J., Palmer, C., Perez-Rontome, M. C., Carter, G., Hynd, A., Romo-Diez, A., Espuny,
 1144 L. D., and Pla, F. R.: Is leaf dry matter content a better predictor of soil fertility than specific
 1145 leaf area? *Ann. Bot.*, 108, 1337–1345, <https://doi.org/10.1093/aob/mcr225>, 2011.

1146 Hoeber, S., Leuschner, C., Köhler, L., Arias-Aguilar, D., and Schuldt, B.: The importance of
 1147 hydraulic conductivity and wood density to growth performance in eight tree species from a
 1148 tropical semi-dry climate. *Forest Ecol. Manag.*, 330, 126–136,
 1149 <https://doi.org/10.1016/j.foreco.2014.06.039>, 2014.

1150 Jónsdóttir, I. S., Halbritter, A. H., Christiansen, C. T., Althuizen, I. H. J., Haugum, S. V., Henn, J. J.,
 1151 Björnsdóttir, K., Maitner, B. S., Malhi, Y., Michaletz, S. T., Roos, R. E., Klanderud, K., Lee,
 1152 H., Enquist, B. J., and Vandvik, V.: Intraspecific trait variability is a key feature underlying
 1153 high Arctic plant community resistance to climate warming. *Ecol. Monogr.*, 93,
 1154 <https://doi.org/10.1002/ecm.1555>, 2022.

1155 Jung, V., Violle, C., Mondy, C., Hoffmann, L., and Muller, S.: Intraspecific variability and trait-
 1156 based community assembly. *J. Ecol.*, 98, 1134–1140, <https://doi.org/10.1111/j.1365-2745.2010.01687.x>, 2010.

1158 Kattge, J., Diaz, S., Lavorel, S., Prentice, C., Leadley, P., Bonisch, G., Garnier, E., Westoby, M.,
 1159 Reich, P. B., Wright, I. J., Cornelissen, J. H. C., Violle, C., Harrison, S. P., van Bodegom, P.
 1160 M., Reichstein, M., Enquist, B. J., Soudzilovskaia, N. A., Ackerly, D. D., Anand, M., Atkin,

1161 O., et al.: TRY - a global database of plant traits. *Glob. Change Biol.*, 17, 2905–2935,
1162 <https://doi.org/10.1111/j.1365-2486.2011.02451.x>, 2011.

1163 Kattge, J., Bonisch, G., Diaz, S., Lavorel, S., Prentice, I. C., Leadley, P., Tautenhahn, S., Werner, G.
1164 D. A., Aakala, T., Abedi, M., Acosta, A. T. R., Adamidis, G. C., Adamson, K., Aiba, M.,
1165 Albert, C. H., Alcantara, J. M., Alcazar, C. C., Aleixo, I., Ali, H., Amiaud, B., et al.: TRY
1166 plant trait database - enhanced coverage and open access. *Global Change Biol.*, 26, 119–188,
1167 <https://doi.org/10.1111/gcb.14904>, 2020.

1168 King, D. A., Davies, S. J., Tan, S., and Noor, N. S. M.: The role of wood density and stem support
1169 costs in the growth and mortality of tropical trees. *J. Ecol.*, 94, 670–680,
1170 <https://doi.org/10.1111/j.1365-2745.2006.01112.x>, 2006.

1171 Kirilenko, A. P., Belotelov, N. V., and Bogatyrev, B. G.: Global model of vegetation migration:
1172 incorporation of climatic variability. *Ecol. Model.*, 132, 125–133,
1173 [https://doi.org/10.1016/S0304-3800\(00\)00310-0](https://doi.org/10.1016/S0304-3800(00)00310-0), 2000.

1174 LeBauer, D. S., and Treseder, K. K.: Nitrogen limitation of net primary productivity in terrestrial
1175 ecosystems is globally distributed. *Ecology*, 89, 371–379, <https://doi.org/10.1890/06-2057.1>,
1176 2008.

1177 Li, C. X., Wulf, H., Schmid, B., He, J. S., and Schaepman, M. E.: Estimating plant traits of alpine
1178 grasslands on the Qinghai-Tibetan Plateau using remote sensing. *IEEE J. Sel. Top. Appl.*
1179 *Earth Obs. Remote Sens.*, 11, 2263–2275, <https://doi.org/10.1109/jstars.2018.2824901>, 2018.

1180 Li, D. J., Ives, A. R., and Waller, D. M.: Can functional traits account for phylogenetic signal in
1181 community composition? *New Phytol.*, 214, 607–618, <https://doi.org/10.1111/nph.14397>,
1182 2017.

1183 Li, Y. Q., Reich, P. B., Schmid, B., Shrestha, N., Feng, X., Lyu, T., Maitner, B. S., Xu, X., Li, Y. C.,
1184 Zou, D. T., Tan, Z. H., Su, X. Y., Tang, Z. Y., Guo, Q. H., Feng, X. J., Enquist, B. J., and
1185 Wang, Z. H.: Leaf size of woody dicots predicts ecosystem primary productivity. *Ecol. Lett.*,
1186 23, 1003–1013, <https://doi.org/10.1111/ele.13503>, 2020.

1187 Liang, X. Y., Ye, Q., Liu, H., and Brodribb, T. J.: Wood density predicts mortality threshold for
1188 diverse trees. *New Phytol.*, 229, <https://doi.org/10.1111/nph.17117>, 2021.

1189 Liaw, A., and Wiener, M.: Classification and Regression by randomForest. *R News*, 2, 18–22,
1190 2002.

1191 Liu, H. Y., and Yin, Y.: Response of forest distribution to past climate change: an insight into
1192 future predictions. *Chinese Science Bulletin*, 58, 4426–4436, [https://doi.org/10.1007/s11434-](https://doi.org/10.1007/s11434-013-6032-7)
1193 013-6032-7, 2013.

1194 Loozen, Y., Rebel, K. T., Karssenber, D., Wassen, M. J., Sardans, J., Peñuelas, J., and De Jong, S.
1195 M.: Remote sensing of canopy nitrogen at regional scale in Mediterranean forests using the
1196 spaceborne MERIS Terrestrial Chlorophyll Index. *Biogeosciences*, 15, 2723–2742,
1197 <https://doi.org/10.5194/bg-15-2723-2018>, 2018.

1198 Loozen, Y., Rebel, K. T., de Jong, S. M., Lu, M., Ollinger, S. V., Wassen, M. J., and Karssenber,

1199 D.: Mapping canopy nitrogen in European forests using remote sensing and environmental
1200 variables with the random forests method. *Remote Sens. Environ.*, 247, 111933,
1201 <https://doi.org/10.1016/j.rse.2020.111933>, 2020.

1202 Madani, N., Kimball, J. S., Ballantyne, A. P., Affleck, D. L. R., van Bodegom, P. M., Reich, P. B.,
1203 Kattge, J., Sala, A., Nazeri, M., Jones, M. O., Zhao, M., and Running, S. W.: Future global
1204 productivity will be affected by plant trait response to climate. *Sci. Rep.*, 8, 1–10,
1205 <https://doi.org/10.1038/s41598-018-21172-9>, 2018.

1206 Martínez-Vilalta, J., Mencuccini, M., Vayreda, J., and Retana, J.: Interspecific variation in
1207 functional traits, not climatic differences among species ranges, determines demographic
1208 rates across 44 temperate and Mediterranean tree species. *J. Ecol.*, 98, 1462–1475,
1209 <https://doi.org/10.1111/j.1365-2745.2010.01718.x>, 2010.

1210 Matheny, A. M., Mirfenderesgi, G., and Bohrer, G.: Trait-based representation of hydrological
1211 functional properties of plants in weather and ecosystem models. *Plant Divers*, 39, 1–12,
1212 <https://doi.org/10.1016/j.pld.2016.10.001>, 2017.

1213 Moles, A. T., Warton, D. I., Warman, L., Swenson, N. G., Laffan, S. W., Zanne, A. E., Pitman, A.,
1214 Hemmings, F. A., and Leishman, M. R.: Global patterns in plant height. *J. Ecol.*, 97, 923–932,
1215 <https://doi.org/10.1111/j.1365-2745.2009.01526.x>, 2009.

1216 Moreno-Martínez, Á., Camps-Valls, G., Kattge, J., Robinson, N., Reichstein, M., van Bodegom, P.,
1217 Kramer, K., Cornelissen, J. H. C., Reich, P., Bahn, M., Niinemets, Ü., Peñuelas, J., Craine, J.
1218 M., Cerabolini, B. E. L., Minden, V., Laughlin, D. C., Sack, L., Allred, B., Baraloto, C., Byun,
1219 C., Soudzilovskaia, N. A., and Running, S. W.: A methodology to derive global maps of leaf
1220 traits using remote sensing and climate data. *Remote Sens. Environ.*, 218, 69–88,
1221 <https://doi.org/10.1016/j.rse.2018.09.006>, 2018.

1222 Myers-Smith, I. H., Thomas, H. J. D., and Björkman, A. D.: Plant traits inform predictions of
1223 tundra responses to global change. *New Phytol.*, 221, 1742–1748,
1224 <https://doi.org/10.1111/nph.15592>, 2019.

1225 NEODC, 2015. NEODC - NERC Earth Observation Data Centre. Natural Environment Research
1226 Council. <http://neodc.nerc.ac.uk/>.

1227 Peng, C. H.: From static biogeographical model to dynamic global vegetation model: a global
1228 perspective on modelling vegetation dynamics. *Ecol. Model.*, 135, 33–54,
1229 [https://doi.org/10.1016/S0304-3800\(00\)00348-3](https://doi.org/10.1016/S0304-3800(00)00348-3), 2000.

1230 Perez-Harguindeguy, N., Diaz, S., Garnier, E., Lavorel, S., Poorter, H., Jaureguiberry, P., Bret-
1231 Harte, M. S., Cornwell, W. K., Craine, J. M., Gurvich, D. E., Urcelay, C., Veneklaas, E. J.,
1232 Reich, P. B., Poorter, L., Wright, I. J., Ray, P., Enrico, L., Pausas, J. G., de Vos, A. C.,
1233 Buchmann, N., Funes, G., Quétier, F., Hodgson, J. G., Thompson, K., Morgan, H. D., ter
1234 Steege, H., van der Heijden, M. G. A., Sack, L., Blonder, B., Poschlod, P., Vaieretti, M. V.,
1235 Conti, G., Staver, A. C., Aquino, S., and Cornelissen, J. H. C.: New handbook for
1236 standardised measurement of plant functional traits worldwide. *Aust. Bot.*, 61, 167–234,

1237 <https://doi.org/10.1071/bt12225>, 2013.

1238 Piao, S. L., He, Y., Wang, X. H., and Chen, F. H.: Estimation of China's terrestrial ecosystem
1239 carbon sink: Methods, progress and prospects. *Science China Earth Sciences*, 65, 641–651,
1240 <https://doi.org/10.1007/s11430-021-9892-6>, 2022.

1241 Potapov, P., Li, X. Y., Hernandez-Serna, A., Tyukavina, A., Hansen, M. C., Kommareddy, A.,
1242 Pickens, A., Turubanova, S., Tang, H., Silva, C. E., Armston, J., Dubayah, R., Blair, J. B.,
1243 Hofton, M.: Mapping global forest canopy height through integration of GEDI and Landsat
1244 data, *Remote Sens. Environ.*, 253, 112165, <https://doi.org/10.1016/j.rse.2020.112165>, 2021.

1245 Qiao, J. J., Zuo, X. A., Yue, P., Wang, S. K., Hu, Y., Guo, X. X., Li, X. Y., Lv, P., Guo, A. X., and
1246 Sun, S. S.: High nitrogen addition induces functional trait divergence of plant community in a
1247 temperate desert steppe. *Plant and Soil*, <https://doi.org/10.1007/s11104-023-05910-1>, 2023.

1248 Reich, P. B., and Oleksyn, J.: Global patterns of plant leaf N and P in relation to temperature and
1249 latitude. *Proc. Natl. Acad. Sci. U. S. A.*, 101, 11001–11006,
1250 https://doi.org/10.1073/pnas.0403588101_2004.

1251 Reich, P. B., and Cornelissen, H.: The world-wide ‘fast-slow’ plant economics spectrum: a traits
1252 manifesto. *Journal of Ecology*, 102, 275–301, <https://doi.org/10.1111/1365-2745.12211>, 2014.

1253 Reich, P. B., Uhl, C., Walters, M. B., and Ellsworth, D. S.: Leaf lifespan as a determinant of leaf
1254 structure and function among 23 Amazonian tree species. *Oecologia*, 86, 16–24,
1255 <https://doi.org/10.1007/BF00317383>, 1991.

1256 Ridgeway, G.: Gbm: generalized boosted regression models. R package version 1.5-6, Available at:
1257 <http://cran.r-project.org/web/packages/gbm/index.html>, accessed 11/02/20092006.

1258 Roderick, M. L., and Berry, S. L.: Linking wood density with tree growth and environment: a
1259 theoretical analysis based on the motion of water. *New Phytol.*, 149, 473–485,
1260 <https://doi.org/10.1046/j.1469-8137.2001.00054.x>, 2002.

1261 Romero, A., Aguado, I., and Yebra, M.: Estimation of dry matter content in leaves using
1262 normalized indexes and PROSPECT model inversion. *Int. J. Remote Sens.*, 33, 396–414,
1263 <https://doi.org/10.1080/01431161.2010.532819>, 2012.

1264 Sakschewski, B., von Bloh, W., Boit, A., Rammig, A., Kattge, J., Poorter, L., Penuelas, J., and
1265 Thonicke, K.: Leaf and stem economics spectra drive diversity of functional plant traits in a
1266 dynamic global vegetation model. *Global Change Biol.*, 21, 2711–2725,
1267 https://doi.org/10.1111/gcb.12870_2015.

1268 Scheiter, S., Langan, L., and Higgins, S. I.: Next-generation dynamic global vegetation models:
1269 learning from community ecology. *New Phytol.*, 198, 957–969,
1270 <https://doi.org/10.1111/nph.12210>, 2013.

1271 Schiller, C., Schmidtlein, S., Boonman, C., Moreno-Martinez, A., and Kattenborn, T.: Deep
1272 learning and citizen science enable automated plant trait predictions from photographs. *Sci.*
1273 *Rep.*, 11, <https://doi.org/10.1038/s41598-021-95616-0>, 2022.

1274 Shangguan, W., Dai, Y. J., Liu, B. Y., Zhu, A. X., Duan, Q. Y., Wu, L. Z., Ji, D. Y., Ye, A. Z., Yuan,

1275 H., Zhang, Q., Chen, D. D., Chen, M., Chu, J. T., Dou, Y. J., Guo, J. X., Li, H. Q., Li, J. J.,
1276 Liang, L., Liang, X., Liu, H. P., Liu, S. Y., Miao, C. Y., and Zhang, Y. Z.: A China data set of
1277 soil properties for land surface modeling. *J. Adv. Model. Earth Syst.*, 5, 212–224,
1278 <https://doi.org/10.1002/jame.20026>, 2013.

1279 Siefert, A., Violle, C., Chalmandrier, L., Albert, C. H., Taudiere, A., Fajardo, A., Aarssen, L. W.,
1280 Baraloto, C., Carlucci, M. B., Cianciaruso, M. V., de, L. D. V., de Bello, F., Duarte, L. D.,
1281 Fonseca, C. R., Freschet, G. T., Gaucherand, S., Gross, N., Hikosaka, K., Jackson, B., Jung,
1282 V., Kamiyama, C., Katabuchi, M., Kembel, S. W., Kichenin, E., Kraft, N. J., Lagerstrom, A.,
1283 Bagousse-Pinguet, Y. L., Li, Y., Mason, N., Messier, J., Nakashizuka, T., Overton, J. M.,
1284 Peltzer, D. A., Perez-Ramos, I. M., Pillar, V. D., Prentice, H. C., Richardson, S., Sasaki, T.,
1285 Schamp, B. S., Schob, C., Shipley, B., Sundqvist, M., Sykes, M. T., Vandewalle, M., and
1286 Wardle, D. A.: A global meta-analysis of the relative extent of intraspecific trait variation in
1287 plant communities. *Ecol. Lett.*, 18, 1406–1419, <https://doi.org/10.1111/ele.12508>, 2015.

1288 Šímová I., Sandel, B., Enquist, B. J., Michaletz, S. T., Kattge, J., Violle, C., McGill, B. J., Blonder,
1289 B., Engemann, K., Peet, R. K., Wisser, S. K., Morueta-Holme, N., Boyle, B., Kraft, N. J. B.,
1290 Svenning, J. C., and Hector, A.: The relationship of woody plant size and leaf nutrient content
1291 to large-scale productivity for forests across the Americas. *J. Ecol.*, 107, 2278–2290,
1292 <https://doi.org/10.1111/1365-2745.13163>, 2019.

1293 Sitch, S., Huntingford, C., Gedney, N., Levy, P. E., Lomas, M., Piao, S. L., Betts, R., Ciais, P., Cox,
1294 P., Friedlingstein, P., Jones, C. D., Prentice, I. C., and Woodward, F. I.: Evaluation of the
1295 terrestrial carbon cycle, future plant geography and climate-carbon cycle feedbacks using five
1296 Dynamic Global Vegetation Models (DGVMs). *Global Change Biol.*, 14, 2015–2039,
1297 <https://doi.org/10.1111/j.1365-2486.2008.01626.x>, 2008.

1298 Smart, S. M., Glanville, H. C., Blanes, M. d. C., Mercado, L. M., Emmett, B. A., Jones, D. L.,
1299 Cosby, B. J., Marrs, R. H., Butler, A., Marshall, M. R., Reinsch, S., Herrero-Járegui, C.,
1300 Hodgson, J. G., and Field, K.: Leaf dry matter content is better at predicting above-ground
1301 net primary production than specific leaf area. *Funct. Ecol.*, 31, 1336–1344,
1302 <https://doi.org/10.1111/1365-2435.12832>, 2017.

1303 Telenius, A.: Biodiversity information goes public: GBIF at your service. *Nord. J. Bot.*, 29, 378–
1304 381, <https://doi.org/10.1111/j.1756-1051.2011.01167.x>, 2011.

1305 Thomas, D. S., Montagu, K. D., and Conroy, J. P.: Changes in wood density of *Eucalyptus*
1306 *camaldulensis* due to temperature—the physiological link between water viscosity and wood
1307 anatomy. *Forest Ecol. Manag.*, 193, 157–165, <https://doi.org/10.1016/j.foreco.2004.01.028>,
1308 2004.

1309 Thomas, S. C.: Photosynthetic capacity peaks at intermediate size in temperate deciduous trees.
1310 *Tree Physiol.*, 30, 555–573, <https://doi.org/10.1093/treephys/tpq005>, 2010.

1311 Thuiller, W., Lafourcade, B., Engler, R., and Araújo, M. B.: BIOMOD – A platform for ensemble
1312 forecasting of species distributions. *Ecography*, 32, 369–373, [62](https://doi.org/10.1111/j.1600-</p>
</div>
<div data-bbox=)

1313 0587.2008.05742.x, 2009.

1314 Trabucco, A., and Zomer, R. J.: Global Aridity Index and Potential Evapo-Transpiration (ET0)
1315 Climate Database v2. CGIAR Consortium for Spatial Information (CGIAR-CSI),
1316 <https://cgiarcsi.community>, 2018.

1317 Vallicrosa, H., Sardans, J., Maspons, J., Zuccarini, P., Fernández-Martínez, M., Bauters, M., Goll,
1318 D. S., Ciais, P., Obersteiner, M., Janssens, I. A., and Peñuelas, J.: Global maps and factors
1319 driving forest foliar elemental composition: the importance of evolutionary history. *New*
1320 *Phytol.*, 233, 169–181, <https://doi.org/10.1111/nph.17771>, 2022.

1321 Van Bodegom, P. M., Douma, J. C., Witte, J. P. M., Ordoñez, J. C., Bartholomeus, R. P., and Aerts,
1322 R.: Going beyond limitations of plant functional types when predicting global ecosystem-
1323 atmosphere fluxes: exploring the merits of traits-based approaches. *Glob. Ecol. Biogeogr.*, 21,
1324 625–636, <https://doi.org/10.1111/j.1466-8238.2011.00717.x>, 2012.

1325 van Bodegom, P. M., Douma, J. C., and Verheijen, L. M. A fully traits-based approach to modeling
1326 global vegetation distribution. *P. Nat. Acad. Sci. USA*, 111, 13733–13738,
1327 <https://doi.org/10.1073/pnas.1304551110>, 2014.

1328 Verheijen, L. M., Aerts, R., Bonisch, G., Kattge, J., and Van Bodegom, P. M.: Variation in trait
1329 trade-offs allows differentiation among predefined plant functional types: implications for
1330 predictive ecology. *New Phytol.*, 209, 563–575, <https://doi.org/10.1111/nph.13623>, 2016.

1331 Wang, H., Harrison, S. P., Prentice, I. C., Yang, Y. Z., Bai, F., Togashi, H. F., Wang, M., Zhou, S.
1332 X., and Ni, J.: The China Plant Trait Database: toward a comprehensive regional compilation
1333 of functional traits for land plants. *Ecology*, 99, 500, <https://doi.org/10.1002/ecy.2091>, 2018.

1334 Webb, C. T., Hoeting, J. A., Ames, G. M., Pyne, M. I., and LeRoy Poff, N.: A structured and
1335 dynamic framework to advance traits-based theory and prediction in ecology. *Ecol. Lett.*, 13,
1336 267–283, <https://doi.org/10.1111/j.1461-0248.2010.01444.x>, 2010.

1337 Wright, I. J., Dong, N., Maire, V., Prentice, I. C., Westoby, M., Diaz, S., Gallagher, R. V., Jacobs,
1338 B. F., Kooyman, R., Law, E. A., Leishman, M. R., Niinemets, U., Reich, P. B., Sack, L., Villar,
1339 R., Wang, H., and Wilf, P.: Global climatic drivers of leaf size. *Science*, 357, 917–921,
1340 <https://doi.org/10.1126/science.aal4760>, 2017.

1341 Wright, I. J., Reich, P. B., Westoby, M., Ackerly, D. D., Baruch, Z., Bongers, F., Cavender-Bares,
1342 J., Chapin, T., Cornelissen, J. H. C., Diemer, M., Flexas, J., Garnier, E., Groom, P. K., Gulias,
1343 J., Hikosaka, K., Lamont, B. B., Lee, T., Lee, W., Lusk, C., Midgley, J. J., Navas, M. L.,
1344 Niinemets, U., Oleksyn, J., Osada, N., Poorter, H., Poot, P., Prior, L., Pyankov, V. I., Roumet,
1345 C., Thomas, S. C., Tjoelker, M. G., Veneklaas, E. J., and Villar, R.: The worldwide leaf
1346 economics spectrum. *Nature*, 428, 821–827, <https://doi.org/10.1038/nature02403>, 2004.

1347 Wullschleger, S. D., Epstein, H. E., Box, E. O., Euskirchen, E. S., Goswami, S., Iversen, C. M.,
1348 Kattge, J., Norby, R. J., van Bodegom, P. M., and Xu, X.: Plant functional types in earth
1349 system models: past experiences and future directions for application of dynamic vegetation
1350 models in high-latitude ecosystems. *Ann. Bot.*, 114, 1–16,

1351 <https://doi.org/10.1093/aob/mcu077>, 2014.

1352 Yan, P., He, N. P., Yu, K. L., Xu, L., and Van Meerbeek, K.: Integrating multiple plant functional
1353 traits to predict ecosystem productivity. *Commun Biol*, 6, 239,
1354 <https://doi.org/10.1038/s42003-023-04626-3>, 2023.

1355 Yang, Y. Z., Zhu, Q. A., Peng, C. H., Wang, H., Xue, W., Lin, G. H., Wen, Z. M., Chang, J., Wang,
1356 M., Liu, G. B., and Li, S. Q.: A novel approach for modelling vegetation distributions and
1357 analysing vegetation sensitivity through trait-climate relationships in China. *Sci. Rep.*, 6,
1358 24110, <https://doi.org/10.1038/srep24110>, 2016.

1359 Yang, Y. Z., Wang, H., Harrison, S. P., Prentice, I. C., Wright, I. J., Peng, C. H., and Lin, G. H.:
1360 Quantifying leaf-trait covariation and its controls across climates and biomes. *New Phytol.*,
1361 221, 155-168, <https://doi.org/10.1111/nph.15422>, 2018.

1362 Yang, Y. Z., Zhao, J., Zhao, P. X., Wang, H., Wang, B. H., Su, S. F., Li, M. X., Wang, L. M., Zhu,
1363 Q. A., Pang, Z. Y., and Peng, C. H.: Trait-Based Climate Change Predictions of Vegetation
1364 Sensitivity and Distribution in China. *Front. Plant Sci.*, 10, 908,
1365 <https://doi.org/10.3389/fpls.2019.00908>, 2019.

1366 Yurova, A. Y., and Volodin, E. M.: Coupled simulation of climate and vegetation dynamics. *Izv.,*
1367 *Atmos. . Ocean. Phy.*, 47, 531-539, <https://doi.org/10.1134/s0001433811050124>, 2011.

1368 Zaehle, S., and Friend, A. D.: Carbon and nitrogen cycle dynamics in the O-CN land surface
1369 model: 1. Model description, site-scale evaluation, and sensitivity to parameter estimates.
1370 *Global Biogeochem. Cy.*, 24, n/a-n/a, <https://doi.org/10.1029/2009gb003521>, 2010.